UNIVERSITY OF CALIFORNIA
RIVERSIDE

The Effects of Quorum-Sensing on the Gut Microbiota and Virulence of *Vibrio cholerae*.

A Dissertation submitted in partial satisfaction
of the requirements for the degree of

Doctor of Philosophy

in

Biochemistry and Molecular Biology

by

Jennifer Y Cho

September 2022

Dissertation Committee:
Dr. Ansel Hsiao, Chairperson
Dr. Jikui Song
Dr. Patrick Degnan

The Dissertation of Jennifer Y Cho is approved:

_____

_____

_____

Committee Chairperson

University of California, Riverside

Acknowledgments

I would like to thank my advisor Dr. Ansel Hsiao for giving me the opportunity to join the lab and work on such an interesting project. Thank you for advise, encouragement, and patience along the journey. I am very grateful for your guidance and allowing me the opportunity to encounter new ideas.

Dr. Song, thank you for offering valuable insights and feedbacks on my project. I really appreciated the time and effort you spent for my qualifying exam and defense. I also had fun doing TA for your lab classes.

Dr. Degnan, thank you for sharing your ideas and thoughts with me. It's always helpful discussing questions with you. I also really appreciated the time and effort for you to serve on my qualifying exam and defense committee. You always ask and provide very insightful questions and thoughts.

Dr. Dingwall, thank you very much for your patients and encouragement when I first started at UCR and throughout the time that I am here. I thank you for serving on my committee despite your busy teaching schedule and I am also very, very happy to see you getting your tenure.

Thank you to the past and present members of the Hsiao lab for your support. It

has been a great pleasure to work with all of you. Jon, you were the first person that I met in this lab and thank you for standing out for me at that time. I valued your carefulness and kindness, and is was a very interesting experience working with you on starting the germ-free mice colonies. Salma, I am very grateful that you were there to go through all the chaos at the beginning of all the mice experience, you are such talented scientists. John, I am also very grateful that we started in this lab together, thank you so much for teaching me as well as all the supports that you have provided. Rui, thank you very much for teaching and assisting me in all the bioinformatics related knowledge, and being such a good friend throughout the journey. I enjoyed all the times that we discuss about each other's project and finding solutions, and the time we went out for a trip. Ethan, it's been a pleasure working with you. You are such a smart person that our conversation as always been enjoyable. Siyi, thank you for your generosity and kindness, I am glad we were able to work together. Katia, I really appreciated your dedication and determination, and I am happy we were able to overlap. Varadh, thank you so much for all your support especially during the tough times for me. You have also been so kind and providing me the support that I needed. It has always been fun to talk to you, I really enjoyed the chats we had. Elyza, I am thankful that you are willing to teach me the experiments that I wanted to

learn and your trust in my ability to discuss about your project. I admire your enthusiastic and thank you for your support.

I would also like to thank my friends at UCR. All the people that I met in my first year, thank you very much, you have made adjusting to busy first year life a lot easier. Yan-Ting, Wei-Hsien, Po-Yao, and Suyeon, thank you all for being here. It has been fun to be friends and roommates with you all and I really enjoyed the trips we took together as well as the journey we had at UCR.

Last, I would like to thank my family for being supportive and patience with me throughout my entire graduate student journey. I am grateful that they are willing to learn about my project and show interest. I could not have gone through the whole process without their support.

The text of this dissertation, in part is a reprint of the material as it appears in the journal Gut Microbes 2021 (Chapter 1) and Frontiers in Cellular and Infection Microbiology (Chapter 2.1). The corresponding author Dr. Ansel Hsiao listed in that publication directed and supervised the research which forms the basis for this dissertation. The RNA-seq data analysis section in Chapter 2.1 and 3.1 was provided by Rui Liu. Raw data discussed in Chapter 3.2 was provided by Dr. Tian Xia (University of

Science and Technology, Wuhan, China).

This work was funded by the National Institute of General Medical Sciences R35GM124724 and National Institute of Allergy and Infectious Diseases R01AI157106 (to Ansel Hsiao).

ABSTRACT OF THE DISSERTATION

The Effects of Quorum-Sensing on the Gut Microbiota and Virulence of *Vibrio cholerae*.

by

Jennifer Y Cho

Doctor of Philosophy, Graduate Program in Biochemistry and Molecular Biology
University of California, Riverside, September 2022
Dr. Ansel Hsiao, Chairperson

Quorum sensing (QS) is a bacterial communication process that allows bacteria to alter gene expression based on environmental signals. Autoinducer-2 (AI-2) is one of these signaling molecules that regulates the virulence of the gastrointestinal pathogen *Vibrio cholerae*, which causes the diarrheal disease cholera that affects millions of people worldwide. Research on healthy and malnourished humans has shown that the structure of gut microbiome is different and differentially able to resist *V. cholerae* colonization, pathogen infection, and host immune response and treatment. However, the effect of AI-2 produced by different bacteria in susceptible and resistant microbiomes on their community and on *V. cholerae* is not well understood. To this end I constructed *Escherichia coli* expressing *luxS* gene from different microbes and combined them with

different model communities of human gut microbes resembling health individuals or individuals recovering from diarrhea and tested in mouse models. We show microbiota-associated biofilm regulation in *V. cholerae* providing resistance against host intestinal environmental stress and AI-2 signal mediated microbiome structural and gene expression change. Our findings suggest that the composition of the gut microbiome is affected by AI-2 signal, and at the time of infection or treatment, the composition is crucial to host resistance against infection. This potentially provides a direction for the prevention and/or improved resistance to pathogen infection as well as immunotherapy.

Table of Content

List of Figure

Chapter 1

Chapter 2

List of Table

Chapter 1 Introduction

Cross-talk between bacteria: Quorum sensing

Quorum sensing (QS) is a bacterial communication system that uses the production and sensing of diffusible signaling autoinducer (AI) molecules to monitor intra- and inter-species population density among both Gram-positive and Gram-negative bacteria, allowing coordinated regulation of effector functions by microbial populations (Rutherford and Bassler, 2012;Pereira et al., 2013) (Table 1-1).

Gram-positive system

AI molecules have a wide variety of chemical structures. Gram-positive bacteria utilize secreted peptides as signaling molecules for QS communication. These peptides, namely autoinducing peptides (AIPs) has variable structures that are synthesized by ribosomes and can be modified post-translationally (Sturme et al., 2002).

One of the signaling pathway in Gram-positive bacteria is the two-component system. Peptides are secreted by ATP-binding cassette (ABC) transporters and cleaved by protease to AIPs. With the increase in population, environmental AIPs starts to accumulate. When The secreted peptides are then detected by two-component receptor

kinase located on cell membrane and activates the kinase via phosphorylation of a conserved His residue. The activated kinase will phosphorylate downstream regulatory receptor by transferring phosphoryl group to Asp residue. This alters the transcription of downstream genes controlled by the regulatory receptor including AIP secretion pathway (Miller and Bassler, 2002;Sturme et al., 2002).

An example of this pathway is the Com system that regulates competence in *Streptococcus pneumoniae* using CSP (competence stimulating peptide). *S. pneumoniae* will first produce a 41-amino acid precursor peptide, ComC, then process it to produce the 17-amino acid peptide CSP (Havarstein et al., 1995;Pozzi et al., 1996). CSP is secreted through ComAB ABC transporter (Hui and Morrison, 1991;Hui et al., 1995). At HCD when CSP has accumulated in the environment, ComD sensor kinase will autophosphorylate and transfer the phosphoryl group to regulator ComE. Phosphorylated ComE activates the expression of *comX* gene which is a σ factor drives the expression of structural genes required for developing competence in *S. pneumoniae* (Lee and Morrison, 1999).

In *Staphylococcus aureus,* virulence in is regulated by two component Agr (accessory gene regulator) system. *S. aureus agrBDCA* operon encodes the elements

required for cell density dependent pathogenicity. AgrD is the 46-amino acid precursor peptide that is further processed by AgrB to from thiolactone intermediate then secreted (Ji et al., 1995;Ji et al., 1997). The AIP is cleaved and become its active from in supernatant. AgrC senses the accumulated AIP and starts the phosphorylation cascade that activates intracellular regulator, AgrA (Peng et al., 1988;Lina et al., 1998). AgrA regulates the transcription of RNAIII, a RNA molecule that regulates cell density dependent pathogenicity (Morfeldt et al., 1995;Koetje et al., 2003). Another common gut pathogen *Clostridium difficile*, also uses Agr system to sense AIP and further regulates the toxin synthesis (Darkoh et al., 2015;Martin-Verstraete et al., 2016).

Another Gram-positive bacteria AIP signaling pathway is the AIP self-signaling pathway. AIPs are synthesized and post-translationally modified then secreted through SacA dependent system. Unlike two-component system, which AIPs are detected by sensor kinase then further activates kinase activity, AIPs are transported into the bacteria through oligopeptide transporter system. *Bacillus subtilis* Phr (phosphate regulator) AIPs is one example. Phr precursor polypeptides has a secretion signal, it becomes the final peptide form after being secreted and cleaved by secreted proteases. The active Phr peptide is then transport back into the cell via ABC transporter family, Opp (oligopeptide

permease) (McQuade et al., 2001). Phr can inhibit Raps (regulator aspartate phosphatase), a phosphatase involved in phosphorylation pathway that regulates transcription of several genes, Phr then further alters downstream gene expression (Bischofs et al., 2009). Currently, AIPs are only known for intraspecies communication and regulation but could possess other biological functions such as antimicrobial properties of lantibiotic nisin peptide produced by *Lactococcus lactis* (Sturme et al., 2002) and potentially influence human tumor progression (De Spiegeleer et al., 2015;Wynendaele et al., 2015).

Gram-negative system

Some Gram-negative bacteria use diffusible molecule acyl-homoserine lactones (AHL) as the communication signal. Unlike AIPs, certain AHLs has been demonstrated to be secreted and sensed by different species of Gram-negative bacteria therefore AHLs can potentially act as interspecies communication signals.

The typical pathway is the LuxI/LuxR QS system that regulates bioluminescence found in the marine bacteria *Vibrio fischeri*. LuxI is responsible for the synthesis of AIs. LuxR protein contains two functional domains, an N-terminal ligand-binding domain,

and a C-terminal DNA-binding domain. As the concentration of autoinducers increases with the rise of the bacterial population, LuxR binds to autoinducers. The LuxR-autoinducer complex then activates the transcription of targeted genes. These AIs are species-specific, it has the core homoserine lactone ring structure plus various acyl tails that provides species specificity (Hawver et al., 2016).

Universal QS signal

This process also occurs between different species in both Gram-positive and Gram-negative bacteria. *Vibrio harveyi* was found to produce autoinducer 2 (AI-2, (2S,4S)-2-methyl-2,3,3,4-tetrahydroxytetrahydrofuran borate) (Higgins et al., 2007) by LuxS enzyme from 4,5-dihydroxy-2,3-pentanedione (DPD) and sensed through LuxP/Q signaling pathway. LuxS homologues are widespread among Gram-positive and Gram-negative bacteria (Pereira et al., 2013). Interestingly, there are different forms of active AI-2, one is identified in *V. harveyi*, a boron containing AI-2 molecule (Chen et al., 2002); in *Escherichia coli* and *Salmonella* spp., AI-2 is a non-borated cyclized DPD derivative (Miller et al., 2004).

Different from the LuxP/Q signaling pathway, *E. coli* and *Salmonella*

typhimurium sense AI-2 through *lsr* system. The *lsr* system was first found in *S. typhimurium* as an operon that includes eight genes (*lsrKRACDBFG*) (Taga et al., 2001). In the *lsr* operon, *lsrACDB* genes encodes the Lsr transporter located in the inner cell membrane. After AI-2 uptake, LsrK kinase will phosphorylate AI-2 in the cytoplasm. The phosphorylated AI-2 further regulates *lsr* operon expression by inactivating the repressor, LsrR (Taga et al., 2001;Taga et al., 2003). LsrR, located upstream of *lsr* operon, represses the expression of both *lsr* operon and itself by binding to the promoter (Xue et al., 2009). LsrF and LsrG are involved in processing the intracellular AI-2 molecule. LsrF is the terminal protein in the AI-2 processing pathway act as a thiolase that catalyzes the transfer of acetyl group from P-HPD (3-hydroxy-2,4-pentadione-5-phosphate, AI-2-phosphate isomer) to coenzyme A, forming dihydroxyacetone phosphate and acetyl-CoA(Marques et al., 2014). LsrG is involved in catalyzing the cleavage of P-DPD to produce 2-phosphoglycolic acid and possibly the first step to stop *lsr* operon expression (Xavier et al., 2007). Although Gram-negative bacteria also possess LuxS enzyme, the detection method is not clear.

Researchers have also discovered a AI-3 system that is independent of LuxS enzyme (Waters and Bassler, 2005). AI-3 molecules are mediated by threonine

dehydrogenase (Tdh) and aminoacyl-tRNA synthetases-related spontaneous cyclization to form pyrazinone family structure (Kim et al., 2020). AI-3 is sensed by QseC receptor found in both *E. coli* and *V. cholerae* (Moreira et al., 2010).

Another metabolite that have impact on bacterial behavior is indole. Host environmental conditions that regulates indole production and extracellular indole concentration can affects indole-producing and non-indole-producing bacteria activity in different ways (Lee and Lee, 2010). Indole molecule has been shown to activate succinate associated genes, spore or biofilm formation, drug resistance, virulence, as well as plasmid stability (Martino et al., 2003;Hirakawa et al., 2005).

Cross-kingdom communication

Direct signaling may also happen cross-kingdom between mammalian host and the pathogen. Some bacterial growth and virulence expression respond to mammalian stress hormones, including *E. coli* and other Gram-negative bacteria. For example, the neuroendocrine stress hormone norepinephrine is capable of stimulating the growth in cell number and the production growth stimulation signals (Lyte et al., 1996b;Freestone et al., 1999) in *E. coli*; addition of norepinephrine to growth media increased *E. coli*

O157:H7 growth rate by several log in 24 hours of growth period. In addition to growth, the production of toxin has also increased. With the supplementation of physiologically relevant concentration of norepinephrine *E. coli* O157:H7 toxin production increased by 100-160 fold during first 12 hours of culture time (Lyte et al., 1996a).Other than hormone produced by host, Bassler lab shown that mammalian epithelial cell from colon, lung, and cervical tissues are capable of producing AI-2 mimic that can be detected by bacterial AI-2 receptor, LuxP/LsrB in *V. harveyi* and *S. typhimurium*. When co-culturing *V. harveyi* AI-2 reporter strain with mammalian epithelial cells, the reporter strain showed 10-50 times more signal activity then hematopoietic origin cell. They also tested with *ΔluxS S. typhimurium* strain carrying an AI-2 inducible *lsr-luxCDABE* transcriptional reporter co-cultured with Caco-2 cells and observed a 100-fold more light production from the reporter. This indicates the host produce an AI-2 mimic that are capable of activate quorum-sensing regulated gene expression through LuxPQ system (Ismail et al., 2016) (Figure 1-1) (Cho et al., 2021).

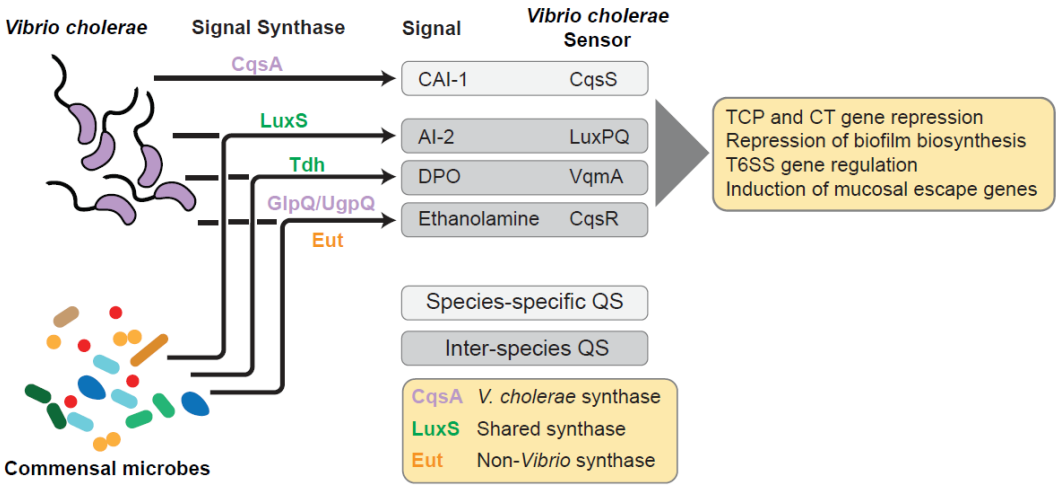

Figure 1-1. Production of small signaling molecules by the gut microbiome influences gene expression in *V. cholerae*.

Gut commensals are able to interface with *V. cholerae* gene regulation during infection through the production of autoinducer (AI) molecules associated with quorum sensing (QS). QS pathways can be species specific or inter-species, and numerous AI signaling molecule/sensor pairs have been described in *V. cholerae*. Broadly, QS activation by intra- and inter-species specific AI signaling in *V. cholerae* can lead to repression of virulence gene expression, and modulation of pathways associated with inter-bacterial competition (e.g., T6SS), and detachment from the mucosa. Thus, premature activation of QS by commensal microbes may disrupt the ability of *V. cholerae* to properly time virulence gene activation during early infection, and affect the outcome of infection *in vivo*.

Table 1-1 Summary of bacterial QS system

Pathway	Bacterial type	Signal	Signal sourse	Downstream effect	References
Intra species					
Com system	Gram-positive	CSP	*S. pneumoniae*	When CSP has accumulated activates the expression of structural genes required for developing competence in *S. pneumoniae*	Havarstein et al., 1995; Pozzi et al., 1996; Hui et al., 1991; Hui et al., 1995; Lee et al., 1999
Agr system	Gram-positive	AIP	*S. aureus*	AgrC sense the accumulated AIP activates the phosphorylation cascade that regulates cell density dependent pathogenicity	Ji et al., 1995; Koetje et al., 1995; Morfeldt et al., 1995; Ji et al., 1997; Lina et al., 1998; Peng et al., 1988
			C. difficile	Regulates the toxin synthesis	Martin-Verstraete et al., 2001; Darkoh et al., 2015
AIP self-signaling	Gram-positive	Phr AIPs	*Bacillus subtilis*	Inhibit Raps involved in phosphorylation pathway phosphorylation pathway and alter gene expression	McQuade et al., 2001; Bischofs et al., 2009
CqsS	Gram-negative	CAI-1	*Vibrios*	Binding of CAI-1 leads to downstream regulator LuxO dephosphorelate and repress *aphA* /upregulate *hapR*, inhibits virulence and biofilm biosynthetic gene expression	Miller et al., 2002; Zhu et al., 2002; Hammer et al., 2003; Shao et al., 2014
Inter species					
LuxP/Q	Gram-negative	AI-2	*V. cholerae*	Binding to AI-2 cause conformational change leads to dephsphorelation of LuxO and repress virulence and biofilm biosynthetic gene expression	Neiditch et al.,2005; Neiditch et al.,2006
CqsR	Gram-negative	Ethanolamine	Host	CrsR represses Qrr sRNA expression and increase *hapR* expression leads to inhibition of colonization in mouse small intestine	Jung et al., 2015; Watve et al., 2019; Watve et al., 2020
VqmA	Gram-negative	DPO	*V. cholerae*	When DPO bound, VqmA upregulates VqmR leads to downregulation of toxin and biofilm synthesis vps genes inhibits infection and virulence expression	Papenfort et al.,2017; Liu et al., 2006; Hai Wu et al., 2019
		Oxygen levels	Environment	Low oxygen level inhibits VqmA to from disulfide bond decrease VqmA activity leades to higher virulence expression	Mashruwala et al., 2020
		Bile salts	Host	Bile salts distrupts VqmA disulfide bound formation leades to increase of *tcpA* and biofilm-associated *vps* gene expression	Mashruwala et al., 2020
Cross-kingdom					
LuxP/Q, LsrB	Gram-negative	AI-2 mimic	Mammalian epithelial cells	The host produced AI-2 mimic can interact with *V. harveyi* LuxP/Q receptor and *S. typhimurium* Lsr system and interfere with bacteria QS regulation	Ismail et al., 2016
		Neuroendocrine stress hormone norepinephrine	Mammalian cells	The presense of norepinephrine in the media is capable of stimulating cellular proliferation and increase toxin production in *E. coli* O157:H7	Lyte et al., 1996; Freestone et al.,1999; Lyte et al.,1996

Vibrio cholerae

Vibrio cholerae is a comma-shaped, Gram-negative gastrointestinal pathogen which has caused cholera pandemics over the last two centuries. It has caused six major pandemics since 1817 and an ongoing seventh pandemics that started in 1961 and reached America in 1991. Cholera is still endemic in many countries lacking clean water sources, poor sanitation, and hygiene infrastructures, affecting millions of people and causing over 100,000 deaths yearly (ECDC, 2021). The most characteristic symptoms of cholera are vomiting and watery diarrhea which cause rapid fluid lose and leads to rapid dehydration, hypotensive shock, and, if untreated, death rate over 50% (Clemens et al., 2017). Although the treatment of oral rehydration can significantly reduce fatality rate, cholera continues to give rise to global health and economical issues (Mogasale et al., 2020) and requires better prevention and therapeutic strategies.

The bacterial strains of *V. cholerae* that cause cholera were discovered by Robert Koch in 1884 (Koch, 1884). While hundreds of serogroups have been identified, including pathogenic and non-pathogenic strains, current knowledge is that the pandemics were caused by only two serogroups, O1 and O139, and two biotypes, classical and El Tor (Finkelstein, 1996;Somboonwit et al., 2017). The spread of *V.*

cholerae from infected patients to other individuals can be through fecal contaminated water sources. Other than the fecal-oral route of infection, *V. cholerae* can also populate aquatic environments such as rivers, and coastal waters with zooplankton and other marine organisms as the natural reservoirs (Halpern et al., 2008). This allows toxigenic *V. cholerae* to spread through contamination of water and food sources into human host. Once infected, *V. cholerae* stars to colonize distal small intestine epithelial cells and produce cholera toxin (CT) and the toxin coregulated pilus (TCP) in response to environmental cues (Waldor and Mekalanos, 1996). TCP is essential for *V. cholerae* colonization of gut epithelial cell, while CT interacts with intestinal cells, leading to endocytosis of the toxin. CT activates G protein and leads to the continuous production of cyclic AMP (cAMP). High level of cAMP causes dramatic efflux of ions and water from infected enterocytes, leading to watery diarrhea releasing the pathogen back into the environment to start the next infectious cycle (Sack et al., 2004).

Cholera effects on the gut microbiome

Until recently, the impact of cholera on the human gut microbiome was much better

understood than the role of the gut microbiome on *V. cholerae* infection outcomes. The profuse watery diarrhea associated with cholera has long been associated with changes in commensal microbial populations; culture-dependent studies have shown that cholera leads to a multi-log reduction in non-*Vibrio* bacteria during acute diarrhea compared to convalescent populations (Gorbach et al., 1970). Recent studies by Hsiao et al. using deep sequencing of fecal 16S ribosomal RNA gene amplicons examined the fecal microbiomes of adult cholera patients in Bangladesh from clinical presentation to 3 months convalescence after the end of diarrhea (Hsiao et al., 2014). In concordance with culturing studies, the diversity of the gut microbiome during cholera dropped dramatically during acute disease, becoming overwhelmingly dominated by streptococci, enterococci, and Proteobacteria. Species more characteristic of healthy human gut microbiomes were detected as very low abundance reservoirs during disease, but over the course of convalescence expanded to re-establish the gut in a manner similar to microbial succession, the ordered process of microbial colonization seen from infancy. Several other culture-independent studies have demonstrated that this transient dysbiosis in microbiome structure seen in cholera can also be caused by malnutrition (Subramanian et al., 2014), and diarrhea of multiple etiologies including rotavirus and pathogenic

Escherichia coli infection (David et al., 2015;Kieser et al., 2018). These environmental insults can be common in cholera-endemic areas and thus potentially drive a reinforcing cycle of microbiome-dependent vulnerability to infection.

In addition to causing diarrhea that disrupt native gut microbial communities, *V. cholerae* can also directly compete with commensals through the use of contact-dependent killing via the T6SS (Ho et al., 2014;Russell et al., 2014). T6SS delivers toxin to 'prey' cells by puncturing the bacterial membrane using a spike and tube structure that also shares functional homology with the T4 bacteriophage, while T6SS-encoding cells are protected via the production of cognate immune proteins (Leiman et al., 2009;Pell et al., 2009;Dong et al., 2013;Fu et al., 2013). *In vitro*, *V. cholerae* is capable of reducing *S. typhimurium* and *E. coli* survival up to 10^5 fold using T6SS (MacIntyre et al., 2010). *In vivo*, mutations in T6SS have driven colonization defects compared to wild-type in suckling mice (Fu et al., 2013;Alavi et al., 2020), infant rabbits (Fu et al., 2013), and *Drosophila* (Fast et al., 2018). Zhao et al. showed that *V. cholerae* was able to directly attack host commensal *E. coli* in the suckling mouse model of infection; commensal *E. coli* load was lowered by ~300 fold in the wild-type group compared to a *vipA*$^-$ T6SS mutant (Zhao et al., 2018). Interestingly, T6SS-mediated killing of *E. coli* led to

additional upregulation of *tcp* and *ctx* virulence genes during infection compared to mice lacking T6SS target microbes via an as-yet undefined mechanism. Separately from contact-dependent T6SS killing, *V. cholerae* can also use T6SS to increase host gut contractility to expel resident bacterial species, for example the expulsion of *Aeromonas veronii* in a zebrafish colonization model (Logan et al., 2018). Taken together, these findings suggest that *in vivo* T6SS interactions with the microbiota plays a complex role in inter-bacterial competition during infection and driving *V. cholerae* fitness in the gut.

Commensal microbes and *V. cholerae* virulence regulation during infection

V. cholerae is a native organism of aquatic environments such as brackish water and estuaries, often complexed with marine organisms such as zooplankton (Colwell et al., 1977;Huq et al., 1983;Tamplin et al., 1990;Colwell and Huq, 1994). In the aquatic reservoir, *V. cholerae* is often found within biofilms that enable attachment to nutritive substrates such as plankton exoskeletons (Huq et al., 1983;Tamplin et al., 1990). These biofilm structures also represent an important host infection mechanism (Watnick and Kolter, 1999) as biofilm-associated *V. cholerae* are much more acid-tolerant than

planktonic cells, which is essential for passage through the stomach acid barrier at the beginning of human infection (Zhu and Mekalanos, 2003). Upon transition into the gut, *V. cholerae* undergoes a carefully orchestrated set of gene expression changes in order to adapt to host-specific environmental stresses and cause disease. This transcriptional program is triggered by a series of environmental signals such as temperature, osmolarity, oxygen concentration, and exposure to host-specific molecules such as bile acids, and leads to the activation of a number of virulence factors critical to colonization, persistence, and pathology (Figure 1-2) (Cho et al., 2021). The two major virulence determinants of *V. cholerae* are Cholera Toxin (CT), which is responsible for the characteristic diarrhea of cholera, and the Toxin-Coregulated Pilus (TCP), which is required for colonization of the intestinal mucosa in both humans and mice (Miller et al., 1987;Herrington et al., 1988). CT is encoded by the *ctxAB* genes on the lysogenic CTXΦ bacteriophage (Waldor and Mekalanos, 1996), and TCP serves both as the receptor for CTXΦ (Shaw and Taylor, 1990;Waldor and Mekalanos, 1996) and in microcolony formation at the intestinal epithelium (Kirn et al., 2000). TCP biosynthetic genes, including that of the primary structural subunit TcpA and accessory colonization factor (*acf*) genes and several transcriptional activators of virulence gene production, are found

on a 40-kb *Vibrio* pathogenicity island (Karaolis et al., 1998). Both *ctxAB* and *tcpA* are activated by the activity of the AraC/XylS-family transcriptional regulator ToxT (DiRita and Mekalanos, 1991;Higgins et al., 1992;Gallegos et al., 1997;Martin and Rosner, 2001). which binds to a degenerate 13-bp DNA sequence known as the 'toxbox' in target promoters (Matson et al., 2007). Several factors comprise a complex regulatory path to ToxT expression. ToxR was the first identified positive regulator of *V. cholerae* virulence (Skorupski and Taylor, 1997), and together with the regulator TcpP activates transcription of *toxT* (Higgins and DiRita, 1994;Hase and Mekalanos, 1998;Childers and Klose, 2007). The expression of *tcpP* is in turn regulated by the transcriptional regulators AphA and AphB, which cooperatively bind to the *tcpP* promoter, while AphB is able to enhance the *toxR* transcription (Xu et al., 2010).

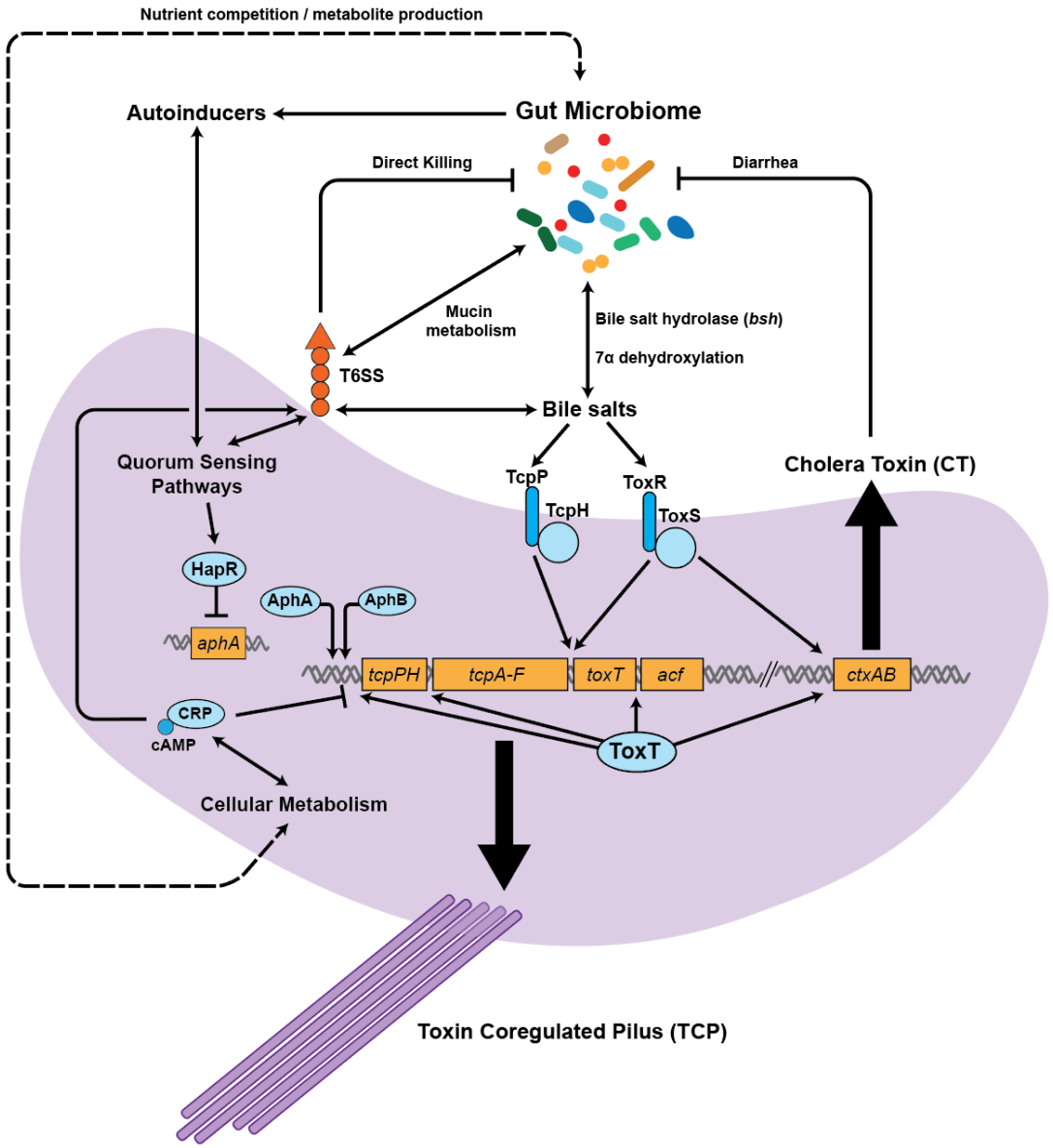

Figure 1-2. Virulence gene expression, including that of the key virulence factors cholera toxin (CT) and the toxin coregulated pilus (TCP), can be influenced by numerous pathways controlled by gut commensals.

The gut microbiome is able to produce or modulate several molecular factors leading to changes in *V. cholerae* virulence gene expression, including the production of quorum sensing autoinducers, the metabolism of bile molecules and host environmental nutrients such as mucin.

Gut microbiome effects *V. cholerae* pathogenesis through QS

In *V. cholerae*, QS is capable of repressing the expression of virulence- and biofilm-associated genes at high cell density (HCD). While at low cell density (LCD), such as during early infection, QS is inactive and virulence gene and biofilm biosynthetic gene expression is active. At LCD, the *V. cholerae* QS regulatory system acts to phosphorylate the regulator LuxO via a phosphorelay protein LuxU (Freeman and Bassler, 1999b;a). Phospho-LuxO is then able to activate the expression of a set of small non-coding regulatory RNAs, Qrr1-4 (quorum regulatory RNAs) (Lenz et al., 2004) that employ a number of mechanisms to suppress QS gene activation, including the *hapR* gene encoding the master QS regulator HapR, and activate production of the virulence activator AphA (Feng et al., 2015). At HCD, when autoinducer concentrations are high, LuxO becomes de-phosphorylated and Qrrs are not produced, allowing for the expression of HapR. HapR is then able to repress virulence gene expression, via direct repression of *aphA*, as well as the expression of biofilm biosynthetic genes (Lenz et al., 2004;Rutherford et al., 2011;Jung et al., 2016).

V. cholerae cells are able to produce a set of AI signals that integrate with LuxO as well as other gene regulatory pathways (Jung et al., 2015;Papenfort et al., 2017). The

V. cholerae AI molecule CAI-1 ((S)-3-hydroxytridecan-4-one) (Higgins et al., 2007;Wei et al., 2011) is synthesized by the enzyme CqsA (Kelly et al., 2009). While long thought to be specific to *Vibrio*s, recent work has demonstrated that pathogenic *E. coli* are also able to sense this autoinducer (Gorelik et al., 2019). CAI-1 levels are monitored by the membrane-bound histidine kinase sensor CqsS (Miller et al., 2002), which acts as a kinase at low cell- and AI-density, auto phosphorylating and transferring this phosphate to LuxU and thence to the regulator LuxO, leading to Qrr sRNA expression and the upregulation of *aphA* and repression of *hapR.* At high cell density and thus high CAI-1 concentrations, CAI-1 binds to CqsS converting it from kinase to phosphatase activity, leading to the dephosphorylation of LuxO (Freeman and Bassler, 1999b;Boyaci et al., 2016). The resulting loss of Qrr sRNA expression leads to the repression of *aphA* and thus virulence gene expression, as well as the repression of biofilm formation via the activity of HapR (Miller et al., 2002;Zhu et al., 2002;Hammer and Bassler, 2003;Shao and Bassler, 2014).

Several other autoinducers produced and sensed by *V. cholerae* are inter-species in nature and thus potentially active during infection of host compartments bearing complex microbial communities. One inter-species autoinducer that is broadly distributed

amongst gut microbes and that plays a role in virulence gene regulation in *V. cholerae* is autoinducer 2 (AI-2), synthesized by the enzyme LuxS from 4,5-dihydroxy-2,3-pentanedione (DPD). Homologs of *luxS* are found in *V. cholerae* (*VC0557*) as well as the genomes of more than 500 Gram-positive and Gram-negative bacterial species (Pereira et al., 2013). In *V. cholerae*, AI-2 is sensed through the LuxP/Q signaling pathway (Neiditch et al., 2005). LuxP is located in the periplasm and forms a heterotetramer when joined with LuxQ. At LCD when AI-2 is not bound, LuxQ acts as a kinase and auto-phosphorylates the cytoplasmic domains, leading to the phosphorylation of LuxU and then LuxO. At HCD, the binding of AI-2 facilitates a conformational change, breaking the symmetry of the LuxPQ heterotetramer, thus, interrupting the phosphorylation cascade and leading to repression of virulence factor expression (Neiditch et al., 2006). Several different active structures of AI-2 have been identified. In *Vibrio*s, AI-2s are produced as a furanosyl borate diester compound ((2S,4S)-2-methyl-2,3,3,4-tetrahydroxytetrahydrofuran borate) (Chen et al., 2002;Higgins et al., 2007), in contrast to the cyclized but non-borated DPD derivative found in *E. coli* and *Salmonella* spp. (Miller et al., 2004). The interspecies nature of these AI-2 molecules is highlighted by bacteria that lack *luxS*, for example *Pseudomonas aeruginosa*, is still capable of detecting AI-2

produced by other bacterial species and accordingly altering gene expression (Duan et al., 2003). In contrast, *V. cholerae* cells are able to produce their own AI-2 and sense other AI-2 forms. This was shown using cell-free supernatants of AI-2 producing *E. coli* that are able to induce gene expression changes in *Vibrio* spp. (Xavier and Bassler, 2005a).

In addition to the CAI-1/AI-2 QS pathways acting through LuxO/HapR described above, several novel signaling molecules and QS receptors have recently been identified. The intestinal metabolite ethanolamine has been shown to regulate *hapR* expression through the regulator CqsR (Jung et al., 2015;Watve et al., 2019;Watve et al., 2020). Ethanolamine is sensed by the CqsR periplasmic CACHE ligand binding domain with high specificity, and addition of ethanolamine repressed Qrr sRNA expression and increased *hapR* expression leading to inhibition of colonization of the mouse small intestine (Watve et al., 2019). Levels of ethanolamine may be controlled and sensed by numerous bacterial pathways. For instance, in pathogens such as enterohaemorrhagic *E. coli* (EHEC), ethanolamine has been shown to increase virulence gene expression (Kendall et al., 2012). Similarly, ethanolamine metabolism and Type III secretion system is regulated by environmental ethanolamine levels in *Salmonella* (Anderson et al., 2015;Anderson and Kendall, 2016), and other common gut pathogens such as

Enterococcus faecalis (Kaval and Garsin, 2018) and *Clostridioides difficile* (Nawrocki et al., 2018) also exhibit ethanolamine-dependent gene regulation. Papenfort et al. demonstrated that 3,5-dimethylpyrazin-2-ol (DPO) acts as a QS signaling molecule in *V. cholerae* (Papenfort et al., 2017). DPO is synthesized from threonine and alanine by the enzyme threonine dehydrogenase (Tdh); threonine metabolism is commonly observed in several intestinal microbes including *E. coli* (Ma and Ma, 2019). DPO is able to bind to the LuxR family transcriptional regulator VqmA, and in so doing leads to the increase in the transcription of the small regulatory RNA VqmR, leading to the downregulation of accessory toxin genes and the *vps* genes involved in biofilm synthesis. Expression of VqmA was previously shown to be deleterious to *V. cholerae* infection and virulence expression via direct activation of HapR without modification of DPO synthesis (Liu et al., 2006).

Recently, Hai Wu et al. have solved the crystal structure of the VqmA-DPO-DNA complex, demonstrating a direct interaction between DPO and the PAS ligand binding domain of VqmA, and speculated that DPO and DNA binding may stabilize VqmA (Wu et al., 2019a). In another study, they observed conformational differences when VqmA is not bound to the target promoter DNA, leading to a possible AI-dependent regulation

differential mechanism (Wu et al., 2019b). Additional work by Mashruwala et al. suggested VqmA activity is related to cell density, environmental oxygen levels, and host produced bile (Mashruwala and Bassler, 2020). In the microaerophilic gut environment, CAI-1 and AI-2 production increased, and VqmA was shown to form disulfide bonds leading to increased transcriptional activity. The presence of bile salts disrupted these disulfide bonds, leading to an observed increase of *tcpA* and biofilm-associated *vps* gene expression. The inter-species nature of DPO and VqmA in the gut is highlighted by recent studies showing that a *Vibrio parahemolyticus*-bacteriophage-encoded VqmA is able to respond to DPO in the gut and mediates cell lysis by activating expression of the phage gene *qtip*. Qtip sequesters the phage cl repressor and leading to the observed bacterial host lysis (Silpe and Bassler, 2019).

The diversity of interspecies signaling molecules produced by commensal microorganisms underlines the complexity of the QS environment of the gut during infection. Several studies have examined the ability of targeted manipulation of QS to affect both gut microbiome structure and outcomes of *V. cholerae* colonization and infection. Experiments conducted by Thompson et al. show that by modifying the Lsr AI-2 transport pathway, transgenic *E. coli* could alter intestinal AI-2 levels in antibiotic-

treated mice, leading to an AI-2 dependent difference in relative abundance between two major bacterial phyla of gut commensals, the Bacteroidetes and Firmicutes (Thompson et al., 2015;Thompson et al., 2016). Duan et al. employed *E. coli* Nissle 1917 as a carrier to express CAI-1 via expression of *cqsA* (Duan and March, 2010). They found that pretreating suckling mice with CAI-1-producing *E. coli* for 8 hours could increase mouse survival by over 90% upon infection with *V. cholerae*, and that co-ingestion of CAI-1-producing *E. coli* and *V. cholerae* resulted in a 25% increase in survival rate post-infection.

QS-mediated interference in *V. cholerae* pathogenesis is not restricted to artificial manipulation. Studies have shown that the common human gut commensal *Blautia obeum* (previously classified as *Ruminococcus obeum*) encodes a functional AI-2 synthase *luxS* that drives reduced *tcpA* expression in *V. cholerae* and mediates microbiome-mediated resistance to infection (Hsiao et al., 2014). In germfree mice inoculated with both *B. obeum* and *V. cholerae*, expression of *luxS* in *B. obeum* increased and *V. cholerae* colonization was ablated. Targeted removal of *B. obeum* from defined microbial communities established in germfree animals dramatically reduced the ability of these microbial assemblages to resist invasion by *V. cholerae*, and transgenic

expression of the *B. obeum luxS* in AI-2-*E. coli* was sufficient to restrict *V. cholerae* colonization in gnotobiotic mice. This signaling was independent of the canonical LuxP AI-2 sensor system; deletion of *luxP* did not rescue the ability of *V. cholerae* to colonize when *B. obeum* was present in the gut. However, expression of *vqmA* was increased during infection in response to *B. obeum*, and *V. cholerae* lacking *vqmA* showed improved colonization in the presence of *B. obeum* compared to wild-type pathogen. Interestingly, *hapR* expression did not seem to respond strongly to increased *vqmA*. Taken together with findings of DPO interaction, these data suggest that this multi-functional AI-sensor/regulator may respond to several QS signaling pathways with different regulatory targets. The dispensability of LuxP to signaling with *B. obeum* AI-2 also suggests that there may be substantial un-characterized diversity in the structure and function of these inter-species autoinducers.

These recent advances in studying cross-species QS signaling in the gut, and the ability of these pathways to interfere with key *V. cholerae* infectious processes such as TCP biogenesis and biofilm production suggest that further characterization of QS in the microbiome may yield novel clinical therapeutic and prophylactic targets for cholera management.

Microbiome-driven modification of the gut chemical environment controls *V. cholerae* gene expression

In addition to QS systems, the action of commensal microbes can affect the levels and function of several other components used by *V. cholerae* to appropriately time virulence gene activity in the gut. One of these major virulence-regulatory components is bile, a digestive secretion that aids in emulsification and solubilization of dietary lipids. Bile is a complex mixture of compounds comprising bile acids, cholesterol, phospholipids, and immunoglobulins (Hofmann, 1999). The synthesis of the predominant bile component, bile acids, occurs in the liver from cholesterol, often in amino-acid conjugated forms containing taurine and glycine. Bile is stored in the gall bladder and secreted into the small intestine in response to food intake. The local pH of the intestine means that bile acids are often found as primary bile salts, and can be further modified by the action of gut bacteria into secondary forms (Ridlon et al., 2006;Jones et al., 2008;Song et al., 2019). Up to 95% of secreted bile acids are reabsorbed within the distal ileum and passed via portal circulation back to the liver to be re-conjugated to amino acids and re-secreted (Dawson and Karpen, 2015;Di Ciaula et al., 2017).

The detergent nature of bile salts and the activities of the various other bile components can have potent bacteriostatic activity, affecting membrane stability and cellular homeostasis; pathogenic and commensal gut microbes have evolved mechanisms to survive and exploit this gut-specific component (Begley et al., 2005). *V. cholerae* bile resistance is mediated by the action of efflux pumps and outer membrane porins in bile salt accessibility to the cell (Provenzano and Klose, 2000;Simonet et al., 2003;Bina et al., 2008;Cerda-Maira et al., 2008). Since bile secretion and re-absorption predominantly occurs in the small intestine, the favored site *of V. cholerae* colonization, this pathogen has evolved mechanisms to take advantage of this intestinal-specific signal in order to time expression of virulence genes (Figure 1-3) (Cho et al., 2021). A set of primary bile salts (e.g., taurocholate, glychocholate) has been shown to activate expression of virulence genes by affecting the structure and function of several key transcriptional regulators of virulence. Taurocholate has been shown to increase TcpP activity by promoting the formation of intermolecular disulfide bond formation and dimerization under microaerophilic/reducing conditions (Yang et al., 2013), and bile salt-induced TcpP-TcpP interactions are further enhanced by the presence of calcium (Hay et al., 2017). Bile salts have also been shown to modulate ToxR activity by preventing

proteolysis of ToxR and promoting formation of ToxRS complexes (Lembke et al., 2018;Lembke et al., 2020). Taurocholate has also been shown to promote detachment from biofilm structures, enabling *V. cholerae* to colonize mucosal surfaces after passage through the gastric acid barrier (Hay and Zhu, 2015). The heterogenous nature of bile means that other bile components have been shown to drive variable effects on *V. cholerae* virulence. For example, unsaturated fatty acids in bile and crude bile can inhibit the transcriptional activity of ToxT (Lowden et al., 2010), and a mixture of bile salts can also reduce the ability of VqmA to mediate QS-dependent repression regulation of biofilm and virulence (Mashruwala and Bassler, 2020).

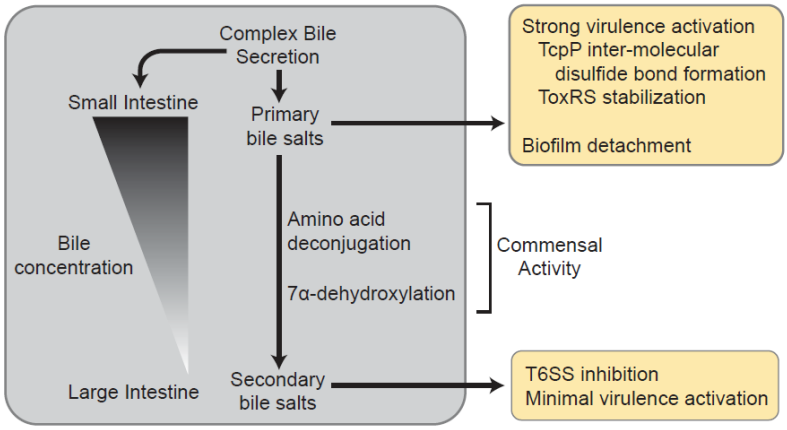

Figure 1-3. Gut microbe bile salt hydrolase changes gut bile composition influences gene expression in *V. cholerae*.

The gut microbiome is able to dramatically shape the composition of the bile salts within the preferred site of *V. cholerae* colonization, the distal small intestine. Bile components can be bacteriostatic but also act as a key signal for microbes in the small intestine, and numerous microbes adapted to this environment have enzymatic pathways that alter the structure and activity of bile salts. In *V. cholerae*, primary bile salts promote strong virulence gene activation through interaction with the TcpPH and ToxRS upstream regulatory complexes, and also promotes detachment from biofilms to allow for spread to host tissues. Commensal activity processes primary bile salts to secondary forms, leading to decreased virulence gene activation *in vivo* and inhibition of type VI secretion activity (T6SS).

One key mechanism for commensal gut microbes to control the bacteriostatic activity of bile is the expression of bile salt hydrolase (*bsh*) enzymes, which mediate the hydrolysis of amino-acid conjugated bile salts and reduces the detergent-like effects of bile and increase bile salt resistance (De Smet et al., 1995;Grill et al., 2000;Chand et al., 2017). The importance of microbial activity in modulating bile composition in the gut can

be seen in germfree mice, where essentially all bile acids in the small intestine are amino acid conjugated, in contrast to conventionally-reared animals (Sayin et al., 2013). Bioinformatics analyses show that BSH is broadly distributed among members of the human gut microbiota, and can be classed into several broad phylotypes that differ in substrate specificity and activity (Song et al., 2019). Thus, the presence and expression of different microbial enzymes can have dramatic effects on the bile acid pool of the intestines, with consequent differential effects on *V. cholerae* gene regulation and responses in these different microbiome contexts.

Recent work by Alavi et al. has demonstrated that the *bsh* activity of the *V. cholerae*-restricting commensal microbe *B. obeum* is able to contribute to *V. cholerae* infection outcomes (Alavi et al., 2020). This work demonstrated that *B. obeum* encodes a *bsh* with high activity against the key virulence-activating factor taurocholate. The presence and activity of *bsh* was shown to be higher in healthy human gut microbiomes *in vitro*, and the fecal metagenomes of healthy Bangladeshi adults were also characterized by higher levels of *bsh* compared to *V. cholerae*-susceptible dysbiotic microbiomes. They demonstrated that this enzymatic activity was able to ablate the induction of *tcpA* expression in response to intestinal tissues through depletion of taurocholate levels, and

that *in vivo*, the presence of *B. obeum bsh* activity was associated with lower *tcpA* expression and *V. cholerae* colonization. These effects were independent of AI-2, as this commensal-encoded enzyme was able to ablate *tcpA* activation by intestinal tissues even when these tissues were boiled to remove AI-2. Expression of *B. obeum bsh* by a natively *bsh*$^{-}$ *luxS*$^{-}$ *E. coli* was also able to significantly reduce *V. cholerae* colonization in suckling mice. These data suggest that differential capacity for bile metabolism by commensal microbes is a key driver of individual- and microbiome-specific differences in *V. cholerae* infection outcome and may serve as a recurrent window of vulnerability to infection by *V. cholerae*.

A combination of microbiota-driven effects on chemical signals in the gut may also be important for the regulation of T6SS-mediated pathogen-commensal competition. Several studies have demonstrated a link between QS and regulation of T6SS; HapR directly regulates T6SS genes (Zheng et al., 2010) and indirectly through the action of QstR (Watve et al., 2015), and QS sRNAs can repress T6SS-related gene expression (Shao and Bassler, 2014). T6SS regulation is also affected by several processes that intersect with the functions of the microbiota. Bile acids are also able to regulate T6SS gene expression, with deoxycholic acid, a secondary bile acid generated via microbial 7-

α-dehydroxylation of cholic acid, shown to inhibit assembly of the T6SS apparatus (Bachmann et al., 2015). Components of mucus, the protective glycoprotein coat at the intestinal mucosa, are able to de-repress T6SS gene expression (Bachmann et al., 2015). Since numerous commensal microbes have been shown to metabolize mucus in the gut environment, and the role of microbes in bile metabolism has been intensively investigated, complex microbiota-driven mechanisms may thus serve as triggers for the control of inter-microbial killing mechanisms during infection.

Chapter 2.1 Microbiota-Associated Biofilm Regulation Leads to *Vibrio cholerae* Resistance Against Intestinal Environmental Stress

Jennifer Y. Cho[1,2], Rui Liu[1,3], Ansel Hsiao[1,4,*]

Affiliations:

[1]Department of Microbiology and Plant Pathology, University of California, Riverside, Riverside, CA 92521, USA.

[2]Department of Biochemistry, University of California, Riverside, California, USA

[3]Graduate Program in Genetics, Genomics, and Bioinformatics, University of California, Riverside, California, USA

[4]Lead Contact

[*]Correspondence: ansel.hsiao@ucr.edu

Abstract

The commensal microbes of the gut microbiota make important contributions to host defense against gastrointestinal pathogens, including *Vibrio cholerae*, the etiologic agent of cholera. As inter-individual microbiota variation drives individual differences in

infection susceptibility, we examined both host and *V. cholerae* gene expression during infection of suckling mice transplanted with different model human commensal communities, including an infection-susceptible configuration representing communities damaged by recurrent diarrhea and malnutrition in cholera endemic areas, and a representative infection-resistant microbiota characteristic of healthy individuals. In comparison to colonization of animals with resistant microbiota, animals bearing susceptible microbiota challenged with *V. cholerae* downregulate genes associated with generation of reactive oxygen/nitrogen stress, while *V. cholerae* in these animals upregulates biofilm-associated genes. We show that *V. cholerae* in susceptible microbe infection contexts are more resistant to oxidative stress and inhibitory bile metabolites generated by the action of commensal microbes, and that both phenotypes are dependent on biofilm-associated genes, including *vpsL*. We also show that susceptible and infection-resistant microbes drive different bile acid compositions *in vivo* by the action of bile salt hydrolase enzymes. Taken together, these findings provide a better understanding of how the microbiota uses multiple mechanisms to modulate the infection-associated host environment encountered by *V. cholerae*, leading to commensal-dependent differences in infection susceptibility.

Keywords: biofilm, *Vibrio cholerae*, pathogenesis, microbiota, bile acids, reactive oxygen species

Introduction

In the transition from the aquatic reservoir into the human gastrointestinal tract, *Vibrio cholerae* encounters multiple host defense mechanisms, including low pH, oxidative stress, and bile acids (Louis and O'Byrne, 2010). Growing evidence indicates that the resident community of gut microbes, the gut microbiota, is also an essential factor affecting host susceptibility to *V. cholerae* infection, using multiple mechanisms to modulate pathogen fitness and gene expression during infection (Hsiao et al., 2014;Alavi et al., 2020;Cho et al., 2021). The gut microbiota is highly complex and varies dramatically between individuals, leading to individual-specific effects on *V. cholerae* susceptibility driven partially by community-specific effects on *V. cholerae* behavior during infection (Hsiao et al., 2014;Alavi et al., 2020). In cholera-endemic areas, environmental insults such as malnutrition and diarrhea of multiple etiologies drive some

individuals' gut communities to recurring damaged or dysbiotic states that are unable to resist the colonization of *V. cholerae* (Hsiao et al., 2014;David et al., 2015;Alavi et al., 2020). Commensal microbes are able to modulate *V. cholerae* fitness and behavior during infection through numerous mechanisms including quorum sensing regulation of virulence genes (Hsiao et al., 2014) and direct competition via type VI secretion system (T6SS) (Zhao et al., 2018). In addition to direct competition and modulating *V. cholerae* transcription during infection, the gut microbiota is also able to broadly modulate gut environmental conditions, such as through manipulation of oxidative conditions as well as host metabolites such as bile. Both of these factors are active during *V. cholerae* infection; transcriptomic studies of cholera patients reveal an increase in expression of host enzymes responsible for oxidative stress (Ellis et al., 2015;Bourque et al., 2018), and microbiota-dependent modulation of bile acid levels has been shown to affect *V. cholerae* virulence gene expression (Alavi et al., 2020).

A key adaptation of *V. cholerae* to environmental stresses is the ability to form biofilms, which in addition to protecting against acid, predation in the aquatic reservoir, and bacteriostatic molecules in the host gut such as bile, also modulates *V. cholerae* infectivity and epidemic spread (Zhu and Mekalanos, 2003;Matz et al., 2005;Hung et al.,

2006;Hay and Zhu, 2015). Here, we show using model human microbiota compositions that commensals are able to differentially affect *V. cholerae* fitness by modulating the expression of biofilm-associated genes in *V. cholerae*. This process intersects with microbiota-specific manipulation of gut redox conditions and bile acid composition that both inhibit *V. cholerae* fitness in a biofilm-dependent fashion. Our findings suggest that the composition and biochemical functions of the gut microbiota are able to use reinforcing mechanisms, leading to commensal-dependent infection-permissive and restrictive conditions in the mammalian gastrointestinal tract.

Methods

Bacterial strains and culture condition

All *V. cholerae* strains were derived from the C6706 O1 El Tor pandemic strain and grown in LB liquid media with appropriate antibiotics at 37℃ with agitation. All anaerobic strains were grown in LYHBHI liquid media (BHI supplemented to 5g/L yeast extract, 5mg/L hemin, 1mg/mL cellobiose, 1mg/mL maltose, and 0.5mg/mL cysteine-HCl) at 37℃ in a Coy chamber under anaerobic conditions (5% H_2, 20% CO_2, balance

N_2) (Alavi et al., 2020). All anaerobic strains used in animal experiments were grown for 48 hours, then 1:100 subcultured into fresh media and grown an additional 48 hours prior to gavage. *vpsL* mutants were constructed using natural transformation based on the published method (Dalia et al., 2014). Approximately 3 kb *vpsL* upstream (forward primer: 5' - GTTAAGAGCACCGATTGCAC - 3', reverse primer: 5' - GTCGACGGATCCCCGGAATCTTCATCACTAGACGCTCCTAAC - 3') and downstream (forward primer: 5' - GAAGCAGCTCCAGCCTACAGCGTATTAAGACAGGGCACTTG - 3', reverse primer: 5' - GCATTTTTTACCGTCAGGGTC - 3') sequence was amplified and added to ends of a trimethoprim resistance (Tm^R) cassettes amplified from SAD530 using primers ABD123 (5' - ATTCCGGGGATCCGTCGAC - 3') and ABD124 (5' - TGTAGGCTGGAGCTGCTTC - 3') by overlapping PCR using Phusion High-Fidelity PCR Master Mix (ThermoFisher scientific). First round of PCR consisted of equimolar *vpsL* upstream fragment, *vpsL* downstream fragment, and Tm^R cassette amplicons with cycle condition of 98℃ for 30 seconds, followed by 15 cycles (94℃ for 10 seconds, 50℃ for 30 seconds, 72℃ for 4 minutes), and 72℃ for 10 minutes. *vpsL* upstream forward primer and downstream reverse primer were added to the PCR reaction and then

continued using cycle conditions as described above. The final PCR product was added to 0.45ml of instant ocean sea salts solution (7mg/ml) with chitin-induced *V. cholerae* and incubated for 16-24 hours at 30℃ stationary, allowing natural competence. 0.5ml LB was then added, and the mixture was incubated for 2-3 hours at 30℃ with agitation. The final mixture was then plated on LB agar plate with 10μg/ml trimethoprim for overnight incubation at 30℃ to select for transformants. The final picked mutants were checked by Sanger sequencing.

Animal experiments

Specific pathogen free (SPF) CD-1 suckling animals were purchased from Charles River Laboratories. Upon receipt, suckling mice were fasted, and an equivalent of about 1mg/g body weight streptomycin was gavaged with 30-gauge plastic tubing. Pups were then placed with a lactating dam for one day before being inoculated with communities and *V. cholerae*. Human gut bacterial strains were prepared by taking a total 300μl of OD_{600} = 0.4 equivalent culture per animal divided evenly across constituent commensal strains. Appropriate amounts of anaerobic strain culture were pooled and pelleted by centrifugation, and resuspended in 25μl of fresh LYHBHI per animal. Mice then received

25µl of the community mixture and 25µl of *V. cholerae* ($1x10^4$-$1x10^5$ CFU) in PBS (Alavi et al., 2020). 4-day old suckling CD-1 mice were fasted for 1.5 hours prior to all gavages. 18 hours after infection, pups were sacrificed, intestinal tissue was homogenized in 5ml of PBS and *V. cholerae* plated on streptomycin LB-agar plate for enumeration and fitness assays. For RNA assays, 1ml of intestinal homogenate from each infected pup was centrifuged at 14000 rpm, the supernatant was removed, and the pellet resuspended in 500µl of TRIzol (Ambion) at -80℃.

Quantitative PCR analysis of model microbiome

DNA was extracted from intestinal homogenate and used as template for model strain detection by quantitative PCR. 500µl of intestinal homogenate was mixed with 210µl of 20% SDS, 500 µL phenol:chloroform:isoamyl-alcohol (24:24:1, Fisher Scientific) and 500µl of 0.1mm Zirconia beads (BioSpec). The mixture was then lysed with bead beater at 2,400 RPM for 3 minutes. The qPCR assay to detect model strain were performed using a universal 16S rRNA gene primer set to detect total bacterial load (forward primer: 5' – GTGSTGCAYGGYTGTCGTCA – 3', reverse primer: 5' – ACGTCRTCCMCACCTTCCTC – 3') (Horz et al., 2005). Each reaction was done in

triplicates with 12.5µl of iQ SYBR Green Supermix (BIO-RAD2), 1µl of 10µM forward and reverse primers, 5.5µl nuclease free water and 5µl of extracted DNA (200 ng/µl).

RNA extraction, RNA-Seq library prep, and sequencing

Total RNA was extracted using TRIzol according to manufacturer instructions. DNA was degraded using Baseline-ZERO DNase (Lucigen), and the samples were then treated with TRIzol again for purification. Sequencing library were prepared using the Ovation Mouse RNA-Seq system with addition of *V. cholerae* enrichment primers (NuGEN). Final libraries were checked using an Agilent Bioanalyzer, and a 75 bp single read sequencing was performed on Illumina NextSeq500.

RNA-Seq analysis

All RNA-Seq sequenced libraries were trimmed using Trimmomatic v0.39 (Bolger et al., 2014) and reads were aligned to mouse and *V. cholerae* genomes, using HISAT2 version 2.1.0 (Kim et al., 2015) with reference genomes GCF_000001635.26_GRCm38.p6 and GCF_000006745.1_ASM674v1. HTSeq (Anders et al., 2015) was used to calculate raw counts. After rRNA and tRNA were removed, differential expression analysis was

conducted using edgeR (Robinson et al., 2009;McCarthy et al., 2012). Statistical analysis and visualization of *V. cholerae* pathway profiles were performed using package clusterProfiler (Yu et al., 2012;Wu et al., 2021) in R with the selected database KEGG, and genes with FDR<0.05 and FC>1 or FC<-1 used for further analyses.

Measurement of H_2O_2 levels in colonized intestines

Intestinal homogenates H_2O_2 levels were measured using the Amplex UltraRed reagent kit (Invitrogen). 50µl of intestinal homogenate is collected and mixed with 50µl of working solution (5mM Amplex UltraRed reagent, 10U horseradish peroxidase, HRP, 0.05M sodium phosphate, pH 7.4) immediately after homogenization. The mixture was incubated at room temperature for 30 minutes and measure absorbance (560nm). The H_2O_2 level was then determined based on H_2O_2 standard curve.

***V. cholerae ex vivo* oxidative stress resistance assays**

50µl of intestinal tissue homogenates collected from *V. cholerae*-infected suckling mice colonized with different commensal groups were incubated with 1mM of hydrogen peroxide for 1 hour at room temperature. After incubation, 10µl of untreated and treated

homogenates were collected, serially diluted, and plated on selective agar to determine survival rates.

Intestinal homogenates *ex vivo* treatment with pure culture

Intestinal homogenates are prepared as described in previously published method (Alavi et al., 2020). Briefly, intestines were collected from 6-day old CD-1 suckling mice fasted for 18 hours and homogenized in 2.5ml sterile water, homogenates were centrifuged and then collect aqueous supernatants. The supernatant was treated at 100℃ for 30 minutes and filter sterilized with 0.22μM filter. The sample was then dried with Savant Integrated Speedvac System (Fisher Scientific) and resuspended in 0.5ml sterile water. 2ml of acetonitrile (Sigma Aldrich) was added to the sample and incubated at room temperature for 20 minutes to deprotienize after vortexing (Humbert et al., 2012). The aqueous layer was then filter sterilized, dried, and resuspended in 0.5ml sterile water. 1.5ml of OD_{600} = 0.4 pure culture was pelleted and resuspended in purified homogenates then incubated anaerobically for 24 hours at 37℃. The culture was heat-treated at 100℃ for 30 minutes then centrifuged. The aqueous layer was then filter sterilized with 0.22μM filter after cooled to room temperature and sent for mass spectrometry analysis.

Quantitative PCR analysis of VPS gene expression

Overnight culture of *V. cholerae* was 1:100 inoculated into fresh LB liquid media containing 100ug/ml streptomycin and grown to OD_{600} = 0.3. 50µM of H_2O_2 or equal volume of PBS was added to the culture and incubated for 2 hours at 37℃ with shaking. The cultures were collected and RNA was extracted using TRIzol according to manufacturer instructions. 2µg of total RNA was then used for reverse transcription PCR using SuperScript™ IV One-Step RT-PCR System (Invitrogen). qPCR assays were preformed using gene specific primer sets targeting *vpsR* (forward primer: 5' – TGGCACACTGCTGCTAAA - 3', reverse primer: 5' – ACATCGACTGCACGAACC - 3'), *vpsT* (forward primer: 5' - ACCCTGATCAAAGGCATGAG - 3', reverse primer: 5' – GTGAGGTCACGACTGAGTTAC - 3'), and *vpsL* (forward primer: 5' - CAGTATGCGAGTGATGGATAATGG - 3', reverse primer: 5' – TCGTGGATCGCCTTTGGT - 3'), with *recA* (forward primer: 5' – ATTGAAGGCGAAATGGGCGATAG - 3', reverse primer: 5' – TACACATACAGTTGGATTGCTTGAGG - 3') as reference gene. Each reaction was done in triplicate with 12.5µl of iQ SYBR Green Supermix (BIO-RAD2), 1µl of 10µM

forward and reverse primers each, 8.5µl nuclease free water and 2µl of 2 fold diluted RT-PCR reaction product.

Measurement of bile acid processing by *B. obeum* BSH

Overnight cultures of *E. coli bsh*^{c} and *E. coli* vector with pZE21 (Alavi et al., 2020) were 1:100 inoculated into fresh LB liquid media containing 50ug/ml kanamycin and incubated for 24 hours at 37℃ with shaking. The cultures were normalized to 1.5ml of OD_{600} = 0.4 culture, pelleted and washed with 1.5ml of PBS. The pellet was resuspended in 1.5ml of PBS containing 2mM of TDCA and transferred to glass tubes then incubated at 37℃ stationary for 24 hours. After the incubation, supernatants were collected by centrifuge and filter-sterilized with 0.22µM filters. Collected supernatants were send for mass spectrometry analysis and test for *V. cholerae* growth inhibition.

***V. cholerae* growth curve measurements**

Supernatants collected as previously described were 1:1 mixed with 1:1000 diluted log phase *V. cholerae* culture in a 96 well plate. OD_{600} was then taken every 30 minutes for

20 hours with BioTek Synergy HTX multi-mode reader under 37℃ with orbital shaking at 180 cpm (6mm) using Gen5 2.09.

Bile acid extraction and preparation from *in vitro* enzymatic assays

Bile acids were extracted from *in vitro* enzymatic assays for LC-MS measurements. An aliquot of 200µl of the assay was acidified to a final concentration of 2% acetic acid. A liquid-liquid extraction was performed with 300µl of ethyl acetate. The supernatant was collected (200µl) and dried down under a stream of nitrogen. Tube content after drying was resuspended in 1ml methanol and diluted 20X for LC-MS analysis.

Liquid chromatography mass spectrometry measurement of bile salts

Standards for TDCA and DCA (1µM) were used to determine retention times and fragmentation patterns for each compound. Chromatographic separations were conducted in a Waters I-class UPLC system using an Acquity UPLC BEH C18 column (2.1 × 100mm, 1.7µM; Waters). Water with 0.1% formic acid (A) and acetonitrile with 0.1% formic acid (B) were used as mobile phases. Sample separation was conducted after 1ul injections with the column kept at 40℃, with a flow rate of 0.4ml/min under the

following gradient: 0 minutes, 10% B; 1 minutes, 10% B; 1.5 minutes, 25% B; 8 minutes, 45% B, 10 minutes, 90% B; 16 minutes, 90% B, 17 minutes, 45% B, 19 minutes, 25% B; 21 minutes, 10% B; 26 minutes, 10% B. Mass spectrometry measurements were conducted in a Synapt G2-Si quadrupole time-of-flight mass spectrometer (Waters). The instrument was operated in negative ion mode under MS/MS conditions with a source capillary voltage of 2.5 kV, source temperature of 150℃, desolvation temperature of 600℃ and desolvation gas at 600L/hr. Leucine enkephalin was used as lock spray standard for mass correction. The following mass transitions (m/z) produced by the indicated collision energies (trap and transfer) were used for signal identification TDCA and DCA (TDCA, 79.95 and 124.00 (CE 40 V); DCA, 343.26 and 391.28 (CE 25 V)). The Quanlynx software (Waters) was used for peak integration and peak area calculation and processing. A quality control sample was produced by pooling equal amounts of samples and used to monitor system stability and reproducibility.

Bile acid growth inhibition of biofilm-associated *V. cholerae*

Overnight *V. cholerae* cultures were 1:100 inoculated into fresh LB liquid media with 100μg/ml streptomycin and 2ml of dilution aliquoted into 100 x 15mm sterilized

polystyrene petri dishes with 10mg glass beads (50-100µm Polysciences), followed by incubation for 24 hours at room temperature with slow shaking (10rpm) (Zhu and Mekalanos, 2003). Planktonic cells were collected by pipetting media, followed by pelleting via centrifugation and resuspension in LB media containing 1mM of different bile acids (diluted from 100x stock solution in dimethyl sulfoxide, DMSO). Beads were rinsed with 1x PBS to remove residual planktonic cells, and the biofilm-associated bacteria on the beads were then treated with 5ml LB liquid media containing 1mM of different bile acids. For both treatments, an identical volume of DMSO as bile acid stock was added to LB liquid media as control. Both planktonic cells and biofilm on the beads were treated for 4 hours, and surviving bacteria were then enumerated by serial dilution and plating.

Statistical analysis

Statistical analysis was performed using GraphPad Prism 9 (Graphpad Software, Inc.). Student's unpaired *t*-test was used to analyze *in vitro* and *ex vivo* CFU and ratio group difference. Mann-Whitney *U*-test was used to analyze *in vivo* CFU level differences

between groups. Comparisons where $P<0.05$ were considered statistically significant. Results are representative of independent repeated experiments.

Results

Bacterial community dependent *V. cholerae* colonization

Previous studies have shown that specific human gut microbiota compositions can affect *V. cholerae* colonization using the antibiotic-cleared infant CD-1 suckling mice model, with dysbiotic gut microbiota being more susceptible to infection compared to prototypical microbial communities characteristic of healthy individuals (Alavi et al., 2020). As the gut microbiota is highly diverse from individual to individual, we used simplified model groups of microbes representative of "healthy" and "unhealthy" or dysbiotic states to examine the effects of microbiota structure on *V. cholerae* behavior during infection. The simplified infection resistant model community (SR) consists of the species representing the major taxa found in either the healthy individuals in Bangladesh (Hsiao et al., 2014), *Blautia obeum* (previously classified as *Ruminococcus obeum*), *Bacteroides vulgatus*, and *Clostridium scindens*. The low-diversity dysbiotic state

induced by recurrent diarrhea or malnutrition was represented by *Streptococcus salivarius* subsp. *salivarius* (SS). 4-day old suckling mice were first treated with streptomycin to remove the host microbiome then co-infected with *V. cholerae* and the community strains after 24 hours. The intestine was collected 18 hours post-infection and homogenized for CFU enumeration of *V. cholerae*, with aliquots of homogenates also stored for host and bacterial RNA-Seq analysis. In accordance with previous findings using healthy and dysbiotic human gut microbiota (Alavi et al., 2020), we repeatedly observed that *V. cholerae* was able to colonize SS-containing animals at around 10^7 CFU; when co-infected with SR, *V. cholerae* colonization was around ~4 fold lower (Figure 2.1-1A). We also verified the colonization of model microbes by measuring total bacterial load using qPCR assay with universal 16S primers after antibiotic treatment and after gavage; total bacterial 16S copy number was significantly higher after bacterial gavage compared to antibiotic treated mice (Figure 2.1-1B). These findings replicate previous studies that these model microbes are capable of colonizing mice intestine (Alavi et al., 2020).

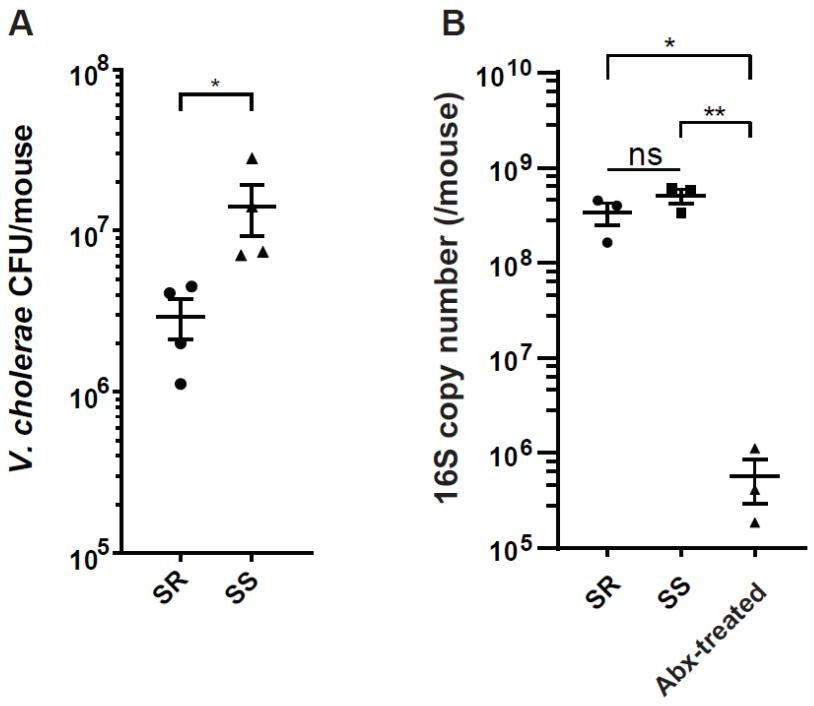

Figure 2.1-1. *V. cholerae* colonization and fitness varies with model commensal microbiota.

A. *V. cholerae* colonization of antibiotic-cleared 5-day old suckling CD-1 mice after co-gavage with model microbial mixtures. B. Bacterial 16S copy number in intestinal homogenates (n=3-4, *: P value<0.05, **: P value<0.01, ns: not significant).

RNA-Seq analysis reveals microbiota-dependent expression of biofilm-associated genes

Alavi et al. determined that one contributor of microbiota-dependent variation in infection resistance was a variable level of commensal-encoded bile salt hydrolase (BSH) that de-conjugates the attached amino acid of the bile acid taurocholic acid (TCA),

leading to differences in induction of virulence gene expression; *B. obeum* (an SR organism) was a key BSH producer, while *S. salivarius* lacked BSH activity (Alavi et al., 2020). To examine other potential contributors to SR/SS infection differences, we examined *V. cholerae* and host gene expression during infection of suckling mice. We extracted RNA from intestinal homogenates of animals colonized with both communities and infected with *V. cholerae* and used RNA-Seq to examine community-dependent *V. cholerae* gene expression patterns. Using pathway analysis with the Kyoto Encyclopedia of Genes and Genomes (KEGG) (Kanehisa and Goto, 2000;Kanehisa, 2019;Kanehisa et al., 2021), we found that *V. cholerae* co-infected with SS significantly upregulated biofilm formation and phosphotransferase system pathways relative to infection of SR mice; in SR mice 16 pathways were increased in expression relative to SS, predominantly metabolic pathways including carbon metabolism, amino acid metabolism and oxidative phosphorylation (Figure 2.1-2A). Biofilm is a population of microbes aggregated and attached to a surface in a matrix of extracellular polysaccharide (EPS), nucleic acid, and proteins. The production and manipulation of *Vibrio* extracellular polysaccharide (VPS) is driven by gene products encoded by two gene clusters *vps*-I (*vpsU*, *vpsA-K*) and *vps*-II (*vpsL-Q*) (Yildiz and Schoolnik, 1999;Fong et al., 2010). We observed that expression of

most VPS genes is upregulated 2-4 fold during infection of SS colonized animals compared to SR colonized animals. Among VPS genes, *vpsL* displayed the strongest difference in expression between microbiota groups, with 4.5 fold higher in expression in SS vs SR. VpsL is known to be essential for forming a stable biofilm structure (Fong et al., 2010). Other than the exopolysaccharide matrix production genes, another *vps*-coregulated protein, Bap1 (biofilm associated protein), also displayed a 2-fold increase in expression in infection of SS animals (Figure 2B). Bap1 is an extracellular matrix protein that modulates biofilm structure and pellicle formation and mediates cell-to-surface adhesion (Fong and Yildiz, 2008;Yan et al., 2016). Biofilms protect microbes, including *V. cholerae*, from environmental stress including extreme environments and host defense mechanism (Roilides et al., 2015;Yin et al., 2019), and increases infectivity (Zhu and Mekalanos, 2003;Tamayo et al., 2010). Our findings suggest that infection of SS-like permissive, dysbiotic microbiota could induce *V. cholerae* to form a more robust biofilm structure either directly or indirectly, leading to stronger defenses against environmental stress.

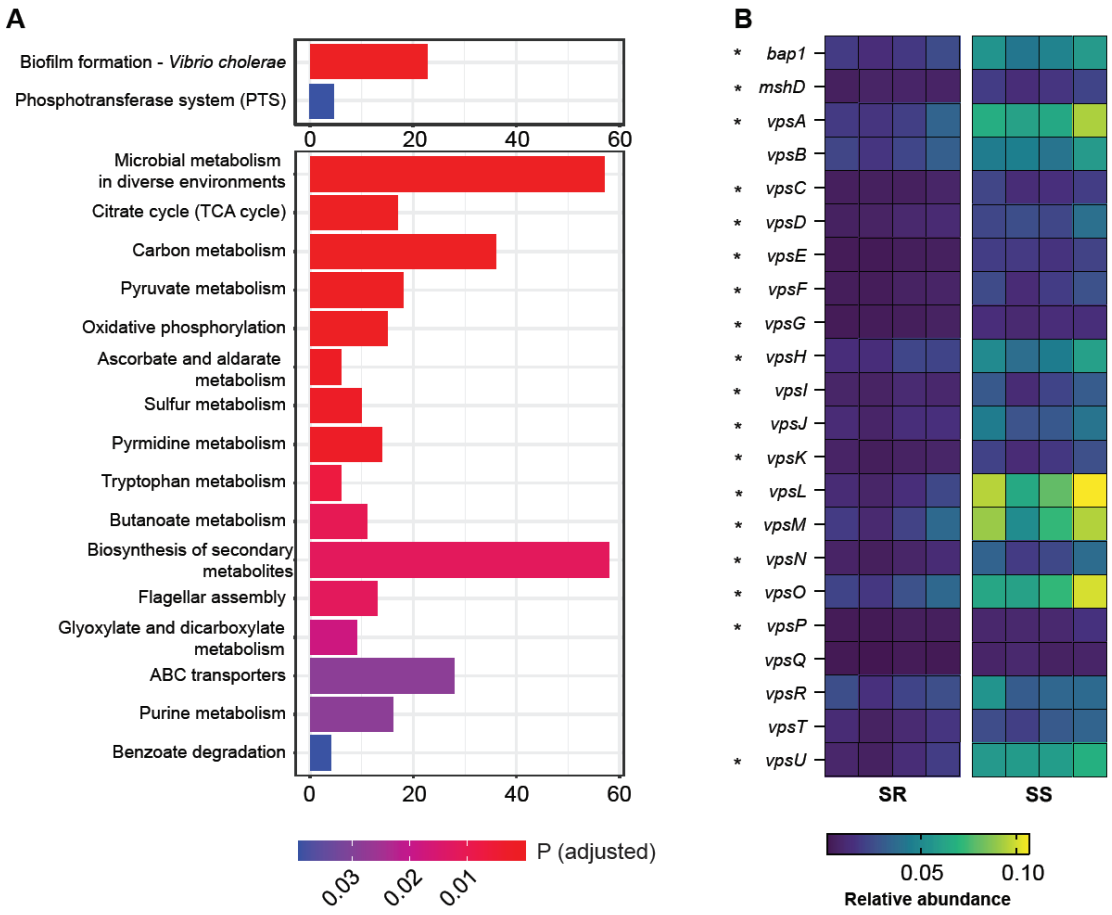

Figure 2.1-2. Differentially gene regulation in *V. cholerae* on co-infection with different model communities.

A. Number of genes involved in indicated KEGG gene pathways relatively significantly upregulated in *V. cholerae* co-infected with SS vs SR (upper panel) and SR vs SS (bottom panel). B. Relative abundance (%) of genes involved in *Vibrio* polysaccharides formation and attachment from *V. cholerae* co-infected with SR or SS. Starred genes (*) are significantly differentially expressed across microbiota groups (*: P<0.005).

Host iNOS and DUOX response towards microbiome structure

Given that the SS triggered the expression of the genes associated with biofilm formation

in *V. cholerae*, and the critical role of biofilms in defense against environmental stresses, we next examined whether the host environment during infection was modulated by the microbiota through transcriptomic measures of host responses to *V. cholerae* infection in the presence of SR and SS model microbes. We found that mice co-infected with SR and *V. cholerae* exhibited a significantly higher expression of *NOS1*, *NOS2*, and *DUOX2* in the total intestine (Figure 2.1-3A-C). *NOS2*, and *DUOX2* are known to involve in the production of compounds such as nitric oxide (NO) and extracellular hydrogen peroxide (H_2O_2), respectively (Geiszt et al., 2003;El Hassani et al., 2005). In response to numerous gastrointestinal infections, host enzymes are able to generate increased local reactive nitrogen stress (RNS) and reactive oxygen stress (ROS), which collectively form a key mechanism to inhibit pathogens (Paiva and Bozza, 2014). Nitric oxide synthases (NOS) catalyze the production of nitric oxide (NO), which includes three different isoforms, NOS1-3. The NO synthesized by NOS1, and NOS3 mainly acts as a neurotransmitter in the brain and peripheral nervous system and maintains a healthy cardiovascular system (Forstermann and Munzel, 2006;Knott and Bossy-Wetzel, 2009). NOS2 is involved in immune response and NO synthesis. ROS synthesis involves the expression of dual oxidase (DUOX) that catalyzes hydrogen peroxide production (Sommer and Backhed,

2015). Prior studies have demonstrated an increase in both ROS and RNS during *V. cholerae* infection; Ellis et al. showed that cholera patients show higher nitric oxide synthase 2 (NOS2) protein abundant during acute-phase (Ellis et al., 2015), while an examination of cholera patients' mucosal gene expression by Bourque et al. demonstrated that dual oxidase 2 (*DUOX2*) and *NOS2* are higher in expression during the acute phase (Bourque et al., 2018).

The resulting increase in NO and H_2O_2 production leads to high local oxidative stress, which forms a key element of the initial host response towards pathogen infection (Kim and Lee, 2014;Król and Kepinska, 2021). These anti-microbial effects are mediated by several pathways, including conversion of NO to peroxynitrite ($OONO^-$), and form $OH\cdot$ and nitrogen dioxide ($\cdot NO_2$) (Nathan and Ding, 2010) to cause oxidative damage on phagocytosed pathogens, and pathogen in phagosome, and H_2O_2 or through catalytic reaction to form hydroxyl radicals ($OH\cdot$) leads to pathogen DNA breakage, base oxidation and deamination, and lipid peroxidation, (Paiva and Bozza, 2014). This increase in ROS production has been observed in cholera patients, as measured by NO metabolite levels in serum and urine (Janoff et al., 1997). Cholera patients' duodenum samples at acute-phase showed more abundant *NOS2* and *DUOX2* transcript levels

compared to convalescent-phase (Ellis et al., 2015;Bourque et al., 2018). Other than higher ROS/RNS enzyme expression, host catalase (*CAT*) gene expression is also induced by infection in the presence of SS (Figure 2.1-3D). Since catalase is an antioxidant enzyme that promotes the conversion and detoxification of ROS and H_2O_2 to prevent oxidative damage to host cells, this further supports an increase in ROS stress during infection of individuals with SR-like microbiota compared to individuals with SS-like commensal microbe. We then measured H_2O_2 production in the homogenates from each model microbiome and found that colonization with the SR community induced significantly higher production of H_2O_2 (Figure 2.1-3E). Given that a significant difference in overall H_2O_2 was observed from total organ samples, local differences in levels of H_2O_2 at epithelial micro-environments as a function of microbiome and infection may be even higher (Bhattacharyya et al., 2014;Ellis et al., 2015;Taylor and Colgan, 2017;Burgueno et al., 2019;Imlay, 2019).

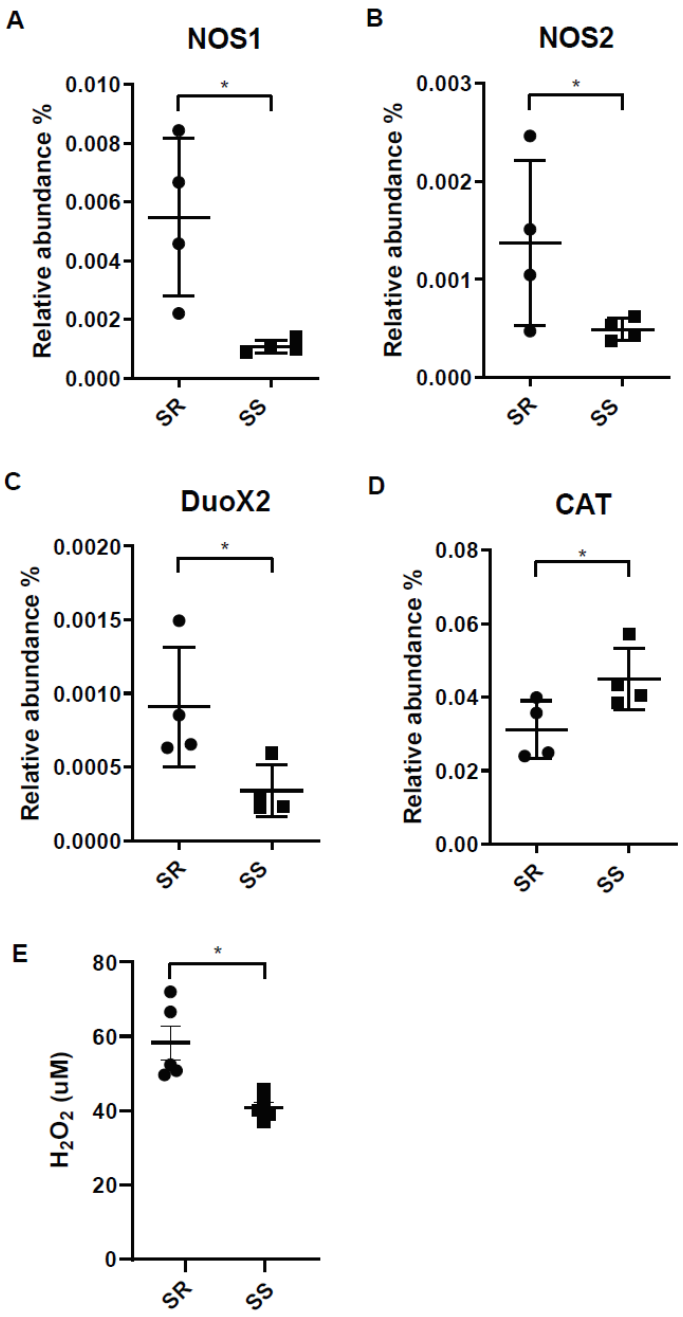

Figure 2.1-3. Community dependent host oxidative stress responses during *V. cholerae* expression.

Host genes involved in the synthesis of reactive nitrogen species A. Nitric oxide synthases 1 (NOS1), B. Nitric oxide synthase 2 (NOS2) and reactive oxygen species C. Dual oxidase 2 (DUOX2), D. Catalase (CAT), E. H_2O_2 level measured from collected intestinal homogenates. (n=4, *: P<0.01)

Differential regulation of biofilm formation leads to oxidative stress resistance

Previous studies have shown that biofilm formation enhances *V. cholerae* resistance towards oxidative stresses driven by early infection (Wang et al., 2018), and our data suggest that SS can induce higher biofilm formation gene expression in *V. cholerae*. To test whether microbiome-dependent differences in biofilm-associated gene expression lead to increase oxidative stress resistance, we used an *ex vivo* ROS survival assay. We co-infected suckling animals with wild-type and biofilm defective *vpsL* mutants (Figure 2.1-4A) and our two model commensal collections. The mutant showed no significant differences in colonization between the two model microbiota (Figure 2.1-4B). We then isolated *V. cholerae* and associated extracellular structures by homogenizing infected small and large intestinal tissues and then treated *V. cholerae*-containing homogenates with H_2O_2. Survival rates of *V. cholerae* were then determined by plating. We found that wild-type *V. cholerae* exhibited >90% H_2O_2 survival after infection of SS-co-colonized small intestine, while *V. cholerae* that colonized SR-bearing animals exhibited only ~55% survival. When the *vpsL* mutant was co-gavaged with the model microbes, this SS-dependent advantage was ablated (Figure 2.1-4C), suggesting biofilm formation was

necessary for this difference in oxidative stress resistance. We observed the same pattern from the large intestine where wile type *V. cholerae* from SS animals exhibited higher levels of *ex vivo* ROS resistance compared to *V. cholerae* from SR animals, and *vpsL* mutants in either microbiota context (Figure 2.1-4D), though the rate of survival in both colonization contacts were significantly reduced compared to small intestine, which may indicate that the regulatory effects of commensal microbes are concentrated at the preferred site of colonization of *V. cholerae*, the distal small intestine. To determine whether biofilm biogenesis was induced by hydrogen peroxide, we treated *V. cholerae* culture with H_2O_2 *in vitro* and examined *vpsR*, *vpsT*, and *vpsL* expression. Quantitative RT-PCR analysis showed no significant differences in expression level between H_2O_2 treated and untreated culture (Figure 2.1-4E), suggesting that other mechanisms, potentially microbial in nature, are responsible for observed *in vivo* microbiome-specific differences in *V. cholerae* biofilm production. Taken together, these findings suggest that i) microbiota-associated biofilm expression leads to different levels of biofilm-dependent ROS resistance in *V. cholerae*, and ii) that this effect is much more substantial in the preferred site of colonization in the distal small intestine. In combination with higher levels of oxidative stress during infection of SR-like communities, this suggests that

modulation of biofilm or biofilm formation potentially contributes to the higher *V. cholerae* colonization level observed during infection of SS-bearing individuals.

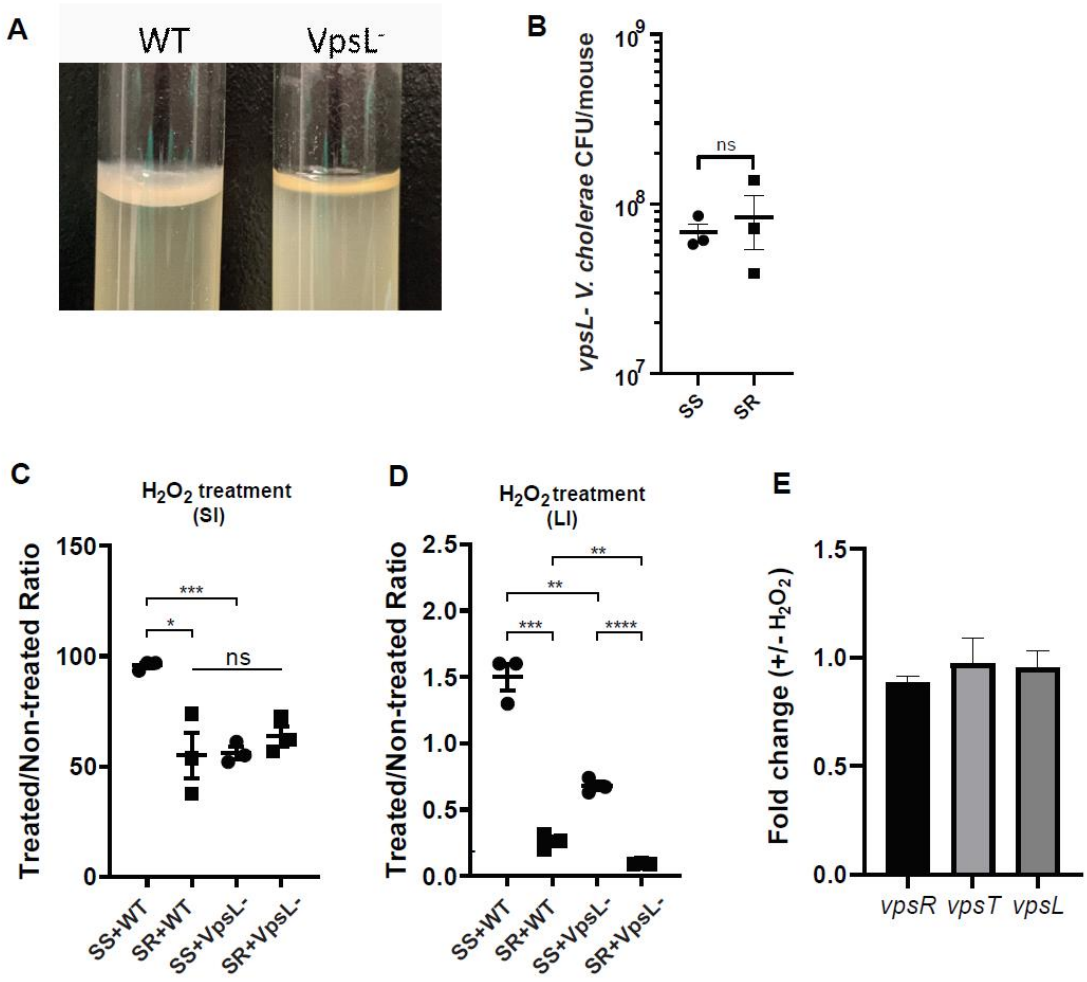

Figure 2.1-4. Presence of different commensal microbes during infection drives different biofilm-dependent *V. cholerae* oxidative stress resistance.

A. Confirmation of disruption of biofilm formation by *vpsL* gene deletion. B. *vpsL* mutant *V. cholerae* colonization co-gavaged with indicated model microbiota. Survival of *V. cholerae* strains in C. small intestine and D. large intestine of antibiotic-cleared suckling mice co-colonized with indicated commensal communities after hydrogen peroxide treatment. E. qPCR quantification of VPS gene expression *in vitro* after hydrogen peroxide treatment (n=3, *t* test, *: P<0.05; **: P<0.01; ***: P<0.001; ****: P<0.0001; ns: not significant)

Microbiota structure and bile salt hydrolase activity modulates bile acid composition and affects *V. cholerae* growth

Since different bile acids have been associated with inhibition of *V. cholerae* growth *in vitro* and regulation of biofilm production (Hay and Zhu, 2015), we examined how host bile might affect microbiota- and biofilm-dependent *V. cholerae* fitness during infection. Bile is a complex mixture secreted by the gallbladder into the proximal intestine in order to aid with the emulsification and absorption of dietary fats. A dominant component of bile are bile acids and their salt forms, the primary forms of which are synthesized in the liver from cholesterol, often in amino-acid conjugated forms. The cycle of bile secretion and subsequent re-absorption in the small intestine and the detergent effects of bile means that commensals and pathogens that target this body site have evolved methods to detoxify bile components and also use them as signaling cues to time body site-specific gene expression programs. One key element of microbial bile response is the expression of bile salt hydrolase (BSH) enzymes, which catalyze the deconjugation of amino acids from primary bile, leading to a reduction in detergent activity and subsequent toxicity (Chand et al., 2017). Subsequent microbial action can also dehydroxylate the sterol backbone of bile acids, leading to a variety of different forms of bile acids that circulate

within the intestine of animals housing resident microbes (De Smet et al., 1995). Taurocholic acid (TCA), an abundant amino-acid conjugated bile species in mouse and human gut, is able to strongly activate the *V. cholerae* virulence regulatory cascade by promoting the formation of disulfide bonds in the upstream regulator TcpP (Fu et al., 2013). In contrast, the de-conjugated form, cholic acid (CA), and the deconjugated and dehydroxylated form deoxycholic acid (DCA), cannot strongly induce virulence. Previous study has shown that SR microbes and SS can help drive differential colonization resistance by modulating the level of TCA conjugation and virulence gene expression (Alavi et al., 2020), however the interaction of *V. cholerae* with other TCA-derived bile acid metabolites has not been well described. This is especially important as DCA generated by BSH-dependent deconjugation of TCA is re-absorbed and reconjugated to taurine by the host, being secreted as taurodeoxycholic acid (TDCA) (Figure 2.1-5A). We therefore used mass spectrometry to analyze the bile salt composition in the intestinal homogenates, before and after incubation with *B. obeum* and *S. salivarius*. We found that TDCA signal in both control and SS are significantly higher than when incubating with *B. obeum* (Figure 2.1-5B). DCA levels in *B. obeum* treated intestinal homogenates were several logs higher compared to *Streptococcus*-treated and

control homogenates (Figure 2.1-5C). The accumulation of DCA suggests that *B. obeum* is able to de-conjugate TDCA to DCA in addition to de-conjugating TCA to CA. To examine whether the *B. obeum* BSH enzyme is able to catalyze this reaction, we examined TDCA and DCA levels in intestinal homogenates incubated with *E. coli* expressing *B. obeum* BSH (bsh^c) compared to isogenic vector strains lacking any endogenous BSH activity. We observed the same low TDCA and high DCA signal pattern compared to vector control (Figure 2.1-5).

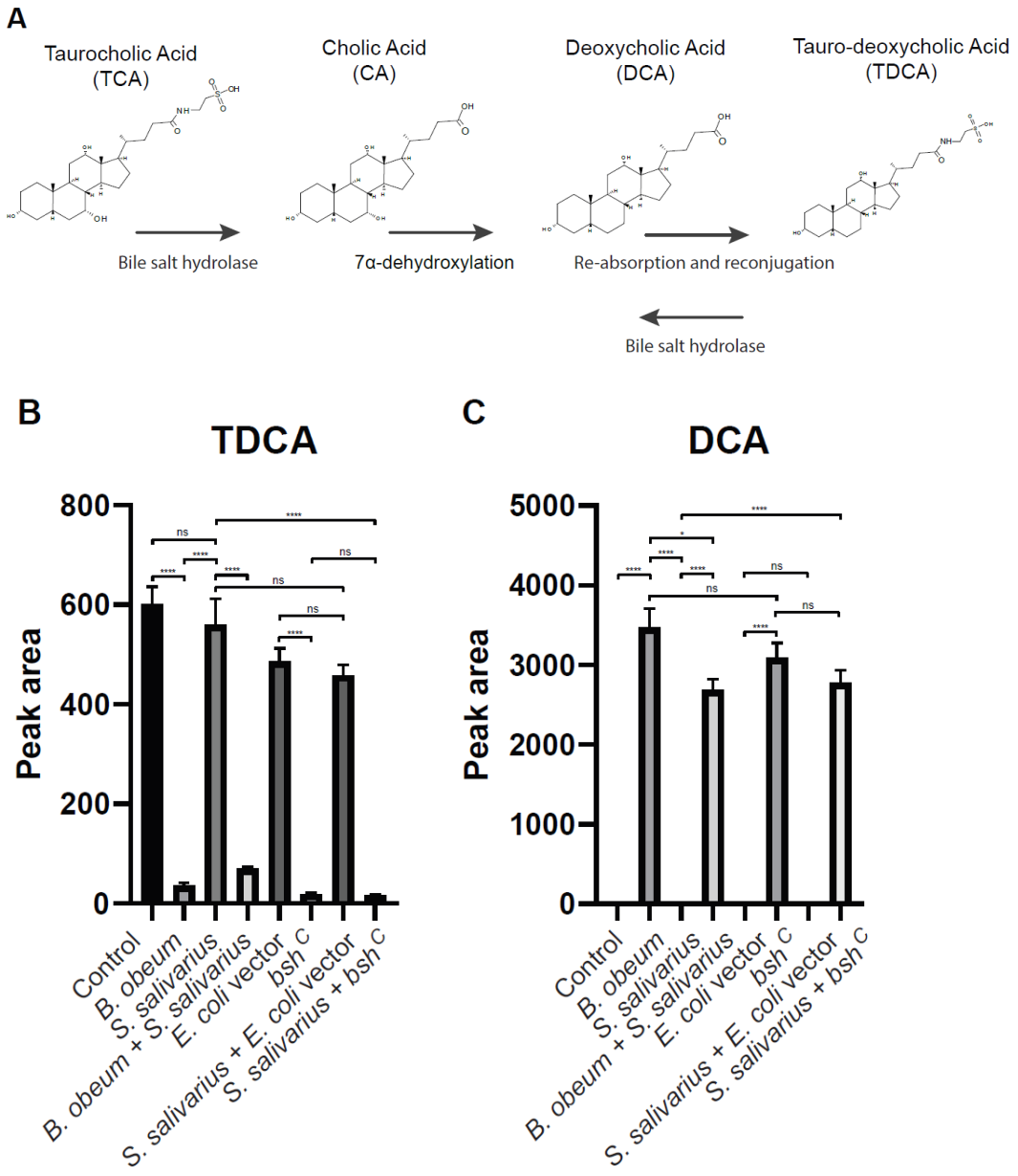

Figure 2.1-5. Bile salt hydrolase-dependent TDCA and DCA levels in infant mouse intestines.

A. Model of microbial modification of bile salt in the gut. B. Tauro-deoxycholate (TDCA) and C. deoxycholate (DCA) levels in intestinal homogenates after incubation with indicated strains. (n=4, *t* test, *: P<0.05; ****: P<0.0001; ns: not significant)

To confirm the conversion from TDCA to DCA via *B. obeum* BSH, pure solutions of TDCA was added to *bsh*^{c} cell pellets in PBS and incubated for 24 hours. The supernatant was collected, filter sterilized, and used for mass spectrometry analysis. Consistent with our previous findings, the level of TDCA remaining was significantly higher in the vector control compared with *bsh*^{c}, while DCA levels were ~600 fold higher in *bsh*^{c} compared to vector control (Figure 2.1-6A-B). Previous studies have shown that DCA is inhibitory to *V. cholerae* growth (Hung et al., 2006). To confirm this, TDCA treated with *bsh*^{C} or vector control was added to fresh *V. cholerae* culture and OD_{600} was taken every 30 minutes for 20 hours. We observed that *V. cholerae* growth was inhibited by *bsh*^{c} processed supernatant compared to vector strain (Figure 2.1-6C). Importantly, the presence of *B. obeum bsh* activity is able to provide inhibitory activity in the presence of *Streptococcus*, supporting the idea that the presence of infection-resistant microbes are able to restore colonization resistance to otherwise susceptible microbiota configurations (Alavi et al., 2020). Taken together, these results indicate that *B. obeum* is capable of converting TDCA to DCA via BSH expression, leading to *V. cholerae* growth inhibition during colonization.

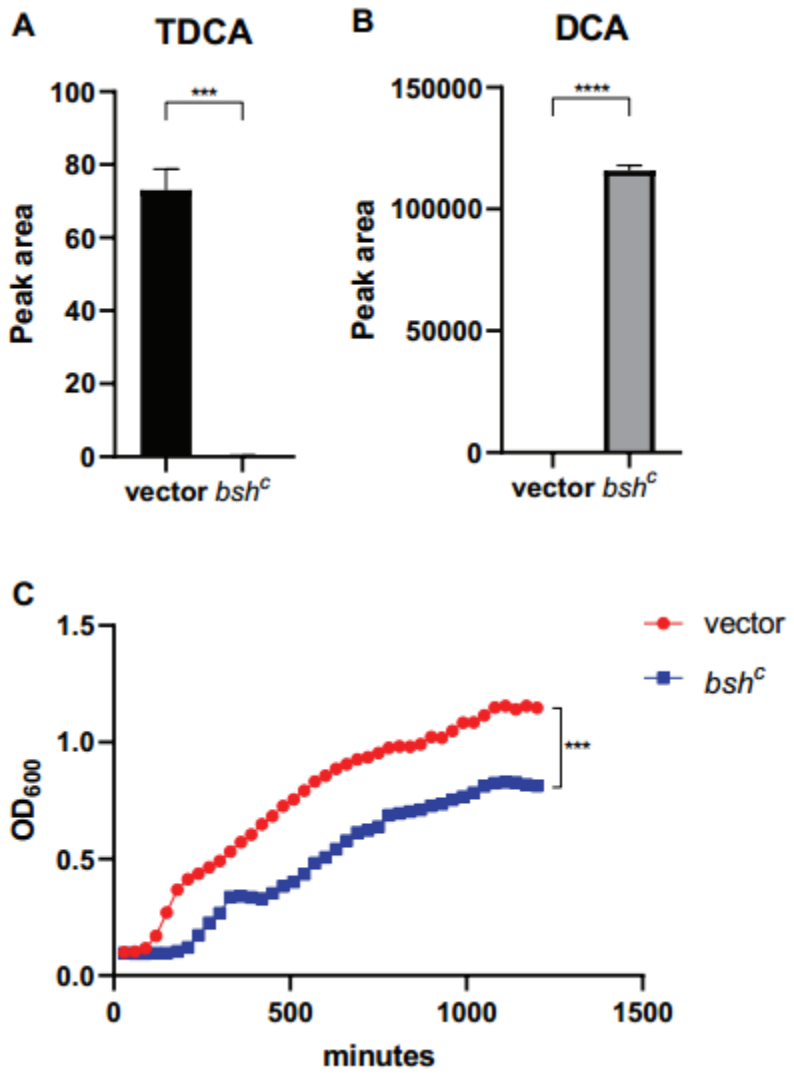

Figure 2.1-6. *Blautia obeum* bile salt hydrolase processes TDCA to DCA leading to inhibition of *V. cholerae* growth.

A. TDCA and B. DCA levels after 24hr incubation of 2mM TDCA with *E. coli* vector and *bsh*^{c} strains as measured by mass spectrometry. C. Effect on *V. cholerae* growth *in vitro* of addition of filtered supernatants from TDCA incubation with the indicated strains. (n=4, *t* test, ***: P<0.001; ****: P<0.0001)

Biofilm dependent bile acid resistance

Previous studies have indicated that crude bile is able to induce biofilm formation, and that biofilm-associated cells are more resistant to bile toxicity (Hung et al., 2006). To test whether biofilm will contribute to *V. cholerae* resistance against different microbially-modified bile acids, we first generated biofilm *V. cholerae* populations in media with beads as a surface for microbial attachment and subsequent biofilm development. We then exposed planktonic and biofilm-formed populations with products of microbial TCA metabolism: TCA, DCA, and TDCA. We found that TCA and TDCA do not significantly affect *V. cholerae* planktonic cell fitness in comparison with no bile acid (Figure 2.1-7A), but that after 4 hours of treatment with 1mM of DCA, planktonic *V. cholerae* exhibited significantly lower survival. In contrast, biofilm-associated *V. cholerae* were insensitive to all bile treatments (Figure 2.1-7B). These repeatable data suggest the formation of biofilm provides *V. cholerae* resistance towards certain bile acids present in the intestinal tract.

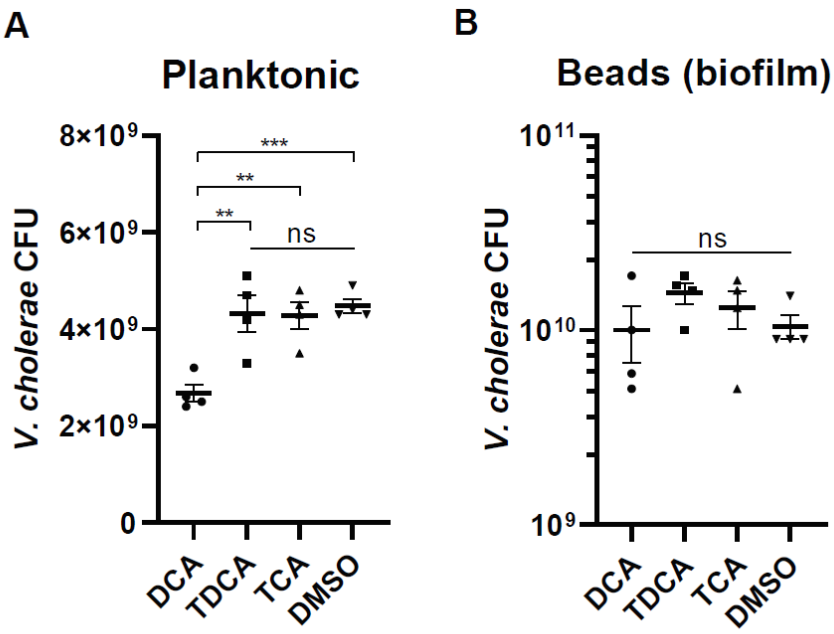

Figure 2.1-7. Biofilm provides *V. cholerae* resistance against secondary bile acid deoxycholate.

Survival of A. planktonic and B. biofilm associated *V. cholerae* after 4 hours of incubation with 1mM of different bile acids including conjugated bile acids taurocholate (TCA) and tauro-deoxycholate (TDCA), and the deconjugated secondary bile acid deoxycholate (DCA). (n=4, T-test, **: P<0.01, ***: P<0.001; ns: not significant)

Discussion

Increasing evidence demonstrates the composition of the gut microbiota influences host defenses against pathogens (Ribet and Cossart, 2015;Cho et al., 2021). This study demonstrates that commensal-dependent manipulation of both *V. cholerae* and host

behavior during infection leads to differential outcomes in *V. cholerae* fitness. *V. cholerae* in the context of infection susceptible communities expresses more biofilm-associated genes, which protects the pathogen against the inhibitory activity of host oxidative mechanisms and inhibitory bile metabolites. The commensal community present during infection in turn affects both mechanisms; SR-colonized mice during infection express significantly higher levels of ROS/RNS production enzymes and display elevated hydrogen peroxide production compared to SS-colonized animals, and we show that one bile acid processing enzyme within the key SR community member *B. obeum* can accumulate deoxycholate, which is inhibitory to planktonic, but not biofilm-associated, *V. cholerae*. These results demonstrate the multi-factorial nature of commensal-associated colonization resistance; prior studies show that the dysbiotic, high Streptoccocus microbiota is more susceptible to *V. cholerae* infection due to the inability to ablate bile-dependent virulence gene activation compared to microbiota containing *B. obeum* (Alavi et al., 2020).

The exact mechanism by which commensal microbes cause differential regulation of *V. cholerae* is not well understood. *V. cholerae* biofilm production *in vitro* is modulated by several pathways, including quorum sensing and bile response (Hung et al., 2006;Hay

and Zhu, 2015). Quorum sensing (QS) plays a key role in the regulation of multiple infection-associated pathways in *V. cholerae* including biofilm production. The sensing of autoinducers leads to a series of dephosphorylation events leading to the repression of the expression of the small RNA regulators Qrr 1-4 (quorum regulatory RNAs) (Lenz et al., 2004). The absence of Qrr sRNAs allows for the expression of the master QS regulator *hapR*, which leads to the repression of the virulence genes and biofilm formation (Miller et al., 2002;Zhu et al., 2002;Hammer and Bassler, 2003;Shao and Bassler, 2014). HapR represses biofilm formation by binding to the regulatory regions of positive regulator *vpsT* and polysaccharide biosynthesis glycosyltransferase *vpsL*, also the first gene of *vps*-II cluster in *V. cholerae* (Waters et al., 2008). Interestingly, production of the inter-species capable autoinducer AI-2 by *B. obeum* has been associated with downregulation of *V. cholerae* virulence and biofilm formation through HapR by transcription regulator VqmA (Liu et al., 2006;Hsiao et al., 2014;Papenfort et al., 2015). While bi-association of *B. obeum* and *V. cholerae* in adult germfree mice revealed no specific transcriptional signatures for biofilm gene regulation in fecal samples, our results suggest significant differences in biofilm regulation in small intestine vs large intestine (Figure 4C-D); compartment-specific microbiota effects on transcription may thus be masked in fecal

transcriptomic data. Treatment with hydrogen peroxide *in vitro* also caused no significant increases in VPS gene expression, further suggesting that the regulation of biofilm is a host environment specific phenotype (Figure 4E). *In vitro* studies have also examined the role of bile salts/acids in biofilm regulation. Hung et al. showed that deoxycholate is able to significantly induce *V. cholerae* biofilm formation in culture (Hung et al., 2006). The presence of bile also has been shown to alter VqmA activity and effect on *V. cholerae* virulence regulation (Mashruwala and Bassler, 2020). While this suggests that the SR community, with the ability to accumulate DCA via the activity of *B. obeum* BSH, should promote biofilm formation, the intersection of other signaling and regulatory pathways such as quorum sensing (Mashruwala and Bassler, 2020), and host oxidative stresses, which lead to increased biofilm formation (Wang et al., 2018), may combine to yield gut compartment- and microbiota-specific effects on *V. cholerae* biofilm regulation.

The role of microbial enzymes in manipulating the host bile acid pool is complex. TCA, CA, TDCA, and DCA are all metabolic products driven by microbial action; in germfree animals, the bile acid pool is almost exclusively amino acid conjugated primary bile molecules such as TCA (Sayin et al., 2013). Microbial BSH activity deconjugates primary molecules such as TCA, generating CA. Further microbial enzymatic action

leads to dehydroxylation of CA to DCA (Molinaro et al., 2018), which can then be reabsorbed by the host, re-conjugated to amino acids, and re-secreted as TDCA (Figure 5A). Thus, multiple commensal pathways can contribute to highly community- and individual-specific bile acid pools. Microbial communities may interact to drive bile acid compositions *in vivo*; both Bacteroides and *C. scindens* within the SR community have been shown to exhibit both BSH and dehydroxylation activity (Kawamoto et al., 1989;Kang et al., 2008). Further complexity is added by the substrate specificity of microbial BSH, which has been grouped into eight phylotypes based on amino acid sequence similarity and substrate specificity (Song et al., 2019). Previous work by Alavi et al. showed that *B. obeum* BSH activity leads to restriction of *V. cholerae* infection by processing TCA, which is a potent activator of key *V. cholerae* virulence genes. In this study, we show that *B. obeum* is also able to process TDCA to DCA; accumulation of DCA leads to inhibition of planktonic, but not biofilm-associated *V. cholerae*. The reduction of *V. cholerae vps* gene expression in SR communities thus reinforces the colonization resistant nature of host intestines bearing SR microbes.

This suggests that infection resistant commensal communities, including *B. obeum*, can control *V. cholerae* fitness during infection by multiple, reinforcing

mechanisms. Production of quorum sensing autoinducers and depletion of conjugated bile acids serving as virulence regulators interrupt the finely calibrate sequence of virulence gene expression regulatory events during early infection, coincident with an increased host oxidative ROS/RNS response compared to the high *Streptococcus* dysbiotic and permissive microbiota. While the precise mechanism leading to lower *vps* gene expression in colonization-resistant communities requires additional work to elucidate, the reduced biofilm formation leads to increased susceptibility to the heightened oxidative stress encountered by *V. cholerae* during infection in these microbiota contexts. Furthermore, *B. obeum* bile salt hydrolase activity not only depletes virulence-gene activating signals such as TCA, but leads to the accumulation of DCA, the growth-inhibitory effects of which are accentuated by reduced *V. cholerae* biofilm production.

Chapter 2.2 Quorum Sensing Regulates *Vibrio cholerae* Fitness Through VqmA

Introduction

During infection *V. cholerae* encounters environmental factors that alter the regulation of virulence gene expression and pathogen fitness. These environmental factors include pH, oxidative states, and molecules. Evidence has shown that gut microbes alter bile composition and effect *V. cholerae* virulence gene expression (Alavi et al., 2020). Further the presence of different microbes also effects host iNOS and catalase expression changing gut environmental oxidative stress (Cho et al., 2022). And expression of *B. obeum luxS* gene is capable of lowering *V. cholerae* colonization in mice model (Hsiao et al., 2014). In particular, modulation of *V. cholerae* quorum sensing (QS) by the gut microbiota may have some of the most important effects on *V. cholerae* virulence.

V. cholerae QS involves several sensing pathways for signaling molecules that are ultimately involved in regulating various key gene expression regulons including motility, susceptibility to antibiotics, biofilm formation, and virulence factor production (Rutherford and Bassler, 2012;Pereira et al., 2013). In *V. cholerae*, there are multiple receptors that senses AI signals and regulates downstream virulence expression including

CAI-1/CqsS signaling pathway (Miller et al., 2002), AI-2/LuxPQ signaling pathway (Neiditch et al., 2005), and a more recently discovered DPO/VqmA signaling pathway (Liu et al., 2006;Papenfort et al., 2015;Wu et al., 2019a) (Figure 2.2-1).

Here, I examine the DPO/VqmA signaling pathway regarding the potential regulation by interacting with *B. obeum* AI-2 signaling molecule. I measured AI-2 activity from different LuxS enzyme source, examined *V. cholerae* gene expression pattern in presence off different AI-2 signal source, and measured *V. cholerae* colonization level with the presence of LuxS expression strain. Result showed that expressing LuxS enzyme from multiple bacteria is capable of producing active AI-2 signal, *V. cholerae* gene expression pattern is different when sensing AI-2 signal from different bacteria, and VqmA could regulate *V. cholerae* colonization dependent on the AI-2 sorce.

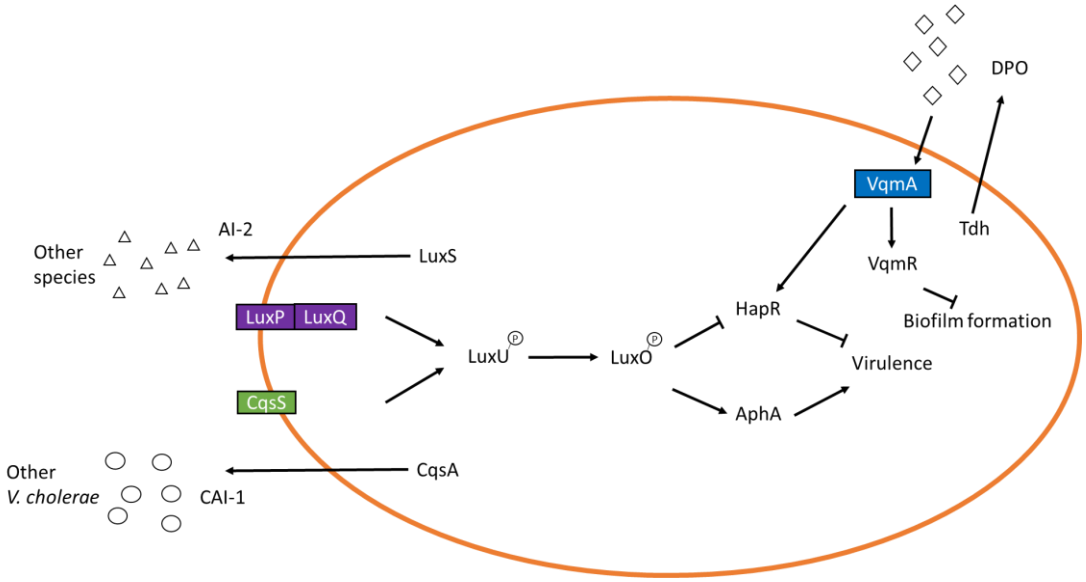

Figure 2.2-1. Model of QS regulating *V. Cholerae* virulence by different AI signals. *V. cholerae* virulence is regulated by QS at different cell densities and environmental signals. At LCD when AI-2 is not bound, LuxQ act as a kinase and auto-phosphorylate the cytoplasmic domains, similar to CqsS by passing phosphoryl group, leads to the phosphorylation of LuxU then LuxO and activates the expression virulence and biofilm formation. When at HCD, the binding of AI-2 facilitates a conformational change breaking the symmetry of LuxPQ heterotetramer prevented the phosphorylation cascade and inactivates the expression of virulence and biofilm formation. The biding of DPO to VqmA also activates the expression of *hapR* and *vqmR*, leads to the inhibition of virulence expression and biofilm formation.

Methods

Bacterial strains and culture condition

All *V. cholerae* strains were derivatives from C6706 O1 El Tor strain and grown in Luria-Bertani (LB) medium under 37℃, shaking at 250 rpm overnight for subsequent use. All anaerobic strains were grown in LYHBHI medium (BHI supplemented to 5g/L yeast extract, 5mg/L hemin, 1mg/mL cellobiose, 1mg/mL maltose and 0.5mg/mL cysteine-HCl) in a Coy chamber at 37℃ (5% H_2, 20% CO_2, balance N_2) then 1:100 subcultured into fresh media and grown an additional 48 hours prior to gavage. All *E. coli* strains were grown in LB medium shaking with 250 rpm under 37℃ overnight, then subcultures into fresh media and grown for overnight prior to gavage.

V. cholerae strain construct

VqmA and PAS domain deleted constitutive expression plasmid was constructed using Gibson assembly master mix (New England BioLabs Inc.). pZE21 vector was linearized PCR using Phusion master mix (ThermoFisher scientific) (forward primer: 5' - TGATATCGAATTCCTGCAGC - 3', reverse primer: 5' - TATCGATACCGTCGACCTCG - 3'). Gene fragment of *vqmA* (forward primer: 5' -

CGAGGTCGACGGTATCGATAATGCCTAACCATCTGACATTAG - 3', reverse primer: 5' - GCTGCAGGAATTCGATATCATTACTGGGCGACAACGTCAAC - 3') and *vqmA* PAS domain deleted (forward primer: 5' - CGAGGTCGACGGTATCGATAATGATTCTTGAAGTTGGTCATTG - 3', reverse primer: 5' - GCTGCAGGAATTCGATATCATTACTGGGCGACAACGTCAAC - 3') was amplified using Phusion master mix. Linearized vector backbone and gene fragment were assembled according to manufacturer's protocol. Assembled product was digested with DpnI to remove vector template then electroporated into an electrocompetent *V. cholerae* and incubated in LB media at 37°C with 250 rpm for 30 minutes and plated on LB agar plates containing 50µg/ml kanamycin. Single colonies are pick and sanger sequenced to confirm the construct. VqmA mutant *V. cholerae* was constructed by SacB selection. pWM91 vector was linearized using XhoI digestion, *vqmA* upstream (forward primer: 5' - GTACCGGGCCCCCCCTGCATAAAGGGGGGATTTC - 3', reverse primer: 5' - GACGTTGTTGCGCCATATCCTCCACTGGAAATG - 3') and downstream (forward primer: 5' - GATATGGCGCAACAACGTCAAGCTGATTG - 3', reverse primer: 5' - TCGATACCGTCGACCATTTCATGTCGCGCCCGA - 3') fragments are amplified using Phusion mater mix. Three fragments where assembled using Gibson

master mix according to manufacturer's protocol and electroporated into an electrocompetent SM10λpir *E. coli*. The plasmid sequence was checked via sanger sequencing, conjugated into *V. cholerae*, and selected on LB agar plates containing 100ug/ml ampicillin and streptomycin then incubate overnight. Single colonies were re-streak onto LB agar plates containing 100ug/ml ampicillin and streptomycin again for colony purification. The purified single colonies were then picked and streaked on a non-selective LB agar plate allowing out-growth for recombination. Mutants were then selected on sucrose plates (5% tryptone, 2.5% yeast, 7.5% agar, and 6% sucrose) by streaking multiple colonies and incubate at room temperature for 2 days. Single colonies were then checked for mutation by PCR.

AI-2 expression strain construct

The *luxS* gene from commensal bacteria were codon-optimized for *E. coli*, placed downstream of the $P_{Ltet\text{-}O\text{-}1}$ constitutive promoter sequence derived from the plasmid vector pZE21, and the resulting construct cloned into vector pMK using the GeneArt Subcloning & Express Cloning Service (ThermoFisher).

AI-2 signal production

AI-2 expression *E. coli* strains were grown overnight in LB media with 50µg/ml kanamycin at 37℃, shaking with 250 rpm. Cultures were then 1:100 subcultured into fresh LB media. Supernatants were then collected at different OD_{600} and filtered with 0.22µM filter.

Bioluminescence assay of AI-2 signal

Supernatant from different LuxS expressing strains were tested by BB170 (*V. harveyi* AI-2 reporter). BB170 was grown at 30℃ shaking in Luria-marine (LM) medium overnight (Bassler et al., 1994). BB170 overnight culture was then 1:1000 diluted into AI bioassay (AB) medium (Greenberg et al., 1979). 90µl of diluted culture was aliquoted into 96-well plates and mixed with 10ul of cell-free supernatant in triplicate. The plates were incubated at 30℃, shaking at 175 rpm for 2 hours, luminescence and OD_{600} were measured every 30 minutes.

Infant mouse experiment

4-day old sucking CD-1 mice (Charles River Laboratories) were fasted for 1.5 hours,

then gavaged with ~1mg/g body weight streptomycin using 30-gauge plastic tubing. The animals were placed with the dam for 1 day. Mice then receive model community strains balanced based on OD_{600} with *V. cholerae* in a 50µL gavage after 24 hours. At 18 hours post-infection, animals were sacrificed and their intestines were homogenized in PBS buffer for CFU measure on LB agar plates containing 200µg/mL streptomycin (Alavi et al., 2020).

Preparation of bacteria inoculum into mice

Each model community bacterium was cultured from glycerol stocks in LYHBHI media for 48 hours at 37°C and then diluted (1:100) in fresh LYHBHI media. After growth for an additional 48 hours, cultures were balanced based on OD_{600}. For inoculation into suckling mice, the equivalent total of 300µl of OD_{600} ~ 0.4 culture divided evenly across community strains was pooled, pelleted by centrifugation, and re-suspended in fresh LYHBHI. Each mouse received this mass of bacterial cells in a maximum gavage volume of 50µl. In mice containing multiple defined communities, normalized mixtures were prepared so that 300µl of OD_{600} = 0.4 equivalent of each community was represented in the final gavage. In mice receiving *V. cholerae*, the total resuspension volume of

commensal strains was 25µl, with the remaining 25µl containing about $1x10^5$ CFU *V. cholerae* in LYHBHI. In mice receiving AI-2 signals, the communities and *V. cholerae* were re-suspended in degassed cell-free supernatant collected from *E. coli* strains harboring different *luxS* gene.

RNA extraction, RNA-seq library preparation and sequencing

V. cholerae strains are subcultured 1:100 from overnight culture into fresh LB media and grown in 37°C at 250 rpm and cell free supernatant was 1:10 added. 1ml of bacteria culture are spin down and collected at OD_{600} ~ 0.4. Total RNA was then extracted using TRIzol reagent according to manufacturer instructions. Extracted total RNA was treated with Baseline-ZERO DNase (Lucigen) to degrade remaining DNA, and then treated with TRIzol again for DNase removal. RNA library were generated using the Ovation Mouse RNA-Seq system with addition of *V. cholerae* enrichment primers (NuGEN). Final libraries were checked using an Agilent Bioanalyzer, and a 75 bp single read sequencing was performed on Illumina NextSeq500.

RNA-seq analysis

All RNA-seq sequencing results are mapped and analyzed with Rockhopper (McClure et al., 2013;Tjaden, 2015;2020). Differential gene expression analysis was done using DEseq (Anders and Huber, 2010) and edgeR (Robinson et al., 2009;McCarthy et al., 2012).

AI-2 identification by mass spectrometry

Cell-free supernatants collected from LuxS expression strains at OD_{600} ~ 0.23 where purified with Bligh and Dyer lipid extraction method (Bligh and Dyer, 1959). The supernatant was mixed with chloroform and methanol (chloroform: methanol: sample, 1:2:0.8, v/v) and the polar layer was taken to dry down and re-suspend in water. Re-suspended samples were then analyzed with mass spectrometry and fractionated with ion exchange chromatography. The collected fractions were the tested with BB170 to look for AI-2 rich fractions.

Statistical analysis

Statistical analysis was performed using GraphPad Prism 9 (Graphpad Software, Inc.).

Mann-Whitney *U*-test was used to analyze *in vivo* CFU level differences between groups. Comparisons where $P<0.05$ were considered statistically significant.

Results

Active AI-2 signals from different LuxS enzymes

AI-2s are synthesized by LuxS from 4,5-dihydroxy-2,3-pentanedione (DPD). LuxS homologues are found in more than 500 bacterial species, in both Gram-positive and Gram-negative bacteria (Pereira et al., 2013). There are different forms of active AI-2, in *Vibrio*, AI-2 molecule contains boron (Chen et al., 2002); in *E. coli* and *Salmonella* spp., AI-2 is a non-borated cyclized DPD derivative (Miller et al., 2004). To test whether if different autoinducers produced by gut commensal microbes will have different effects on *V. cholerae* colonization, we cloned *luxS* genes from a phylogenetically diverse selection of gut commensals and expressed them in *ΔluxS E. coli*. The sequences of these *luxS* homologs were codon optimized for *E. coli* and constitutively expressed under the pLtet-O1 promoter. With AI-2 being a secreted signaling molecule, supernatant was collected from *E. coli* expressing these *luxS*- and filtered. Filtered cell-free supernatants

were then detected via the BB170 (AI-1 sensor -, AI-2 sensor +) bioassay (Bassler et al., 1994). I was able to observe strong induction of bioluminescence from all of the LuxS expressing strain compare to negative control. These result indicated difference source of the LuxS enzyme are capable of producing detectable AI-2 signal (Figure2.2-2).

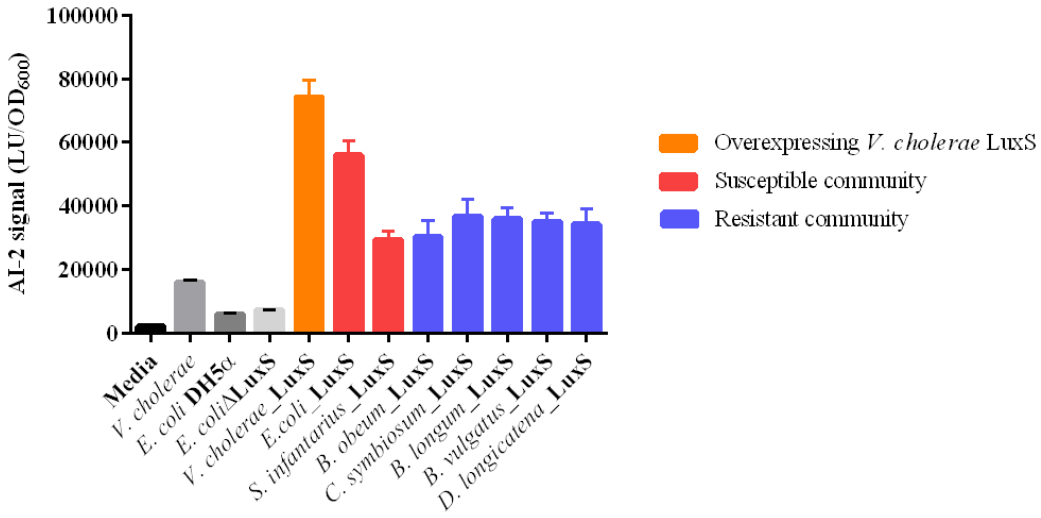

Figure 2.2-2. AI-2 signal detection from LuxS expression *E. coli* strain.
AI-2 signals from different LuxS enzymes cloned from members of human gut microbiome tested with BB170 bioassay. AI-2 signals are produced by LuxS from different strain and reported as luminescence normalized by OD_{600} of the reporter strain.

AI-2 signal dependent *V. cholerae* colonization *in vivo*

There are multiple factors that can regulate *V. cholerae* virulence and its ability to colonize the host. Hsiao et al. has found co-culturing *V. cholerae* with *E. coli* expressing *B. obeum luxS* has a reduced expression of *tcp*. *V. cholerae* has a lower colonization level

when co-colonized with *B. obeum luxS* expression strain comparing to a vector control in gnotobiotic mice (Hsiao et al., 2014). This suggested that the restriction of *V. cholerae* colonization from microbiome could also be due to AI-2 signal composition. We then focused on AI-2 signals from *Streptococcus infantarius*, strain from the susceptible model community, and *Blautia obeum* (previously classified as *Ruminococcus obeum*), strain from resistance model community that has been shown to reduce *V. cholerae* colonization in previous studies (Hsiao et al., 2014;Alavi et al., 2020) (Table 2.2-1).

Table 2.2-1. List of bacterial strains in the model community. Bold highlighted strains are the constructed *luxS* gene sequence source from the community.

Resistant	Susceptible
Dorea longicatena	***Escherichia coli***
Bacteroides Caccae	***Streptococcus infantarius***
Bacteroides vulgatus	*Enterococcus faecalis*
Dorea formicigenerans	*Streptococcus salivarius subsp. salivarius*
Collinsella aerofaciens	*Streptococcus salivarius subsp. thermophilus*
Ruminococcus torques	
Eubacterium rectale	
Faecalibacterium prausnitzii	
Bacteroides thetaiotaomicron	
Blautia obeum	
Clostridium scindens	
Bactreroides uniformis	
Bifidobacterium longum	

To test the effect of different AI-2 signal on *V. cholerae* colonization, we co-infected *V. cholerae* with different model community in an antibiotic cleared infant mice model. Consistent with previous findings, *V. cholerae* was able to colonize better with a model community that represents the disrupted microbiome (Susceptible) compared to a model community that represents a 'healthy' microbiome (Resistant) (Alavi et al., 2020). Interestingly, when introducing AI-2 signals of bacteria from the two model communities, we found that *V. cholerae* colonization level has no significant difference between susceptible community with or without the addition of *Streptococcus* AI-2, but when *B. obeum* AI-2 signal was added to the susceptible community, *V. cholerae* colonization level was significantly lower than only with susceptible community (Figure2.2-3). This suggests that LuxS enzyme from different microbes are capable of producing different AI-2 signal that could affect *V. cholerae* colonization.

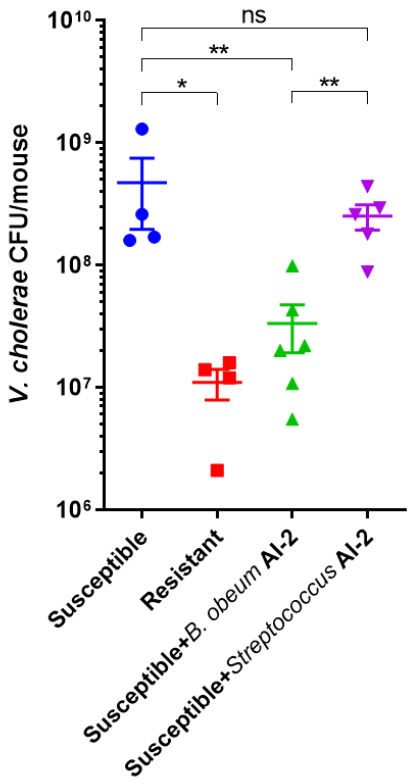

Figure 2.2-3. AI-2 produced by *B. obeum* is capable of restoring resistance against *V. cholerae* colonization in an infant mice model.
V. cholerae colonization of 5-day old infant CD-1 mice after co-gavage with model microbial mixtures. (n=3-4, *: P value<0.05, **: P value<0.01, ns: not significant).

AI-2 signal lead to differential *V. cholerae* gene expression pattern through VqmA

Given that *B. obeum* AI-2 signal is able to resist *V. cholerae* colonization, we next want to determine the mechanism. Previously Hsiao et al. observed that *V. cholerae* VqmA transcript abundance was significantly higher in *B. obeum* co-colonization compare to mono-colonized mice (Hsiao et al., 2014). VqmA has been proven to be able to regulate

the expression of VqmR and HapR (Liu et al., 2006;Papenfort et al., 2015). To further exam the interaction between *B. obeum* AI-2, *Streptococcus* AI-2, and VqmA, we overexpressed full length VqmA as well as PAS domain deleted VqmA in *V. cholerae*, cultured with cell free supernatant and collect RNA at mid-log phase. RNA-seq analysis of the expression pattern show *V. cholerae* may respond to *B. obeum* AI-2 molecules via the PAS domain and is different from *Streptococcus* AI-2 (Figure 2.2-4). This response is dominating *V. cholerae* response to *Streptococcus* AI-2. This suggests a potentially novel role of this protein in sensing several forms of autoinducers related to *V. cholerae* gene expression.

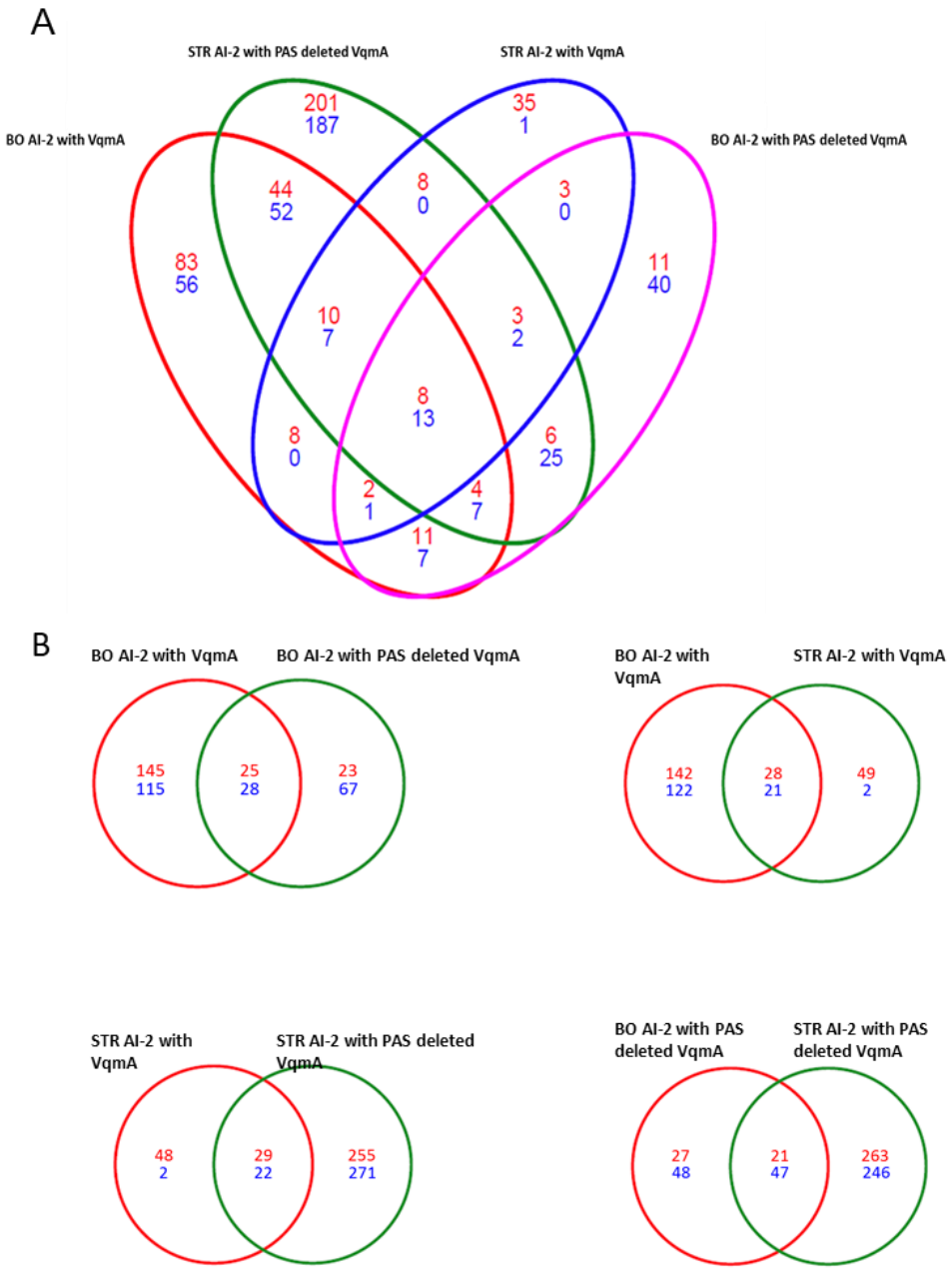

Figure 2.2-4. Gene expression pattern Venn diagram of *V. cholerae* overexpression full length or PAS truncated VqmA under different AI-2 signal.

A. Total comparison of *V. cholerae* gene expression pattern under different conditions. The numbers suggest genes being differentially regulated with the presence of AI-2 signal comparing to negative control. B. Breakdown of group comparison. Blue: number of upregulated genes; Red: number of down regulated genes. BO: *B. obeum*, STR: *Streptococcus*.

VqmA PAS domain dependent *V. cholerae* colonization

With VqmA-DPO-DNA complex crystal structure solved demonstrating the PAS domain ligand binding interaction with DPO (Wu et al., 2019a) and the suggestion from previous data, we want to look at the direct effect of *B. obeum* AI-2 on *V. cholerae* colonization through interaction with VqmA PAS domain *in vivo*. Wild type and PAS domain truncated *V. cholerae* were co-infected with *E. coli* expressing *B. obeum luxS*, *Streptococcus luxS*, and *luxS* negative control respectively. Result show that with the presence of *B. obeum* AI-2, *V. cholerae* colonization was restricted comparing with no signal present; where with *Streptococcus* AI-2, there was no significant difference in *V. cholerae* colonization level. When PAS domain is removed, this AI-2 dependent colonization difference phenotype no longer existed (Figure 2.2-5).

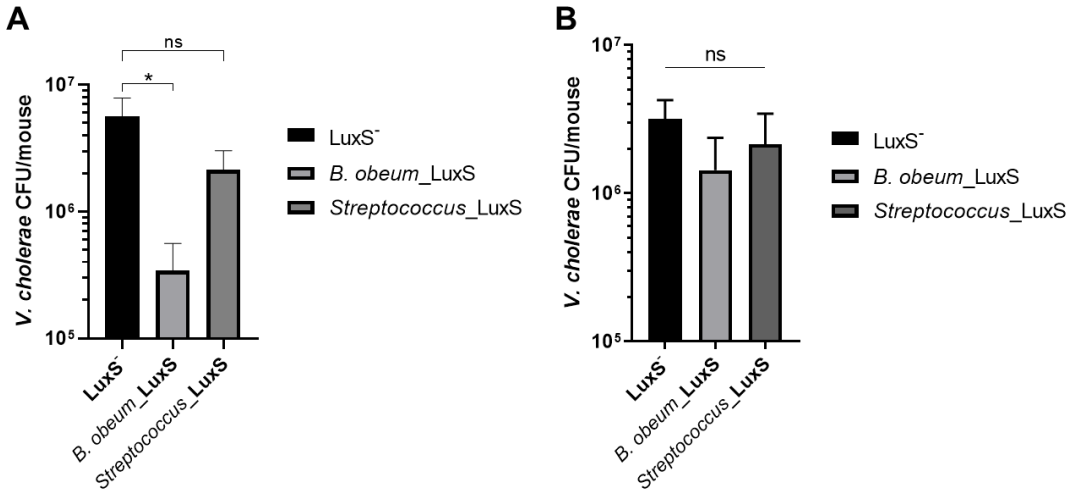

Figure 2.2-5. VqmA PAS domain dependent *V. cholerae* colonization difference in response to AI-2 signal.

A. Wild type *V. cholerae* with full length VqmA colonization level co-infected with *luxS* expression strain in infant mice intestine. B. PAS domain truncated *V. cholerae* colonization level co-infected with *luxS* expression strain in infant mice intestine. (n=5, *: P value<0.05, ns: not significant)

AI-2 signaling molecule analysis with mass spectrometry

Currently, the known AI-2 signaling molecule was identified and purified through the binding with its receptor (Chen et al., 2002;Miller et al., 2004) and culture based bioluminescence, high-performance liquid chromatography (HPLC), or mass spectrometer as a sensor system (Bassler et al., 1994;Campagna et al., 2009;Thiel et al., 2009;Song et al., 2014). We attempt to use mass spectrometry to identify possible chemical structure of both *B. obeum* and *Streptococcus* AI-2 molecule by comparing the

chemical component in cell-free supernatant when expressing respective *luxS* gene while using LuxS$^-$ *E. coli* as background. We were only being able to find a peak that showed up in both AI-2 expression strain that was unique to LuxS$^-$ strain at 213.96 m/z while there was a significant amount of background noise. The evidence suggests this molecule could have a SO_3 group, but we were unable to determine the structure and the fact that it exists in both *luxS* expression strains, it is unlikely to be the AI-2 molecule. We also try to fractionate the supernatant in order to reduce background noise. The fractions collected was then tested with BB170 assay to identify potential target fraction that contain AI-2 molecules. Unfortunately, none of the fraction showed induction of luminescence in BB170 bioassay. This could be due to low abundance of the molecule or potentially unstable structure of the molecule.

Discussion

Increasing evidence demonstrated the importance of gut microbiome composition influencing host defense against pathogens in a wide variety of mechanism (Cho et al., 2021). There are multiple factors that could affect *V. cholerae* fitness from gut

microbiome either directly or indirectly. In this chapter, we show quorum sensing dependent regulation of *V. cholerae* gene expression and colonization through transcription factor VqmA. *V. cholerae* fitness to host infection is mediated by the structure of gut microbiome. A more diverse community that represents a healthy human microbiome is capable of restricting *V. cholerae*'s ability to colonize host compare to a less diverse community that are similar to a dysbiotic microbiome (Alavi et al., 2020). The introducing of exogenous signal produced from *B. obeum* AI-2 synthase, *luxS*, to the susceptible microbiome restores the restriction phenotype (Figure 2.2-3). The expression of *B. obeum luxS* gene has shown to induce the expression of *V. cholerae* transcription factor, VqmA (Hsiao et al., 2014). By analyzing VqmA amino acid sequence, it was previously identified as a LuxR family transcriptional regulator. LuxR type proteins were first described as quorum sensing related pheromone receptor and transcription regulators in *V. fischeri* in 1983 (Engebrecht et al., 1983). LuxR and its homolog has been found involved in QS in multiple bacteria and leads to various downstream regulation. This type of protein has a characteristic structure of DNA binding site at carboxyl terminus and a AI binding site at amino terminus (Fuqua et al., 1996;Patankar and Gonzalez, 2009). As a LuxR-type protein, VqmA contains a Per-Arnt-Sim (PAS) ligand binding domain, a

common domain found in signaling protein involved in signal transduction, and a DNA-binding domain (Papenfort et al., 2017;Wu et al., 2019a). The PAS domain is an important sensor domain that can be involved in monitoring various environmental factors including light, oxygen level, redox status, chemical ligand, as well as energy level (Glagolev, 1980;Baryshev et al., 1981;Taylor, 1983). VqmA is able to bind to DPO (3,5-dimethylpyrazin-2-ol) synthesized by Tdh (threonine dehydrogenase) from threonine and alanine (Ma and Ma, 2019) and lead to increasing expression of small regulatory RNA VqmR. Co-crystallization of VqmA-DPO-DAN indicated a VqmA dimer bound to two DPO molecules mainly through hydrophobic interactions. The hydroxyl of DPO was fixed by Lys-101 and six-membered ring was sandwiched by Phe-99 and Phe-67 (Wu et al., 2019a). Huang et al. showed that VqmA contain basal transcriptional activity without binding to DPO, the interaction with DPO leads to VqmA conformational change and increase in activity (Huang et al., 2020). Other than interacting with DPO, VqmA regulation strength is also influenced by oxygen level, bile salts, and redox. The change in theses environmental cues alters VqmA DNA binding activity through altering disulfide bond formation and leads to the regulation of biofilm structural gene *vpsL* and toxin coregulated pilus gene *tcpA* expression (Mashruwala and Bassler, 2020). Our data

suggests that VqmA could also interacts with *B. obeum* AI-2 signal through PAS ligand binding domain and alters *in vivo* colonization level in *V. cholerae* (Figure 2.2-4,5). Based on the research done by Huang et al., 2′-hydroxyl or 2′-carbonyl group is necessary for binding and promoting VqmA activity and the structure of DPO (Huang et al., 2020), we could hypothesize that the structure of *B. obeum* AI-2 is more similar to the non-borate version. Amino acid alignment also demonstrated *B. obeum* LuxS has a higher similarity against *E. coli* LuxS and a conserved binding site. With these information, we could adjust the experimental set up for mass spectrometry to try to identify *B. obeum* AI-2 structure. The understanding of AI-2 signaling molecules interspecies communications are very limited due to the difficulty of isolating AI-2 molecule, a receptor pair is required in order to identify a AI-2 molecule structure by crystallography. By further adjusting the conditions, the combination of both detection and fractionating supernatants containing AI-2 molecules could potentially identify these molecules in a more efficient manner.

Chapter 3.1 Quorum sensing effect on microbiome composition

Introduction

Quorum sensing (QS) is a signal communication process in the bacterial community, and this is currently a developing field in which we are slowly building up our understanding of how the process works. QS controls multiple bacterial behaviors, including bioluminescence, competence, biofilm formation, virulence expression, and more, through sensing signaling molecules called autoinducers (AIs) in the environment. Gram-positive bacteria intra-species communication is via using autoinducer peptides (AIPs) as signaling molecules, which can range from 5 to 17 amino acids and in the form of circular or linear (Okada et al., 2005;Bouillaut et al., 2008;Thoendel et al., 2011;Rutherford and Bassler, 2012). Unlike Gram-positive bacteria, Gram-negative bacteria use acyl-homoserine lactones (AHLs) that have a N-acylated homoserine-lactone ring structure and with the 4–18 carbon acyl chain modifications (von Bodman et al., 2008;Galloway et al., 2011). This process also occurs between different species. LuxS, the enzyme that catalyzes the production of autoinducer 2 (AI-2) signaling molecule, was found present among Gram-positive bacteria and Gram-negative bacteria (Pereira et al.,

2013). It has been shown that the expression of *B. obeum luxS* gene alone is capable of inhibiting *V. cholerae* colonization in the germ-free mouse model (Hsiao et al., 2014), indicating direct inter-species communication.

The composition of the gut microbiome is associated with human diseases and the host's ability to resist gut pathogen colonization (Hsiao et al., 2014;Jandhyala et al., 2015). Experiments conducted by Thompson et al. have shown that by using *E. coli* to alter signal levels, AI-2 can modulate the structure of gut microbiota, influencing bacterial behaviors and restoring the balance between Bacteroidetes and Firmicutes (Thompson et al., 2015;Thompson et al., 2016). Although with the increasing research on the QS process, the understanding of these environmental signaling molecules' role in mediating microbiome structure in a healthy configuration and providing protection against pathogens is still limited.

Here, I infected germ-free mice with defined model community and human fecal sample with the presence of LuxS expressing strain then analyzed microbiome structure and gene expression pattern. The result indicated that exogenous AI-2 will shift the microbiome structure and alters overall bacterial behavior.

Method

Bacterial culture condition

All *E. coli* strains are inoculated in LB media and grown overnight under 37℃ at 250 rpm for subsequent experiments. Anaerobic strains were grown at 37℃ in a Coy chamber under anaerobic conditions (5% H_2, 20% CO_2, balance N_2) in LYHBHI media (BHI supplemented to 5g/L yeast extract, 5mg/L hemin, 1mg/mL cellobiose, 1mg/mL maltose, and 0.5mg/mL cysteine-HCl) (Alavi et al., 2020). All anaerobic strains were inoculated in LYHBHI media and grown for 48 hours, then 1:100 subcultured into fresh media and grown for another 48 hours before gavage.

Animal experiment

Germ-free C57BL/6J mice were bred and maintained in plastic gnotobiotic isolators at the University of California, Riverside. 5-8 week old mice were fasted for 30 minutes and gavaged with 100µl 1M $NaHCO_3$ 20 min prior to introduction bacteria. An equal amount of culture density between resistant, susceptible, and AI-2 producing *E. coli* strains were normalized based on $OD_{600,}$ then pooled, pelleted by centrifuge, and resuspended in fresh LYHBHI. Human fecal slurries were normalized so that each adult mouse received ~16µg

of microbial genomic DNA and ~10^9 CFU AI-2 producing *E. coli*. Fecal pellets were collected across the course of the experiment. Mice were sacrificed 4 or 14 days after the introduction of bacteria, and three equal sections of the small intestine were collected. Samples were homogenized in PBS for CFU counts on LB agar plates.

DNA extraction and 16S sequencing

For fecal samples, pellets were resuspended in 500µl PBS and used for DNA extraction. For intestinal samples, the small intestine was separated into three sections according to length and homogenized in 5ml PBS, 500µl of homogenates were used for DNA extraction. ~500µl 0.1mm glass beads (BioSpec), 210µl SDS %20, and 500µl neutral phenol:chloroform:isoamyl-alcohol (24:24:1, Fisher Scientific) were added to each sample, and samples were then purified as described previously (Hsiao et al., 2014).

Bacterial 16S ribosomal RNA gene V4 variable region was amplified in 25µl of PCR reaction using 1µl of extracted DNA as the template, 10µl Platinum Hot Start PCR Master Mix (ThermoFisher), 13µl PCR-grade water, and 0.5µl of forward and reverse primers (10 µM). PCR cycle conditions were 94°C for 3 min, followed by 30 cycles (94°C for 45 sec, 50°C for 60 sec, 72°C for 90 sec), and 72°C for 10 min, then hold at

4°C. An equal amount of each amplicon was pooled and purified using QIAquick PCR purification columns (Qiagen) and then sequenced with the Illumina MiSeq platform.

Quantitative PCR to determine bacteria and AI-2 strain abundance

To determine the bacterial load, DNA extracted from the fecal pellet and distal intestine was used as the template for the qPCR assay. Universal 16S primer set (Forward: 5'-GTGSTGCAYGGYTGTCGTCA -3', reverse: 5'- ACGTCRTCCMCACCTTCCTC -3') (Horz et al., 2005) was used to determine total bacterial load and AI-2 strain-specific primers, *E. coli luxS* mutant (No signal) (Forward: 5'- CGCCTGTTAATCGCCAATTT -3', reverse: 5'- AAAAGAATGCCAGGTTGAACG -3'), *B. obeum luxS* expresser (BO_LuxS) (Forward: 5'- GTATGACCAGCCCGAATGAA -3', reverse: 5'-CGGACCAAATTCTGCATGATTAC -3'), and *S. infantarius luxS* expresser (STR_LuxS) (Forward: 5'- CCATTGTGAAAGCACCGTATG -3', reverse: 5'-GCTGCACCAGACGAATATCA -3') to determine each AI-2 producing strain. Quantitative PCR reaction was performed in triplicates and consisted of 12.5 µL of iQ SYBR Green Supermix (BIO-RAD2, Hercules, CA), 0.25 µL of forward and reverse

primers at 10 µM concentration, 10 µL nuclease-free water and 2 µL of DNA (250 ng/µL).

RNA extraction and RNA-seq library preparation

Total RNA was extracted from fecal pellets resuspended in nuclease-free water and 500µl of homogenized distal small intestinal tissue using TRIzol according to manufacturer instructions. DNA was removed by Baseline-ZERO DNase (Lucigen) digestion and purified with TRIzol. Sequencing libraries were prepared using Stranded Total RNA Prep with Ribo-Zero Plus (Illumina), analyzed using Agilent Bioanalyzer, and 75 bp single read sequencing was performed on Illumina NextSeq500.

16S sequencing analysis

All 16S sequencing libraries were analyzed using QIIME 2 version 2022.2, where sampling depth was set at 1000 (Bolyen et al., 2019). Visualization of PCoA plots was performed using ggplot2 (Wickham, 2016).

RNA-Seq analysis

Taxonomic profiling of the microbial community was analyzed with MetaPhlAn3 (Beghini et al., 2021), of which a species' value depends on its overall genomic abundance and the average transcriptional level of its unique marker genes. Functional profiling of transcript was done using HUMAnN3 (Beghini et al., 2021), and the cpm of the gene family and the pathway abundance was used for the following analysis. Statistical analysis of gene differential expression was performed using MaAslin2 (Mallick et al., 2021), with the settings: model=NEGBIN, normalization=NONE, min-prevalence=0.1, min-abundance=0.0001.

Results

AI-2 signal shifts microbiome structure

Gut microbes are capable of modifying AI-2 pools in the gut via synthesis and scavenging which in turn can alter community composition (Sperandio et al., 2003;Thompson et al., 2015). To determine the specific impacts of AI-2 produced by gut Firmicutes associated with V. cholera resistance or susceptibility we used LuxS mutant *E.*

coli as control (no signal) and expressed *luxS* gene of *S. infantarius* (STR_LuxS) or *B. obeum* (BO_LuxS) co-gavaged with both resistant and susceptible model community (Table 3.1-1) into germ-free mice and collected fecal pellets along the course of the experiment and sacrificed the animals at day 14.

Table 3.1-1. Model community strains used in the germ-free experiment.

Resistant	Susceptible
Dorea longicatena	*Enterococcus faecalis*
Bacteroides caccae	*Streptococcus salivarius*
Bacteroides vulgatus	*Streptococcus infantarius*
Dorea formicigenerans	*Streptococcus thermophilus*
Collinsella aerofaciens	
Blautia torques	
Eubacterium rectale	
Faecalibacterium prausnitzii_cc	
Bacteroides thetaiotaomicron- VPI	
Blautia obeum	
Clostridium scindens	
Bacteroides uniformis	

We examined total bacterial abundance using qPCR targeting 16S DNA, there was no difference in whole bacterial load in earlier time points and distal small intestine at the time of collection, but after day 7 there was a significant difference between with and without signal groups (Figure 3.1-1A-B). The AI-2 producer and non-producer *E. coli* loads were significantly different in fecal pellets, not distal small intestine, but when

counting CFUs, no signal strain was not detectable (Figure 3.1-1C-D, and G). When looking at the relative abundance of the signal strains, the was no difference between the AI-2 producing strains where non-producer was significantly lower than the other two groups fecal samples, and showed no difference between the three groups in the distal small intestine (Figure 3.1-1E-F).

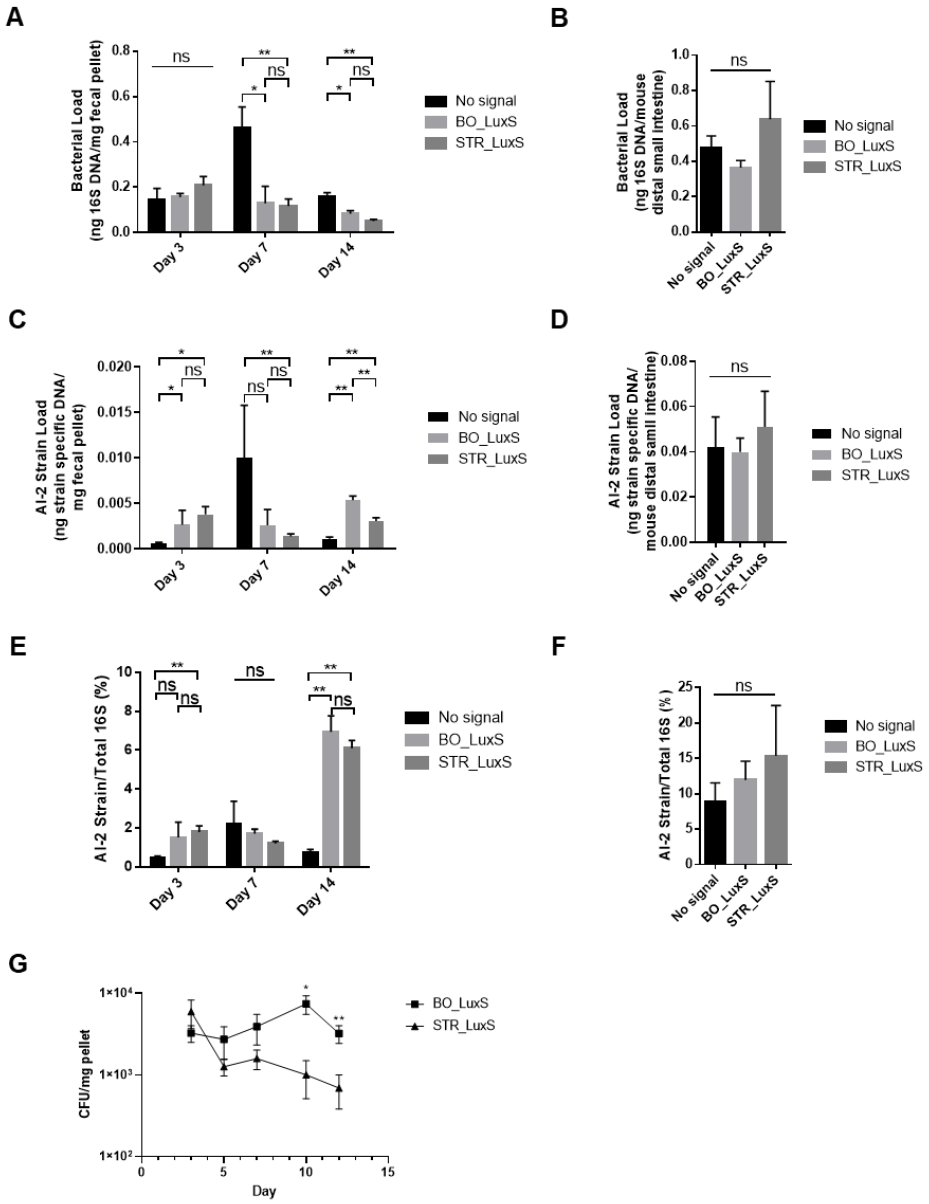

Figure 3.1-1. Total bacterial and AI-2 signal strain 16S DNA load in adult germ-free mice containing indicated microbiomes.

Total Bacterial 16S DNA load in A. fecal pellets, B. distal small intestine. Total AI-2 expressing strain load in C. fecal pellets, D. distal small intestine. Percentage of AI-2 producing strain to total bacterial load in E. fecal pellets, F. distal small intestine. G. AI-2 producing *E. coli* CFU in fecal pellets. (Mann-Whitney U-test, *. P<0.05; **: P<0.01; ns: not significant; No signal: *luxS* mutant *E. coli* group; BO_LuxS: *B. obeum luxS* expressing *E. coli* group; *S. infantarius luxS* expressing *E. coli* group)

We then identified gut microbiome structure by 16S sequencing. Results show that on day 3 there was no significant separation between with or without the addition of AI-2 nor with the AI-2 source. The microbiome structure started to diverge with the addition of AI-2 by day 7 post-gavage. Both fecal pellet and distal small intestine showed strong differences at day 14, while some samples from community with BO_LuxS overlapped with no signal group in the distal small intestine (Figure 3.1-2). While pairwise unweighted UniFrac distances showed the same trend, on day 14, fecal pellet showed significance between the two signals with STR_LuxS closer to no signal group (Figure 3.1-3). These results suggest that the AI-2 signal can shape the microbiome structure, but either the difference between *B. obeum* AI-2 and *S. infantarius* AI-2 is insignificant or, due to the low abundance of the producer, is not capable of diverging between the two after 14 days of colonization. Further analysis of microbiome composition with analysis of the composition of microbiomes (ANCOM) indicated that *Faecalibacterium prausnitzii* was statistically difference between the groups. *F. prausnitzii* percentile abundances are lower in the two *luxS* expression groups compared to the no signal group. Based on the KEGG database, although *F. prausnitzii* contains

LuxS enzyme, the two known AI-2 receptor was not found. *F. prausnitzii* abundance may be affected by the AI-2 signal through a non-direct regulation due to the change in other microbial behavior.

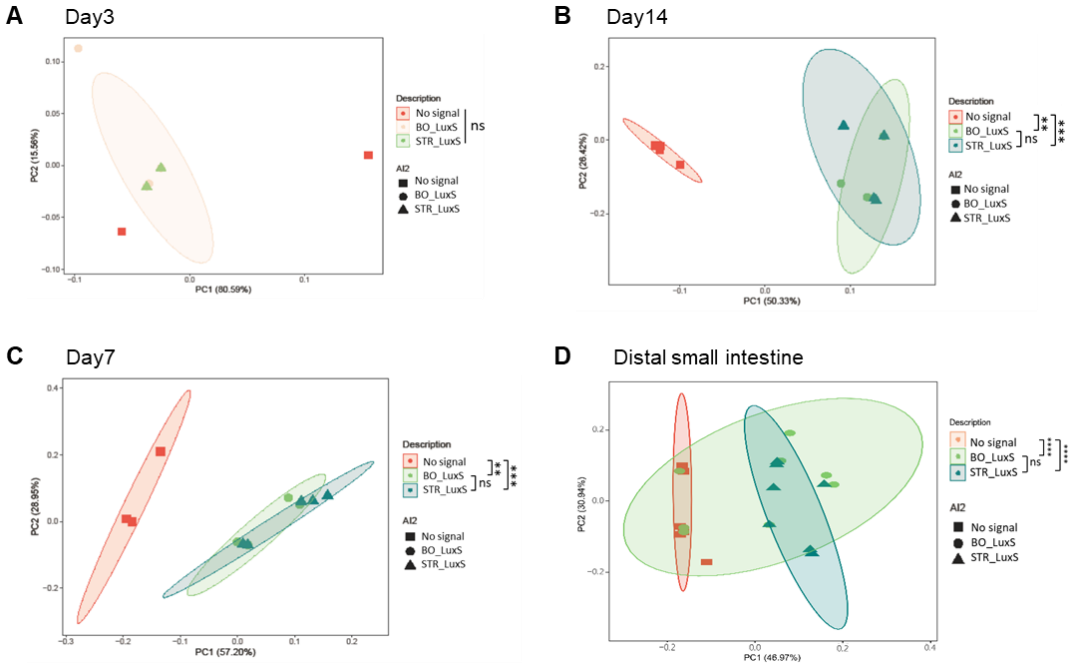

Figure 3.1-2. The addition of AI-2 drives microbiome structure change.
Principal coordinates analysis (PCoA) of microbiome community diversity based on unweighted UniFrac distance of A-C. fecal pellet sample collected days post-inoculation of bacteria into germ-free mice as labeled, and D. distal small intestine. % variance explained shown in each axis; Ellipses show 95% confidence intervals. (**: P<0.01; ***: P<0.005; ****: P<0.0001; ns: not significant; No signal: *luxS* mutant *E. coli* group; BO_LuxS: *B. obeum luxS* expressing *E. coli* group; *S. infantarius luxS* expressing *E. coli* group)

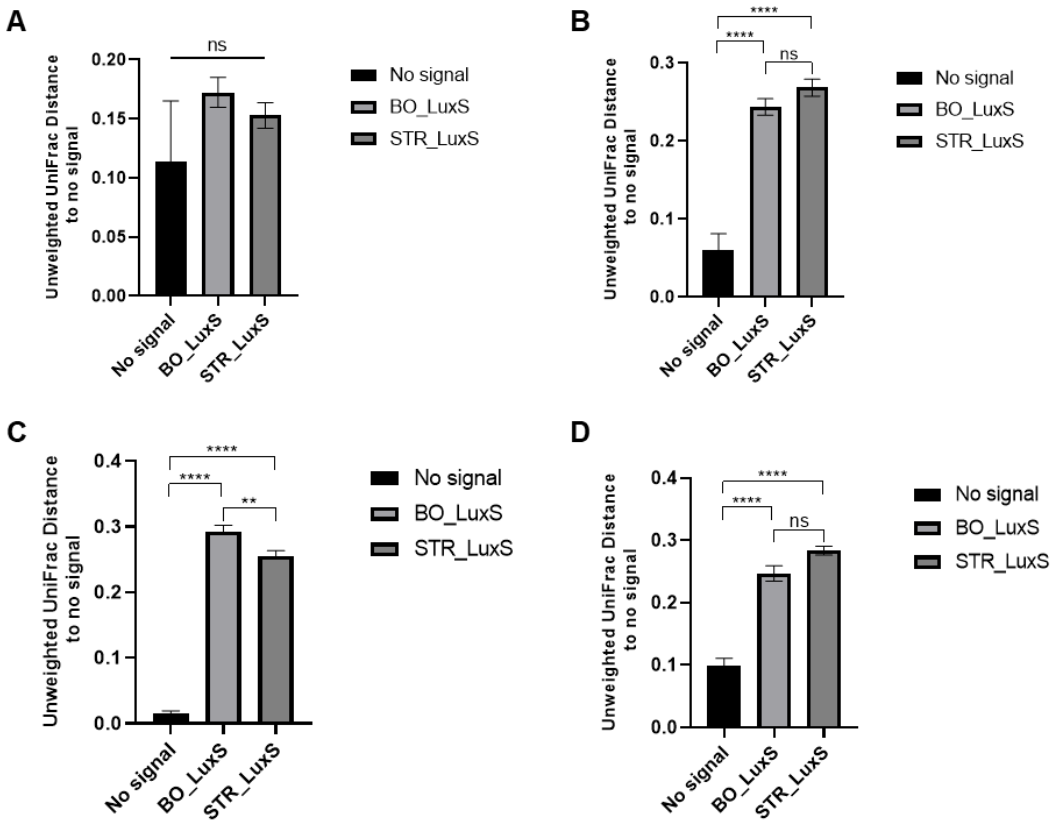

Figure 3.1-3. Pairwise unweighted UniFrac distances to no signal samples.
A. day 3, B. day 7, day 14 post-inoculation of bacteria into germ-free mice, and D. distal small intestine. (Mann-Whitney U-test, **: P<0.01; ***: P<0.005; ****: P<0.0001; ns: not significant; No signal: *luxS* mutant *E. coli* group; BO_LuxS: *B. obeum luxS* expressing *E. coli* group; *S. infantarius luxS* expressing *E. coli* group)

Except for using a model community, we also inoculated from healthy human donors' communities using fecal pellet slurries and co-gavaged with AI-2 producing *E. coli* strains. We included two donors that were shown to possess differences in the ability to restrict *V. cholerae* colonization (Alavi et al., 2020). Human donor A was slightly

different in total 16S DNA load (Figure 3.1-4A-B) with AI-2 expressing strain showed no difference in bacterial load between the two expressers, but when comparing relative abundances to total bacterial *B. obeum luxS* expressing strain was higher (Figure 3.1-4C-F). We also observed that the signal expressing *E. coli* has colonization dropped by three logs by day 4 post-gavage and with about 10^2 CFU in the distal small intestine (Figure 3.1-4G-H).

16S sequence analysis on the fecal samples showed a difference between no signal with *S. infantarius* AI-2 in fecal samples on day 3 based on PCoA results. On day 4, the fecal sample indicated the addition of *B. obeum* AI-2 drives the structure to be different from the other two groups, but the microbiome in the distal small intestine showed no difference between the groups. Pairwise unweighted UniFrac distances analysis showed no significant difference between the groups at different time points (Figure 3.1-5).

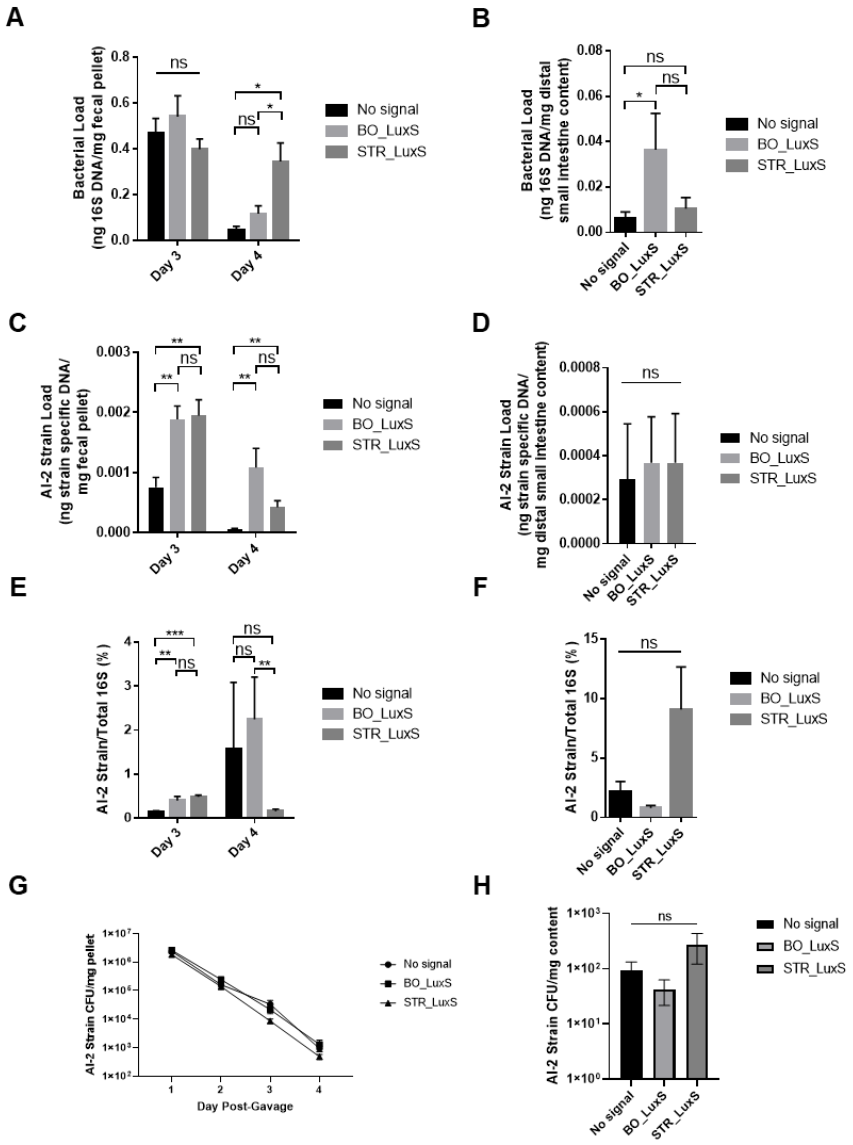

Figure 3.1-4. Total bacterial and AI-2 signal strain 16S DNA load in adult germ-free mice with human donor A fecal microbiome.

Total Bacterial 16S DNA load in A. fecal pellets, B. distal small intestine. Total AI-2 expressing strain load in C. fecal pellets, D. distal small intestine. Percentage of AI-2 producing strain to total bacterial load in E. fecal pellets, F. distal small intestine. AI-2 producing *E. coli* CFU in G. fecal pellets, H. distal small intestine. (Mann-Whitney U-test, *. P<0.05; **: P<0.01; ***: P<0.005 ns: not significant; No signal: *luxS* mutant *E. coli* group; BO_LuxS: *B. obeum luxS* expressing *E. coli* group; *S. infantarius luxS* expressing *E. coli* group)

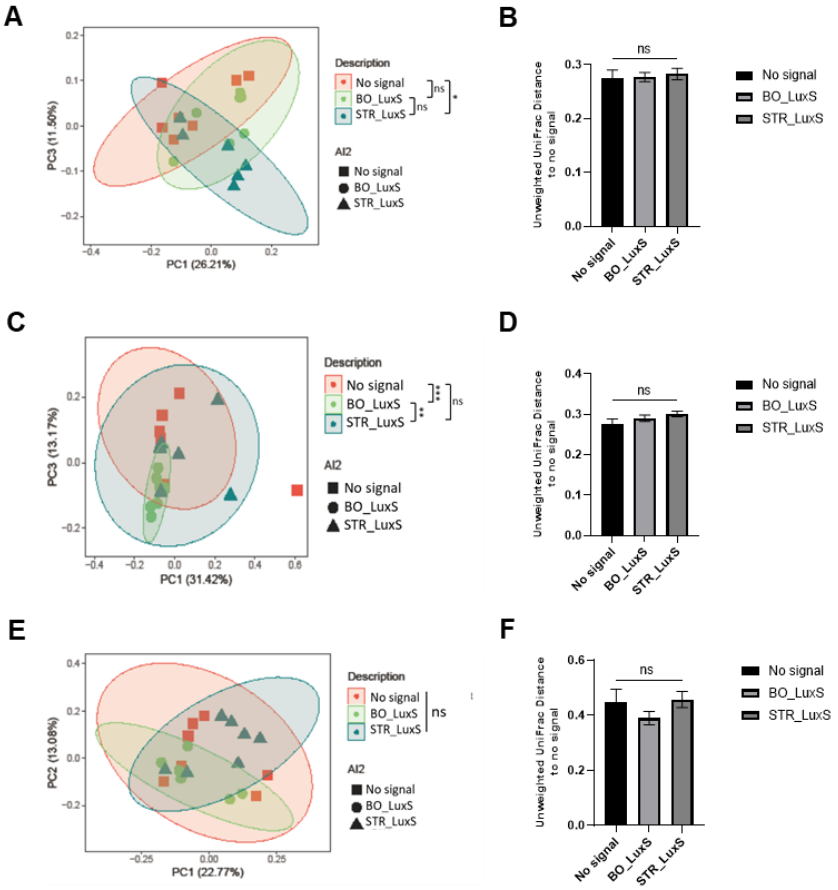

Figure 3.1-5. Human donor A PCoA and Pairwise unweighted UniFrac distances analysis.

PCoA plot of A. day 3 fecal pellet, C. day 4 fecal pellet, E. distal small intestine sample. Pairwise unweighted UniFrac distances of B. day 3 fecal pellet, D. day 4 fecal pellet, F. distal small intestine sample. (*. P<0.05; **: P<0.01; ***: P<0.005; ns: not significant; No signal: *luxS* mutant *E. coli* group; BO_LuxS: *B. obeum luxS* expressing *E. coli* group; *S. infantarius luxS* expressing *E. coli* group)

Human donor B showed no significant difference in total bacterial load and no difference between the two AI-2 producing strains, but both were higher than the non-producing strain (Figure 3.1-6A-F). CFU counts also showed that non-producing strain

was not detectable after 4 days in both fecal pellet and distal small intestine (Figure 3.1-6G-H). Unlike donor A, donor B PCoA showed no difference in the fecal samples. The distal small intestine content indicated a difference between no signal and *S. infantarius* AI-2 group pairwise unweighted UniFrac distances analysis indicated a difference between the two AI-2 signal added groups (Figure 3.1-7). This difference in microbiome response to AI-2 signal between the two donors could be due to microbiome composition variation leading to the disparity of microbial behavior.

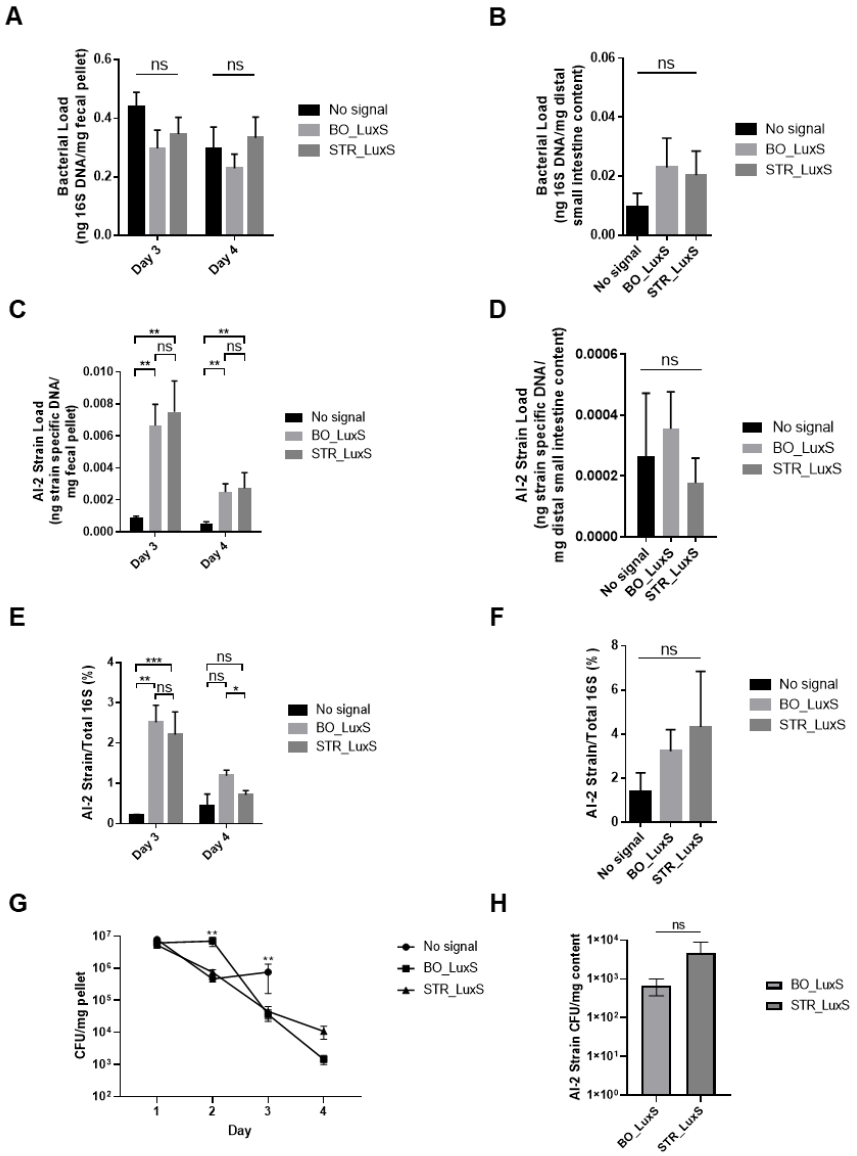

Figure 3.1-6. Total bacterial and AI-2 signal strain 16S DNA load in adult germ-free mice with human donor B fecal microbiome.

Total Bacterial 16S DNA load in A. fecal pellets, B. distal small intestine. Total AI-2 expressing strain load in C. fecal pellets, D. distal small intestine. Percentage of AI-2 producing strain to total bacterial load in E. fecal pellets, F. distal small intestine. AI-2 producing *E. coli* CFU in G. fecal pellets, H. distal small intestine. (Mann-Whitney U-test, *. P<0.05; **: P<0.01; ***: P<0.005 ns: not significant; No signal: *luxS* mutant *E. coli* group; BO_LuxS: *B. obeum luxS* expressing *E. coli* group; *S. infantarius luxS* expressing *E. coli* group)

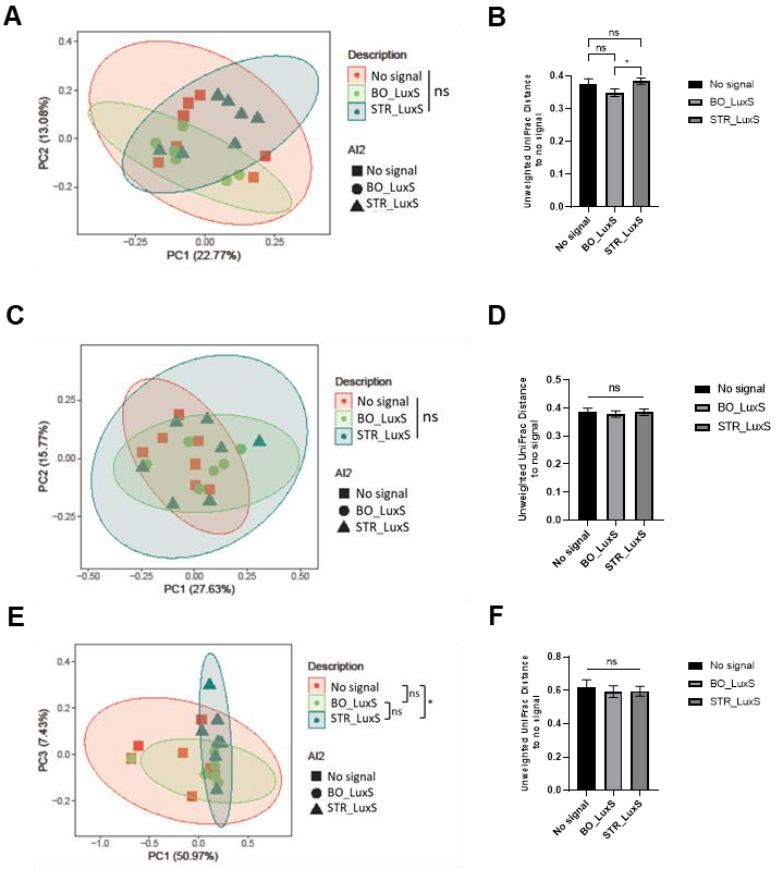

Figure 3.1-7. Human donor B PCoA and Pairwise unweighted UniFrac distances analysis.

PCoA plot of A. day 3 fecal pellet, C. day 4 fecal pellet, E. distal small intestine sample. Pairwise unweighted UniFrac distances of B. day 3 fecal pellet, D. day 4 fecal pellet, F. distal small intestine sample. (*. P<0.05; **: P<0.01; ***: P<0.005; ns: not significant; No signal: *luxS* mutant *E. coli* group; BO_LuxS: *B. obeum luxS* expressing *E. coli* group; *S. infantarius luxS* expressing *E. coli* group)

AI-2 signal leads to different transcriptional activity

Given that the presence of the AI-2 signal is capable of changing the structure of the microbiome, we further analyzed the transcriptomic pattern from the model community

sample of the day 3 pellets. When comparing the relative abundance of each community strain based on 16S analysis and Metatranscriptomics analysis, we found that while *Bacteroides* spp. has a relatively high relative abundance but the transcript abundance was low. In comparison, *B. obeum* was not the most abundant strain in the microbiome, but its transcript was most abundant, being close to 50% of total transcripts (Figure 3.1-8). Although we did not observe a significant difference between each group based on 16S analysis (Figure 3.1-4A), Metatranscriptomics analysis showed diverging from with or without exogenous AI-2 signal on day 3 (Figure3.1-9).

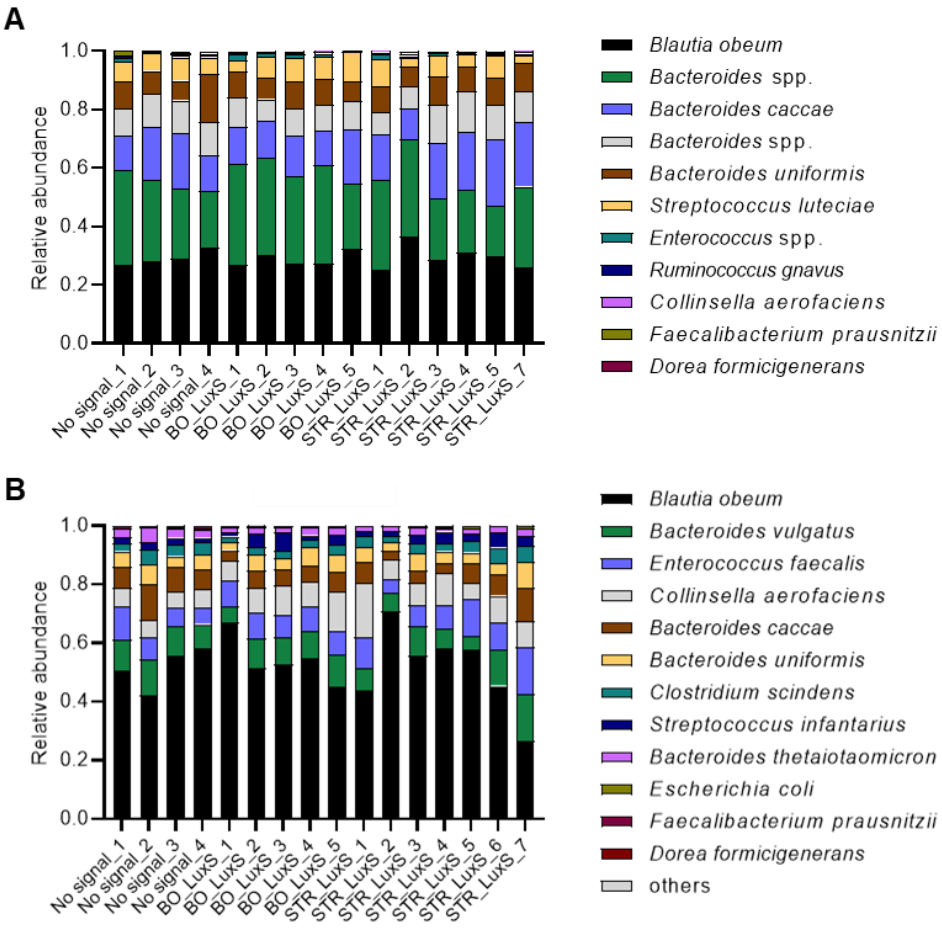

Figure 3.1-8. Bacterial activity was different from the structure.
Relative abundance of each strain based on A. 16S sequencing analysis, B. RNA-seq Metatranscriptomics analysis of day 3 fecal pellet total transcripts of defined model communities.

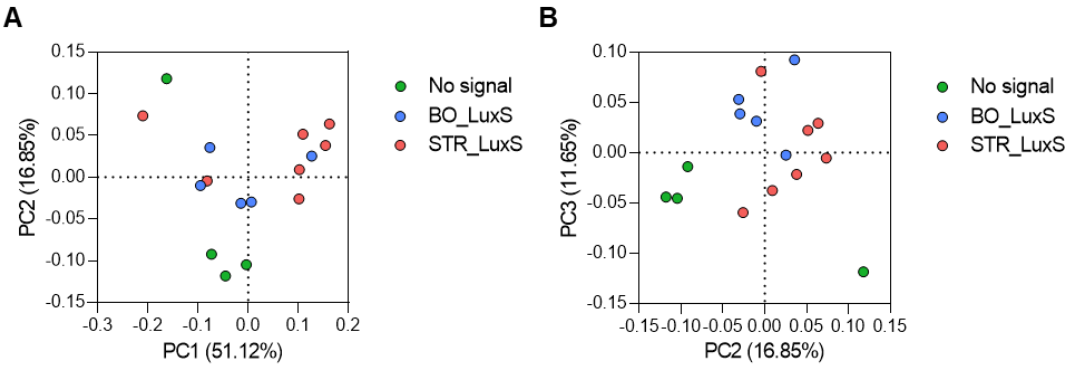

Figure 3.1-9. PCoA of microbiome Metatranscriptomics analysis.
PCoA plot of day 3 fecal pellet with A. PC1 and PC2, B. PC2 and PC3 based on Bray Curtis distance.

When comparing to the no signal group, Metatranscriptomics analysis demonstrated that the differences in transcript expression patterns were different between the two signals. Although most of the transcripts are unidentified proteins, the microbiome in both signal groups increases metabolic-related proteins like cysteine synthase. In STR_LuxS, DNA-binding protein HU which is involved in multiple bacterial survival-related mechanisms, growth, virulence genes expression, and many other processes was upregulated (Stojkova et al., 2019), potentially indicating that *S. infantarius* AI-2 induces bacterial survival and virulence direct or indirectly (Figure 3.1-10).

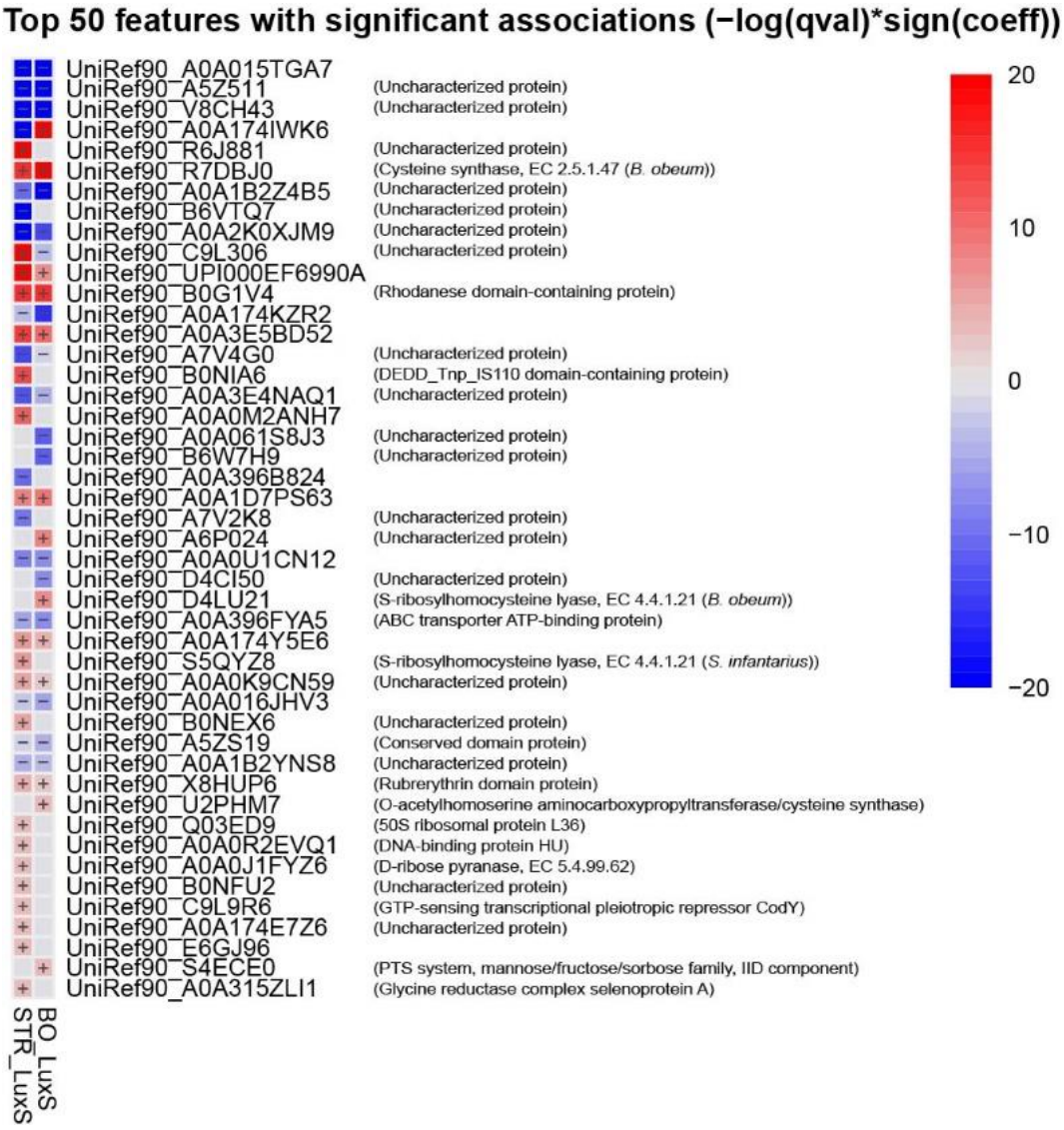

Figure 3.1-10. Metatranscriptomics analysis showing features that are significantly different using no signal group as control.

Scale represents -log(qvalue)*sign(coeff), positive value indicating upregulation, negative value indicating downregulation.

When directly comparing the two signal groups, fewer features were significantly different most of them being uncharacterized protein. However, BO_LuxS shows to have

higher cysteine synthase expression than the STR_LuxS and the LuxS enzyme (Figure 3.1-11). The synthesis of the AI-2 molecule is catalyzed by LuxS cleaving S-ribosylhomocysteine (SRH) into homocysteine and 4,5-dihydroxy-2,3-pentanedione (DPD). DPD is an unstable linear molecule and will spontaneously cyclize and form the final AI-2 molecule (Schauder et al., 2001;Chen et al., 2002;Winzer et al., 2002) (Figure 3.1-12). Although the gene is identified as *B. obeum* cysteine synthase and LuxS enzyme, most likely coming from the *B. obeum luxS* expressing strain, these results could still potentially suggest the overall change in global quorum sensing, metabolism, and growth. More detailed analysis on individual bacterial gene expression is needed.

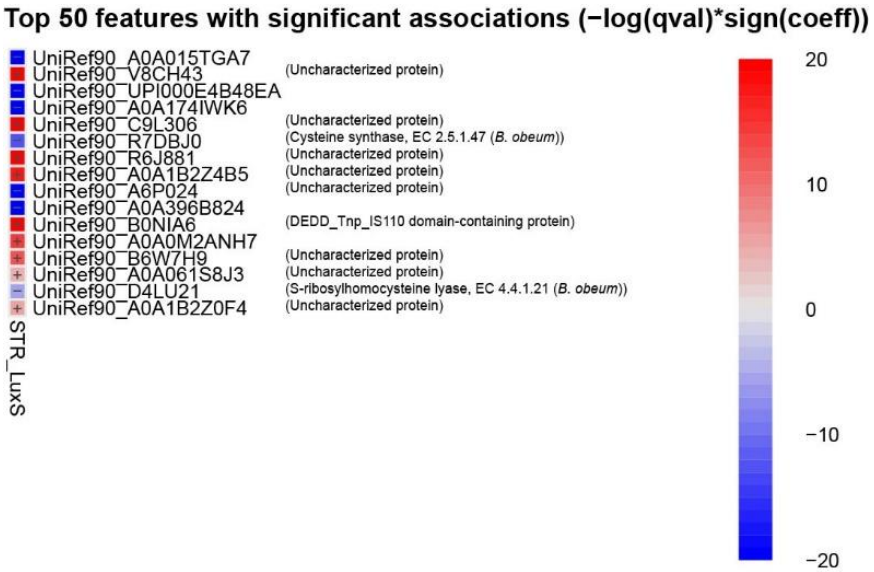

Figure 3.1-11. Metatranscriptomics analysis showing features that are significantly different between AI-2 signal groups.
Scale represents -log(qvalue)*sign(coeff), positive value indicating upregulation, negative value indicating downregulation

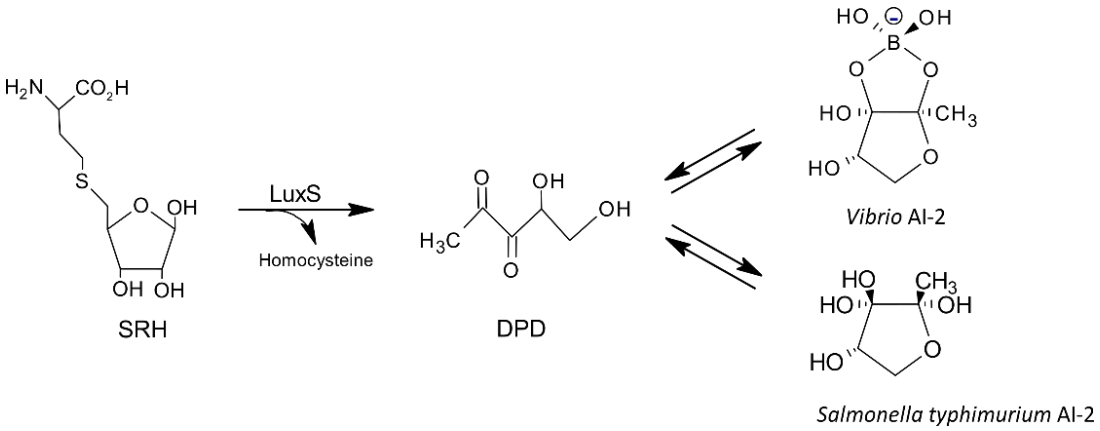

Figure 3.1-12. AI-2 biosynthesis pathway.

Discussion

With building evidence indicating human gut microbiota affects the host's ability to defend against pathogen infection, multiple factors could lead to the alteration of microbiome composition (Cho et al., 2021). This chapter focused on the AI-2 signaling molecule, expressed by both Gram-positive and Gram-negative bacteria. Currently, AI-2 molecules are found in two forms, a boron-containing and a non-borated cyclized DPD derivative (Miller et al., 2004). The manipulation of AI-2 levels changes microbiome structure and gene expression (Xavier and Bassler, 2005a;Thompson et al., 2015). By introducing *luxS* mutant *E. coli* and expressing *luxS* gene from *B. obeum* and *S. infantarius,* results show that adding exogenous AI-2 source will start to shift model

microbiome structure 7 days post-inoculation (Figure 3.1-2,3) and the change of the structure could be through an indirect mechanism.

Results also suggest the ability of AI-2 signal effecting microbiome structure depends on the microbiome's overall composition (Figure 3.1-5,7). Analyzing the gene expression profile at day 3 post-gavage demonstrated that bacteria's relative abundance is quite different from transcripts. This difference suggests that although with low abundance, certain bacteria can be more active and potentially plays a critical role (Figure 3.1-8). Although the microbiome structure has not yet started to diverge significantly on day 3, adding AI-2 shifts gene expression patterns away from the control group (Figure 3.1-9). Interestingly, we found that DNA-binding protein HU, involved in bacterial survival and growth (Stojkova et al., 2019), was upregulated in *S. infantarius luxS* expression group (Figure 3.1-10). We also observed the differential expression of genes involved in the biosynthesis of AI-2, suggesting regulating the global AI-2 level (Figure 3.1-10,11). Further analysis of Metatranscriptomics of different microbes are need to gain more information on the impact of each strain.

Research has indicated the microbiome's importance in defending and regulating the host response against pathogen infection (Hsiao et al., 2014;Alavi et al., 2020), and

with increasing evidence showing that the QS process alters the microbiota structure, transcriptomic behavior, and host immune response (Thompson et al., 2015;Zargar et al., 2015;Li et al., 2019), understanding the QS process in controlling bacterial behavior within the microbiome has become more crucial.

Chapter 3.2 Enrichment of Quorum Sensing Pathway in Gut Microbiome Associated with Response to Immune Checkpoint Inhibitor Treatment

Jennifer Y. Cho[2,3,15] Xunhui Cai[1,15],, Lijun Chen[4], Yufeng Liu[1], Fenghu Ji[1], Katia Salgado[2], Siyi Ge[2], Dehua Yang[5], Hui Yu[6,7], Jianbo Shao[6], Ming-Wei Wang[5], P. Andrew Futreal[8], Boris Sepesi[9], Don Gibbons[10], Yaobing Chen[11], Guoping Wang[11,12], Chao Cheng[13], Meng Wu[14,*], Jianjun Zhang[8,10,*], Ansel Hsiao[2,*], Tian Xia[1,11,12,*]

Affiliations:

[1]School of Artificial Intelligence and Automation, Huazhong University of Science and Technology, Wuhan, China

[2]Department of Microbiology and Plant Pathology, University of California, Riverside, Riverside, USA

[3]Department of Biochemistry, University of California, Riverside, California, USA

[4]Department of Pathology, School of Basic Medicine, Tongji Medical College, Huazhong University of Science and Technology, Wuhan, China

[5]The National Center for Drug Screening, Shanghai Institute of Materia Medica, Chinese Academy of Sciences, Shanghai, China

[6]Clinical Laboratory, Wuhan Children's Hospital, Wuhan, China

[7]Tongji Medical College, Huazhong University of Science and Technology, Wuhan, China

[8]Department of Genomic Medicine, The University of Texas MD Anderson Cancer Center, Houston, Texas, USA

[9]Department of Thoracic and Cardiovascular Surgery, The University of Texas MD Anderson Cancer Center, Houston, Texas, USA

[10]Thoracic/Head and Neck Medical Oncology, The University of Texas MD Anderson Cancer Center, Houston, Texas, USA

[11]Institute of Pathology, Tongji Hospital, Tongji Medical College, Huazhong University of Science and Technology, Wuhan, China

[12]Department of Pathology, School of Basic Medicine, Tongji Medical College, Huazhong University of Science and Technology, Wuhan, China

[13]Department of Medicine, Baylor College of Medicine, Houston, Texas, USA

[14]Department of Immunology, Harvard Medical School, Boston, MA, USA

[15]these authors contributed equally to this work

[*]Correspondence: meng_wu@hms.harvard.edu (M.W.), jzhang20@mdanderson.org

(J.Z.), ansel.hsiao@ucr.edu (A.H.), tianxia@hust.edu.cn (T.X.)

Summary

The human gut microbiome modulates tumor microenvironment and influences response to immune checkpoint inhibitors (ICI). Here, we designed a pathway-centric computational pipeline and analyzed three independent clinical cohorts of metastatic melanoma patients treated with anti-PD-1. Our analyses discovered quorum sensing (QS) and ABC transporters pathways significantly enriched in responders to anti-PD-1 vs non-responders. Furthermore, we found that 8 synthase (*luxS*) genes for the QS signal AI-2 from different species were identified with significant differential abundances between responders and non-responders in a clinical cohort. Follow-up microbiota transplant experiments showed that inter-species signaling by different QS AI-2 molecules can act on overall community function to promote the colonization of *Akkermansia muciniphila*, which has been reported to associate with superior response to ICI. Together, our data suggest a role for QS/ABC transporters pathways in modulation of microbiome and anti-tumor immunity in cancer patients.

Introduction

Cancer immunotherapy is considered to be the "fifth pillar" of cancer therapy, joining the ranks of surgery, chemotherapy, radiation, and targeted therapy (Oiseth and Aziz, 2017). The principle of immunotherapy is to boost or restore ability of the immune system to detect and destroy cancer cells by overcoming mechanisms by which tumors evade and suppress the immune response (Disis, 2014). Immune checkpoint inhibitors (ICIs) targeting cytotoxic T-lymphocyte-associated protein 4 (CTLA-4) (Halpert et al., 2016) and the programmed cell death protein 1 (PD-1) (Van der Kooij et al., 2017) have revolutionized the therapeutic landscape of many cancer types. However, responses to ICIs are often heterogeneous. A recently recognized important host factor that could contribute to inter-patient heterogeneity is differential composition of the patients' gut microbiome, which has been shown to affect antitumor immunity and therapeutic efficacy from ICIs (Frankel et al., 2017;Gopalakrishnan et al., 2018;Matson et al., 2018;Routy et al., 2018).

Interactions between the host immune system and microbiome have been recently scrutinized to identify immunogenic bacteria species that may impact responses to ICI therapy through facilitating recruitment and activation of $CD8^+$ T cells, identifying

several potential bacterial determinants (Frankel et al., 2017;Gopalakrishnan et al., 2018;Matson et al., 2018;Routy et al., 2018;Gharaibeh and Jobin, 2019;Lee et al., 2022). Gopalakrishnan et al. found higher abundance of *Faecalibacterium prausnitzii* (*F. prausnitzii*) in responders (R) compare to non-responders (NR) with metastatic melanoma treated with anti-PD-1 (Gopalakrishnan et al., 2018), while in a different cohort of patients with metastatic melanoma, Matson et al. reported that response to anti-PD-1 therapy was associated with an increased abundance of a consortium of eight species driven by *Bifidobacterium longum* (*B. longum*) (Matson et al., 2018). In another study, of metastatic melanoma patients, Frankel et al. observed that responders to anti-PD-1 therapy were enriched for *Dorea formicogenerans* (*D. formicogenerans*) (Frankel et al., 2017). In non-small cell lung cancer, Routy et al. observed increased relative abundance of *Akkermansia muciniphila* (*A. muciniphila*) in anti-PD-1 R compared to NR (Routy et al., 2018).

This species-centric approach to identify consistent microbial biomarkers for predicting efficacy to ICI is limited by rapid evolution at strain level, the enormous inter-individual heterogeneity in human gut microbiomes (Thursby and Juge, 2017), and the inability to convert taxon-level data to mechanistic molecular understanding of how candidate

microbes drive associated phenotypes. Rather than focusing on specific bacterial strains, we hypothesize that gut microbiome may share common molecular pathways that functionally impact host immune repertoire may be critical determinants for response to ICIs. To test this, we designed a computational pipeline using metagenomic shotgun sequencing data analysis of human gut microbiome to identify significantly enriched molecular pathways across different patient cohorts. With our computational pipelines, we demonstrated that quorum sensing (QS) and ABC transporters pathways were significantly enriched between R and NR groups, and then explored the potential mechanisms of QS/ABC transporter molecules of gut microbiota in the three ICI clinical cohorts. Finally, we designed a mouse colonization model to confirm the association of QS AI-2 molecules with the fitness of immune-modulatory species, and demonstrated that indirect QS effects on commensal communities can drive the abundance of key taxa independent of direct signal interaction.

Methods

QS pathway functional characterization

AI-2 mediated QS system were obtained from KEGG 'Quorum sensing' pathway. Representative reaction pathway shown in Figure 3A. The abundance of microbial genes related AI-2 mediated QS system with significant differential abundance was identified from supplementary table 1.

Phylogenetic analysis

LuxS sequences were aligned and a phylogenetic tree was generated using MEGA version X (Kumar et al., 2018). Sequences were aligned and analyzed by ClustalW using the default setting. The phylogenetic tree was generated using the aligned result by UPGMA Tree using the default setting.

Bacterial growth conditions

Strains incorporated into the defined human gut community are listed in Table S2. All strains were grown in LYH-BHI liquid media (BHI supplemented to 5 g/L yeast extract, 5 mg/L hemin,1 mg/mL cellobiose, 1 mg/mL maltose and 0.5 mg/mL cysteine-HCI). In

order to optimize the growth of *A. muciniphila*, LYH-BHI media was supplemented with 3% of porcine mucin. All cultures were placed inside a static incubator at 37 ℃ for 48 hours under anaerobic conditions (5% H_2, 20% CO_2, balance N_2), and then, subcultured at 1:100 in fresh LYH-BHI media for 48 hours prior to use. All *E. coli* strains containing *luxS* expression constructs were grown aerobically in Luria broth medium (LB media) with agitation at 37 ℃ overnight, and subcultured at 1:100 in fresh LB media overnight prior to use.

Generation of AI-2 expression strains

E. coli strains overexpressing the *luxS* enzymes of *S. infantarius* or *B. obeum* were constructed using an *E. coli luxS* mutant strain (BW30045). The *B. obeum luxS* coding region (from genome position 33,305-33,784) and the *S. infantarius luxS* coding region (from genome position 414,476-414,994) were codon-optimized for *E. coli*, placed downstream of the $P_{Ltet\text{-}O\text{-}1}$ constitutive promoter sequence derived from the plasmid vector pZE21, and the resulting construct cloned into vector pMK using the GeneArt Subcloning & Express Cloning Service (ThermoFisher). These expression constructs were then

amplified and inserted into the *endA* gene of the *E. coli* genome using primers (forward: 5'-CCAAAACAGCTTTCGCTACGT TGCTGGCTCGTTTTAACACGGAGTAAGTGTTAGAAAAATTCATCCAGCA-3', reverse: 5'-GGTTGTAC GCGTGGGGTAGGGGTTAACAAAAAGAATCCCGCTAGTGTAGGCGGGCAGTG AAAGGAAGGCC-3').

BB170 AI-2 bioassay

Cultures of signal-producing *E. coli* strains or *luxS*- parental strains were grown overnight in LB, and subcultured 1:100 into 12 mL of LB and grown with agitation at 37 ℃ until $OD_{600} \approx 0.2$, centrifuged, and the supernatant filtered using 0.22 μm filters. AI-2 activity in the resulting cell-free supernatants was then assessed using the BB170 bioassay (Bassler et al., 1994). Briefly, overnight cultures of reporter strain *BB170* in LM medium were diluted at 1:1000 in AB medium and 10 μL of cell-free supernatant or heat-treated cell-free supernatant were then added to 90 μL of BB170 dilution. The luminescence and OD_{600} of each sample were measured immediately and after ~3 hours growth at 30 ℃ with agitation.

Infant mouse colonization

Four-day-old CD-1 suckling mice were purchased from Charles River Laboratories. All animal protocols were approved by University of California, Riverside's Institutional Animal Care and Use Committee. To deplete the gut microbiota, the suckling mice were fasted for 1.5 hours and treated with approximately 1 mg/g body weight of streptomycin by gavage with a 30-gauge plastic tubing. Pups were then placed back with a lactating dam. After 24 hours, the mice were separated into three groups ($n = 7$), and each mouse received a maximum gavage volume of 50 μL of a defined bacterial mixture. The bacterial mixture for gavage consisted a total microbial mass of 300 μL of $OD_{600} = 0.4$ per inoculum, divided into (i) 45% microbial community, 20% *E. coli* expressing *luxS* from either *Streptococcus*, *B. obeum*, or empty expression vector, and 35% of *A. muciniphila* or (ii) equal quantities of *E. coli* strains and *A. muciniphila*. Gavaged mice were placed in at 30 ℃ for 16 hours and then sacrificed. The small and large intestines were dissected, separated, and homogenized in 5 mL LYH-BHI followed by DNA isolation.

Quantitative PCR analysis of bacteria abundance

To determine the abundance of *A. muciniphila* relative to the bacterial load, DNA extracts were isolated from both small and large intestines of colonized suckling mice. 500 µL of intestinal homogenates were mixed with 500 µL 0.1mm Zirconia beads (BioSpec), 210 µL SDS 20%, 500 µL phenol:chloroform:isoamyl-alcohol (24:24:1, Fisher Scientific) and lysed using a bead beater at 2,400 RPM for one minute. Next, qPCR assays were performed using primers specific to *A. muciniphila* (Forward: 5'-CAGCACGTGAAGGTGGGGA-3', reverse: 5'-CCTTGCGGTTGGCTTCAGATC-3') and a primer set targeting the total bacterial load (Forward: 5'-CTCCTACGGGAGGCAGCAG-3', reverse: 5'-TTACCGCGGCTGCTGGCAC-3'), *B. longum* (Forward: 5'-GTTCCCGACGGTCGTAGAG-3', reverse: 5'-GTGAGTTCCCGGCATAATCC-3'), and *F. prausnitzii* (Forward: 5'-GATGGCCTCGCGTCCGATTAG-3', reverse: 5'-CCGAAGACCTTCTTCCTCC-3'). Each reaction was performed in triplicates and consisted of 12.5 µL of iQ SYBR Green Supermix (BIO-RAD2, Hercules, CA), 0.25 µL of forward and reverse primers at 10 µm concentration, 10 µL nuclease free water and 2 µL of genomic DNA (500 ng/µL).

Results

QS and ABC transporters pathways were enriched in multi ICI clinical cohorts

We first applied metagenomic shotgun sequencing data analysis to Matson et al.'s dataset (n = 39, 15R, 24NR) and Gopalakrishnan et al.'s dataset (n = 25, 14R, 11NR), which collected gut microbiome sample from patients with metastatic melanoma treated with anti-PD-1 (Frankel et al., 2017;Gopalakrishnan et al., 2018;Matson et al., 2018). Pathway analysis on these two data sets revealed 19 pathways in Matson et al.'s cohort (Figure 3.2-1A), and 5 pathways in Gopalakrishnan et al.'s cohort (Figure 1B) that were statistically enriched (false discovery rate, FDR < 0.05). The 19 pathways in Matson et al.'s cohort included QS, ABC transporters, phosphotransferase system, ribosome, aminoacyl-tRNA biosynthesis, flagellar assembly, base excision repair, protein export and lysosome, and other metabolism pathways, while the 5 pathways in Gopalakrishnan et al.'s cohort were QS, ABC transporters, bacterial secretion system, cationic antimicrobial peptide resistance and carbon fixation in photosynthetic organisms (Figures 3.2-1A and 1B).

We also analyzed a recently published anti-PD-1 therapy in melanoma patients, which performed shotgun metagenomic sequencing of 223 fecal samples obtained from

15 recipients and 7 donors (Davar et al., 2021). For each recipient, they sequenced one pre-fecal microbiota transplantation (FMT) sample (obtained 7 to 21 days before FMT) and all available post-FMT samples (obtained weekly for 12 weeks and then every 3 weeks for as long as the patient remained on trial). The data indicated that QS and ABC transporters pathways were the top two most significantly enriched pathways (Figure 3.2-1C). Taken together, the QS and ABC transporters pathways were enriched in all three independent clinical cohorts, suggesting that these pathways may affect microbial-driven divergence in response to ICI therapy.

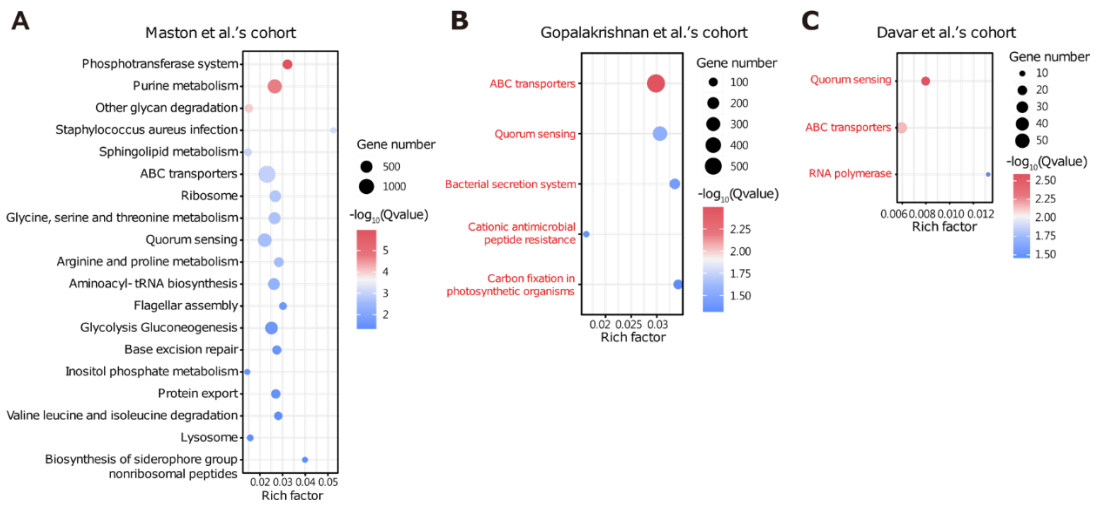

Figure 3.2-1. Metagenomic data analysis of metastatic melanoma patients treated with ICI therapy from Matson et al.'s, Gopalakrishnan et al.'s and Davar et al.'s cohorts.

Pathway enrichment analysis based on genes with significantly different abundance from A. Matson et al.'s, B. Gopalakrishnan et al.'s, and C. Davar et al.'s cohorts, respectively. y-Axis indicates the pathway name; x-axis indicates rich factor. Rich factor is the ratio of the number of differentially abundant genes annotated in a pathway term to the number of all genes annotated in this pathway term. Greater rich factor means greater intensiveness. The bubble size indicates the number of genes. The color bar indicates the corrected *P* value, red represents higher value, blue represents lower value.

The analysis of Frankel et al.'s dataset (n = 39, 24R, 15NR), which collected gut microbiome sample from patients with metastatic melanoma treated with various anti-PD-1 drugs (Frankel et al., 2017), found that QS, excluding ABC transporters was also significantly enriched between R and NR (Figure 2.3-2).

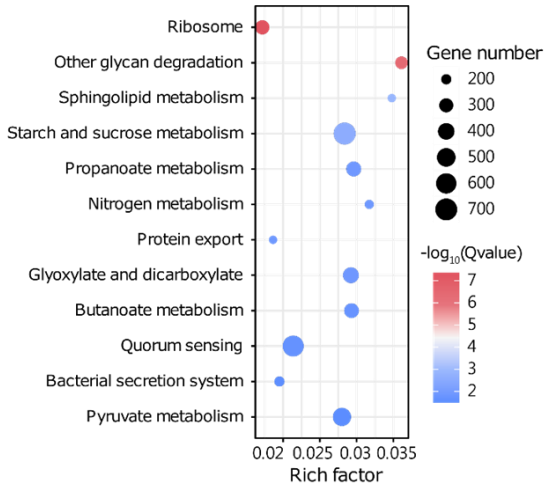

Figure 3.2-2. Pathway enrichment analysis based on genes with significantly different abundance from Frankel et al.' cohort.

y-Axis indicates the pathway name; x-axis indicates rich factor. Rich factor is the ratio of the number of differentially abundant genes annotated in a pathway term to the number of all genes annotated in this pathway term. Greater rich factor means greater intensiveness. The bubble size indicates the number of genes. The color bar indicates the corrected *P* value, red represents higher value, blue represents lower value.

LuxS homologues from different species differ in abundance between R and NR

Gut bacteria use QS to efficiently synchronize behaviors across populations in response to changes in population density and community species composition by producing and sensing diffusible signaling molecules called autoinducers (AIs) (Li et al., 2019). These signals can be species-specific or inter-species in nature, with the best characterized of the latter systems being the autoinducer-2 (AI-2) system. Among all autoinducer-related genes with significant differential abundance between R and NR sample groups, we

found that a total of 8 *luxS* (AI-2 synthase) genes in Matson et al.'s dataset (Figure 3.2-3A and Figure 3.2-4). The abundance of gene 1373611, 1271590, 1432971, 1440705, 1741886, and 1464080 were significantly elevated in R group ($P < 0.05$, Wilcoxon rank-sum test, log2 (fold change) ≥ 1, Figure 3.2-4). Second, the abundance of gene 1253822 and 144119 were significantly down-regulated in R group ($P < 0.05$, Wilcoxon rank-sum test, log2 (fold change) ≤ -1, Figure 3.2-4). Interestingly, while overall reads mapping to *luxS* were not significantly different between NR and R groups in all three ICI cohorts (Figure 3.2-3C), we found that *luxS* genes can be grouped into distinct clusters based on sequence similarity (Figure 3.2-3B), which displayed differential abundance in NR and R groups, suggesting that *LuxS* expression and thus AI-2 production may not be uniform across gut commensals. To identify the evolutionary relationship of these *luxS* genes to publicly available gut species representative of broader gut microbial diversity, we constructed a phylogenetic tree. The UPGMA phylogenetic tree revealed that these differentially abundant genes were distributed across nine major clusters (Figure 3.2-3B). For the down-regulated LuxS homologues, gene 1253822 clustered with *Dorea longicatena* (Figure 3.2-3B and 3D). Of note, the top 3 significantly up-regulated genes, 1432971, 1741886, and 1464080, clustered with *B. longum* (Cluster 9), *D.*

formicigenerans (Cluster 1), *F. prausnitzii* (Cluster 6), respectively (Figure 2B and 2D), which have been reported to potentially influence the response of ICI treatment by promoting the recruitment and activation of $CD8^+$ T cells (Frankel et al., 2017;Gopalakrishnan et al., 2018;Matson et al., 2018). In addition, we showed that *LuxS* clusters 7, and 8 were enriched in R group, while Cluster 1 and Cluster 2 *luxS* were enriched in both R and NR groups depending on sequence. These genes mapped to phylum Firmicutes, a significantly phylogenetically and biochemically diverse group of gut commensal microorganisms (Jandhyala et al., 2015).

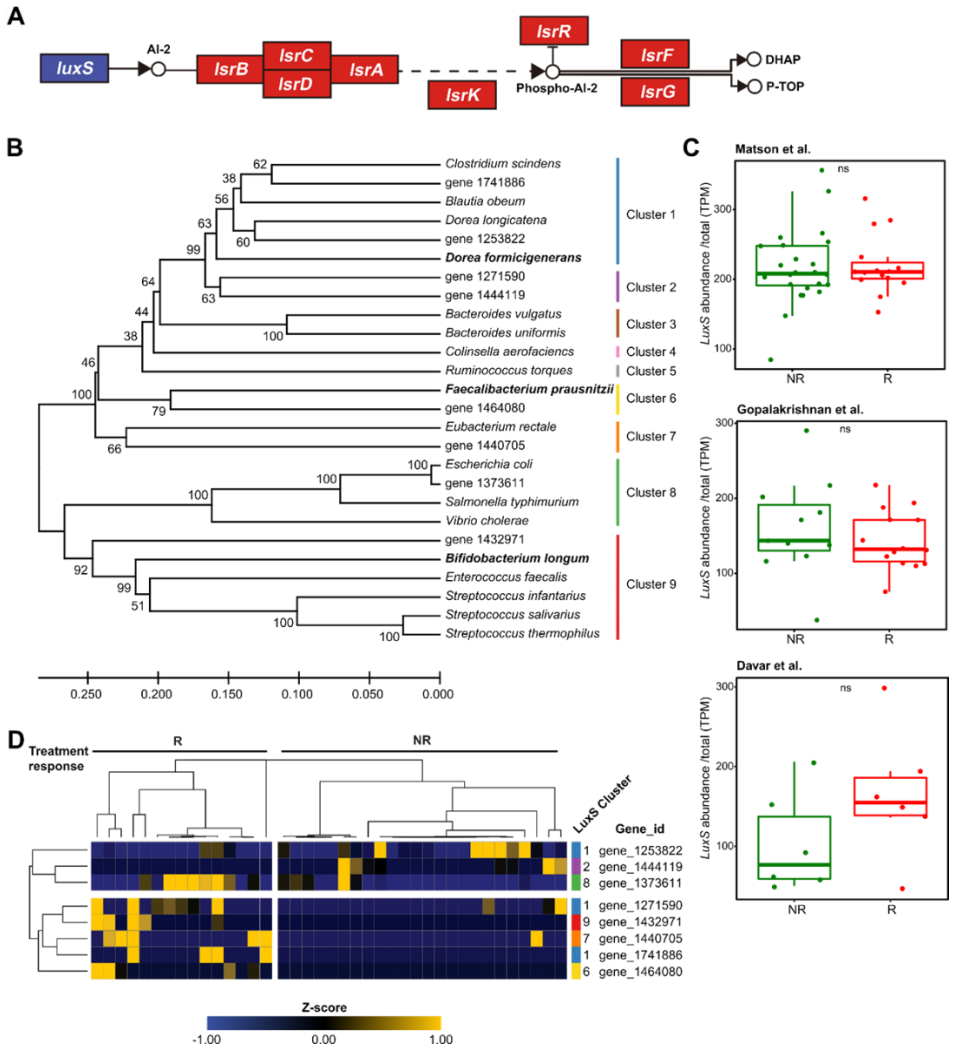

Figure 3.2-3. AI-2 mediated QS system have differential abundance between R and NR in three ICI cohorts.

A. Model for production, regulation, transport and modification of AI-2 in the KEGG database. Circles represent intermediate metabolites. DHAP, dihydroxyacetone phosphate; P-TOP, 3,3,4-trihydroxy-2-pentanone-5-phosphate. B. Nucleotide similarity of *LuxS* sequences from one ICI cohort and selected human gut-associated microbes. The scale bar refers to evolutionary distances in substitutions per site. The numbers at tree nodes refer to percentage bootstrap values after 1000 replicates. Colors represent different clusters. C. Boxplot of the total abundance of *LuxS* in Matson et al.'s, Gopalakrishnan et al.'s and Davar et al.'s cohorts. TPM, transcripts per million. ns, not significant. Wilcoxon rank-sum test. D. Heatmap of the differentially abundant genes related to *LuxS* between R and NR in Matson et al.'s cohort.

Additionally, some bacteria, such as *Escherichia coli* (*E. coli*), can quench the AI-2 signal produced by a variety of species present in the gut environment, and thus can influence AI-2–dependent bacterial behaviors (Marques et al., 2014). This process involves uptake of AI-2 via an ATP binding cassette (ABC) transporter (encoded by lsr*ACDB*), followed by phosphorylation (*lsrK*) and consequent intracellular sequestration (*lsrF* and *lsrG*, Figure 3.2-3A). Within the KEGG QS pathway, we identified 14 genes in the canonical Lsr system for AI-2 sensing, including *lsrA*, *lsrD*, *lsrF*, *lsrG* and *lsrK*, that were differentially enriched between R and NR in two of the three ICI cohorts (Figure 3.2-5). All these results suggest that AI-2 mediated QS system is a potentially important and relevant molecular pathway underpinning gut microbiota mediated response to cancer ICI therapy.

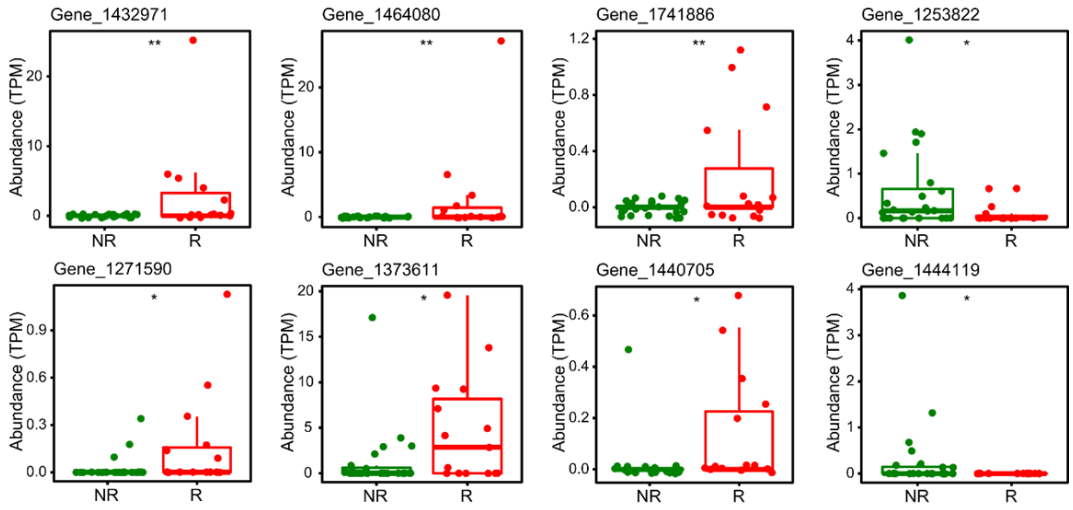

Figure 3.2-4. Boxplot of the significant differential abundance genes related to *LuxS* in Matson et al.'s cohort.

TPM, transcripts per million. (*, adjusted $P < 0.05$; **, adjusted $P < 0.01$; ***, adjusted $P < 0.001$; Wilcoxon rank-sum test.)

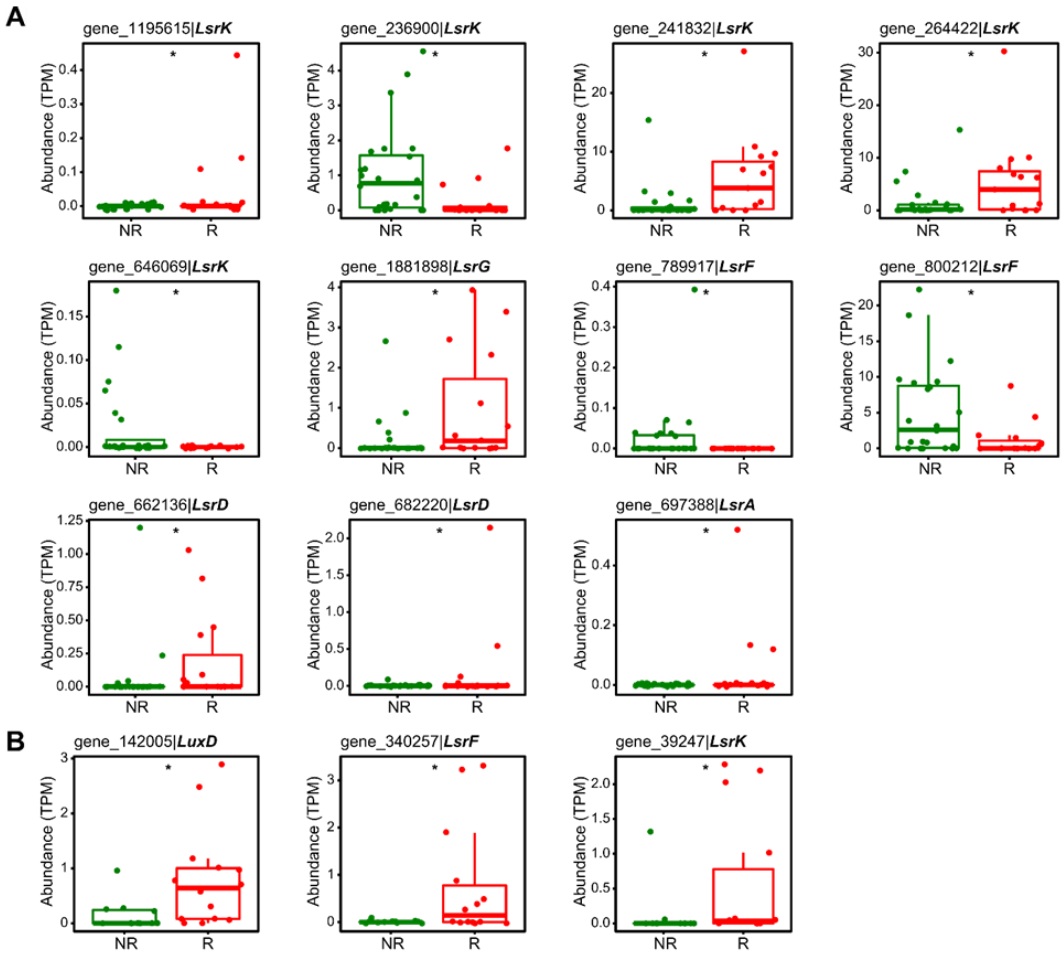

Figure 3.2-5. Boxplot of the significant differential abundance genes related to lsr*ADFGK*.

A. Matson et al.'s cohorts. B. Gopalakrishnan et al.'s cohorts. (* adjusted $P < 0.05$; ** adjusted $P < 0.01$; *** adjusted $P < 0.001$. Wilcoxon rank-sum test.)

AI-2 was associated with colonization of immunogenic strains in mouse model

To examine the role of AI-2 in driving the fitness or behavior of immune-modulatory species, we first examined the genome of *A. muciniphila*, previously shown to have higher abundance in patient responded to ICI treatment (Routy et al., 2018), for putative

homologs to known AI-2 related pathways. We mapped *A. muciniphila* against the KEGG database to identify putative QS pathways. Although one ABC transporter family homolog, Opp (oligopeptide permease) (McQuade et al., 2001) was identified, strikingly, no *luxS*, *lsr*, or *luxPQ* homologs were identified, and *A. muciniphila* also does not encode a Com or Agr autoinducer peptide (AIP) sensing/regulation system. These findings suggested that the relationship of *A. muciniphila* abundance to AI-2 may be an indirect one working via the effect of bacterial signaling on the rest of the gut commensal community. Similar to *A. muciniphila*, *B. longum* have not been reported to carry *lsr* or *luxPQ* AI-2 receptors, but does possess functional *luxS* (Sun et al., 2014). A recently published work has identified homologs to RbsB-type AI-2 receptors and showed AI-2 dependent biofilm formation in *B. longum* (Liu et al., 2021). To confirm this, we used a suckling mouse colonization model (Alavi and Hsiao, 2020) where the putative immunogenic taxa *A. muciniphila, B. longum*, and *F. prausnitzii* were co-colonized with transgenic Δ*luxS E. coli* modified to express the AI-2 synthase enzymes from two human gut commensals, *Blautia obeum* (*B. obeum*, cluster 1) and *Streptococcus infantarius* (*S. infantarius,* cluster 9), whose genomes contain *luxS* homologs of high sequence variability (33.3% amino acid identity, 33.6-34.2% amino acid identify with *E. coli* LuxS,

Figure 3.2-3B). The luxS enzymes of these different species were codon-optimized for expression in *E. coli*, and stably integrated in single copy into the *E. coli* chromosome and driven by the same constitutive promoter. Constitutive expression of these different AI-2 synthase enzymes drove consistent AI-2 signal levels in the filtered supernatants (Figure 3.2-6A) when measured using the *Vibrio* BB170 bioassay, suggesting that these enzymes produce AI-2 signals able to mediate cross-species communication.

Next, we designed an experiment to explore the association of AI-2 molecules with immune-modulatory species in a mouse colonization model. Three groups of mice received the immunomodulatory strain *A. muciniphila*, a defined human gut commensal community, and either i) Δ*luxS E. coli*, or *E. coli* expressing the *luxS* enzyme of two different human gut commensals, (ii) *B. obeum* and (iii) *S. infantarius*. The background model microbiome was based on healthy US human gut microbiomes, and included *A. muciniphila*, *B. longum*, *D. formicigenerans*, and *F. prausnitzii* (Table 3.2-1). qPCR with universal 16S primers showed similar overall microbial load, and no statistically significant differences between AI-2 signal types in either compartment (Figure 3.2-6B). We found using quantitative PCR with *A. muciniphila*-specific primers that the presence of *E. coli* expressing AI-2 from *B. obeum* was associated with a significantly increased

abundance of *A. muciniphila* in the small intestine and large intestine compared to Δ*luxS E. coli* (Figure 3.2-6C). In contrast, a potentially direct interaction between cognate AI-2 pathways was observed for *B. longum*, which displayed increased abundance in the presence of cluster 9 LuxS signal products, i.e. in the presence of *E. coli* expressing the *Streptococcal luxS* (Figure 3.2-6D), while *F. prausnitzii* did not significantly respond to either signal type (Figure 3.2-6E). *A. muciniphila*, was unexpected given that it lacks canonical AI-2 receiver genes. To determine if these effects were mediated via changes in community behavior or if they were direct response of *A. muciniphila* to the AI-2, we co-colonized this immunomodulatory organism with either Δ*luxS E. coli* or *E. coli* expressing the *B. obeum luxS* alone (Figure 3.2-6F) and we observed no statistically significant signal-dependent colonization phenotype. These data indicate that the *A. muciniphila* is responding to indirect effects of AI-2 signaling to other community members.

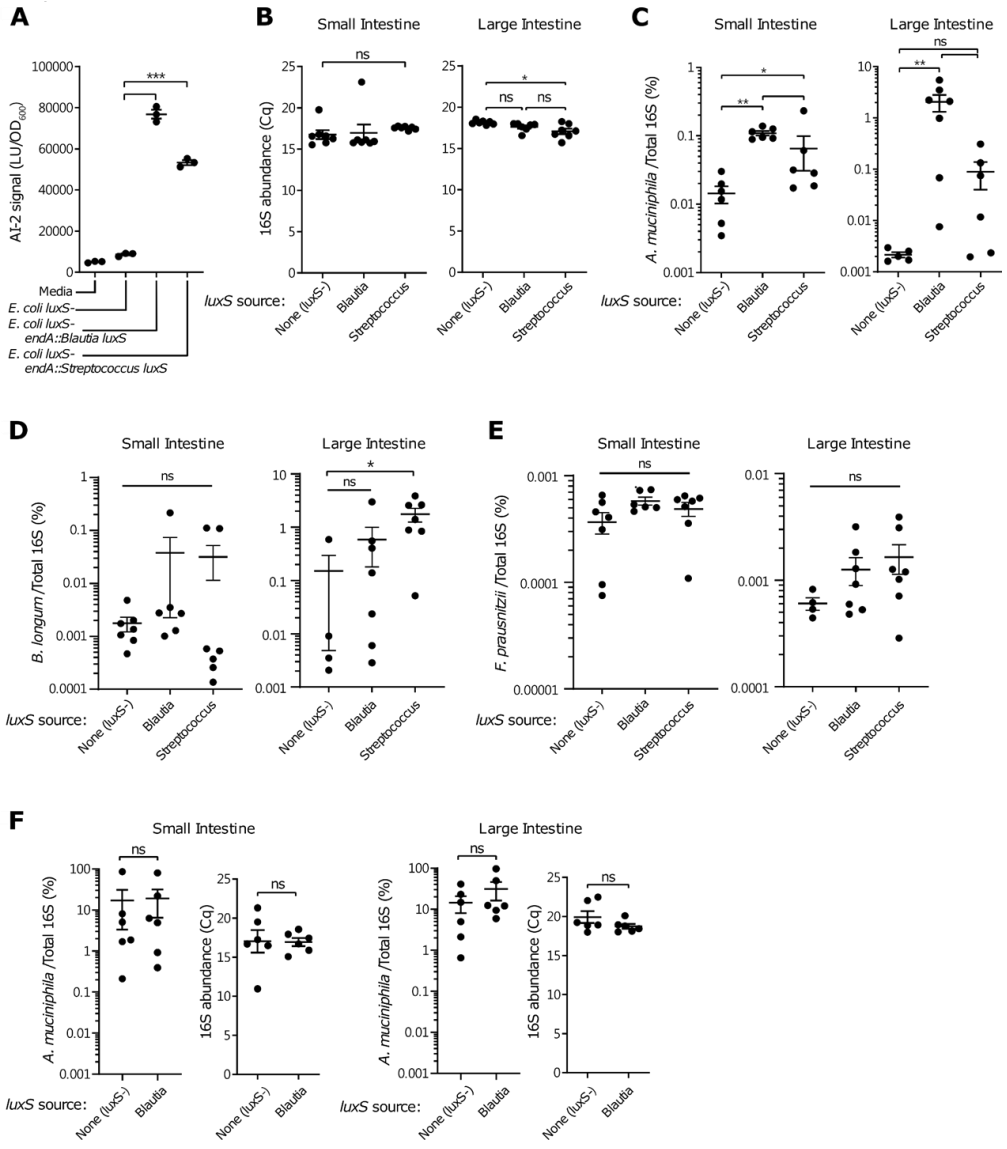

Figure 3.2-6. Commensal-encoded AI-2 quorum sensing signals promote *A. muciniphila* colonization.

A. AI-2 signal levels of cell-free supernatants from indicated bacterial strains. B. Overall 16S levels measured by quantitative PCR. C. Colonization of *A. muciniphila* with defined model community and *E. coli* expressing AI-2 signals from indicated bacteria. D. Colonization of *B. longum* with defined model community and *E. coli* expressing AI-2 signals from indicated bacteria. E. Colonization of *F. prausnitzii* with defined model community and *E. coli* expressing AI-2 signals from indicated bacteria. F. *A. muciniphila* levels when co-colonized with bacteria expressing indicated AI-2 signals. (*, $P < 0.05$; **, $P < 0.01$, ***, $P < 0.001$. Mann-Whitney U test.)

Taken together, our results suggest that AI-2 signal sources are not homogenous within the gut, and that different LuxS enzymes are able to produce signal that differentially affects specific gut taxa vis direct and indirect mechanisms, depending on the overall structure of the gut microbiome. These signal-dependent effects can modulate the levels of putative immune-modulatory taxa that are associated with R and NR outcomes for immunotherapy.

Table 3.2-1 List of healthy US human gut microbes.

Bacterium	Phylum	Strain Name	NCBI Taxonomy ID
Bifidobacterium longum subsp. *longum*	Actinobacteria	DSM 20219	565042
Collinsella aerofaciens	Actinobacteria	ATCC 25986	411903
Dorea formicigenerans	Firmicutes	ATCC 27755	411461
Eubacterium rectale	Firmicutes	ATCC 33656	515619
Faecalibacterium prausnitzii	Firmicutes	DSM 17677	411483
Bacteroides vulgatus	Bacteroidetes	ATCC 8482	435590
Blautia obeum	Firmicutes	ATCC 29174	411459
Clostridium scindens	Firmicutes	ATCC 35704	411468
Akkermanisa muciniphila	Verrucomicrobia	ATCC BAA-835	239934

Discussion

The role of the human microbiome on cancer progression and response to cancer therapy have recently been under investigation. Several studies have suggested that gut

microbiota can modulate response to ICIs across several cancer types (Frankel et al., 2017;Gopalakrishnan et al., 2018;Matson et al., 2018;Routy et al., 2018). Gut microbes may impact antitumor immunity via a number of mechanisms, including interaction of microbial components or products with antigen-presenting cells (APCs), which can help prime an adaptive immune response; induction of cytokine production by APCs or lymphocytes, and the effects of microbial metabolites (Helmink et al., 2019). Notably, there was only modest overlap in these checkpoint blockade responsive microbiome signatures across cohorts, though some phylogenetic commonalities exist among identified bacterial taxa in studies utilizing different checkpoint inhibitors (Lee et al., 2022). At the species level there is enormous inter-individual heterogeneity in gut microbiomes, which has hindered efforts to define a core microbiome shared between healthy individuals. Instead, the functional capacity of the microbiota, as defined abundances of genes involved in metabolic pathways, has been advanced as a better metric for defining a core healthy microbiota (Huttenhower et al., 2012;Integrative, 2014); indeed, the basic categories of metabolic pathways were more evenly represented across individuals as compared to bacterial taxonomy (Huttenhower et al., 2012).

Recently, Gharaibeh and Jobin (Gharaibeh and Jobin, 2019) also performed

functional analysis to the same cohorts from Matson et al. and Gopalakrishnan et al. as in the current study. In their pioneer work, 869 and 653 KOs from these two datasets respectively were found to have significantly different abundance between R and NR groups, but further pathway analyses were not performed. By using KO to annotate gene function and depicted enriched pathways based on genes with significant differential abundance, over 52,000 and 22,000 genes were identified with significant differential abundance from Matson's and Gopalakrishnan's cohorts respectively. Pathway level analysis identified significantly enriched ABC transporters and QS pathways across three independent ICI cohorts of metastatic melanoma. ABC transporters are members of a transport system super family, with representatives in all phyla, from prokaryotes to humans (Polgar and Bates, 2005). In gut microenvironment, bacteria use ABC transporters to uptake a large variety of nutrients, biosynthetic precursors, trace metals, and vitamins from the intestinal lumen, while exporting sterols, lipids, drugs, and a large variety of primary and secondary metabolites. Knocking out of oligopeptides ABC transporter *oppD* can alter the ability of the bacterium to trigger cytokine (TNF-α, IL-6 and IL-1b) release from infected macrophages (Dasgupta et al., 2010). We hypothesize that gut microbiota use ABC transporters system to secrete bacterial products into the

lumen, which act as antigens can be internalized by dendritic cells in the intestinal lamina propria (Arques et al., 2009), and thus, contribute to ICI therapy by favoring recruitment and activation of $CD8^+$ T cells.

QS process enables bacteria in a population to synchronize their actions and engage in group behaviors. The most commonly studied QS signals belong to one of the following three categories: acylated homoserine lactones (AI-1), used by Gram-negative bacteria; peptide signals, used by Gram-positive bacteria; and AI-2, used by both Gram-negative and Gram-positive bacteria (Jimenez and Sperandio, 2019). Of these systems, AI-2 is the only one thought to be an inter-species signaling system, capable of mediating communication within and across many bacterial species. The autoinducer AI-2 is synthesized via the action of the enzyme LuxS and has been shown to be mediated by several pathways. In *Vibrio* species, a transmembrane LuxPQ protein complex recognizes the AI-2 molecule, initiating a phosphorelay via adapter proteins that leads to modulation of the activity of a complex set of downstream transcriptional regulators (Bassler et al., 1994;Zhu et al., 2002), while the Lsr system in *E. coli* and *Salmonella* encodes for an ABC-type transporter complex that moves AI-2 from the environment to the cytoplasm, where it is phosphorylated, sequestering the signal in the cell and allowing it to mediate

transcriptional regulatory changes in the bacterial cell (Xavier and Bassler, 2005b). Despite the abundance of AI-2 signaling homologs in the gut microbiome, very few studies have attempted to define the community effects of AI-2 manipulation. Engineered strains of *E. coli* with modified Lsr system expression to sequester AI-2 signal from the gut environment of mice has been observed to drive changes in the composition of the gut microbiota (Thompson et al., 2015), suggesting that the manipulation of AI-2 levels have great potential in maintaining microbiota homeostasis. Our results suggest that there is substantial AI-2 signal diversity based on different types of the AI-2 synthase LuxS, and that differential addition of these LuxS products in a gut community can affect the abundance of immunomodulatory species.

Our studies investigate the potential role of *A. muciniphila* associated with response to cancer immunotherapy. However, no relevant literature regarding the products of AI-2 by *A. muciniphila* has been published. Our results show that LuxS orthologs from different species were identified with significant differential abundance between R and NR in one ICI cohorts. In addition, we found that the provision of exogenous AI-2 from the common human gut commensal *B. obeum*, but not Streptococcus species, promote *A. muciniphila* colonization in the small and large

intestine of animals. This suggests that microbial AI-2 is able to affect the gut microbiome to favor the expansion of immunomodulatory species, and that separate AI-2 products of the AI-2 synthase enzyme LuxS can drive divergent community phenotypes. Of note, Meger et al. (Mager et al., 2020) identify inosine as a metabolite produced by *A. muciniphila* and *Bifidobacterium pseudolongum* that markedly increases the level of intratumoral and splenic $CD4^+$ and $CD8^+$ T cells and further enhance the efficacy of ICI therapy in mouse model. In addition, the outer membrane protein Amuc of *A. muciniphila* strengthens the antitumor immune response in subcutaneous melanoma and colorectal tumor-bearing mice, through activating toll-like receptor 2 signaling pathway (Shi et al., 2020). Therefore, these data support a mechanistic model where AI-2 action on the overall microbiota promotes accumulation of *A. muciniphila* that then can increase the efficacy of ICI therapy and antitumor immune response via inosine and Amuc production in the gut microenvironment. Furthermore, Zargar et al. (Zargar et al., 2015) demonstrated that AI-2 from nonpathogenic bacteria affect host immune function by stimulating the expression of inflammatory cytokine IL8, suggesting that AI-2 directly mediate interkingdom communication between the microbiome and the host in the gastrointestinal tract. In conclusion, our findings suggest that AI-2 is likely a vital

regulatory molecule for gut microbiota response to cancer ICI therapy, and that further investigation of the effect of other bacterial AIs including AI-1 and AIP signals as well as other potential AI-2 variants are warranted.

Chapter 4 Conclusion

Summary

Bacteria communicates using signaling molecules to alter its behavior and lead to changes in microbiome structure. Gut microbiome varies between individuals due to multiple factors including health statues. When individual's gut microbiome is in a dysbiotic state, it becomes more vulnerable to pathogen infection then individual with normal gut microbiome acting as barrier against pathogens. Therefore, studying bacterial communication processes affecting gut microbiome structure is critical to prevent pathogen infection.

In chapter 2, results demonstrated the ability of model microbes representing simplified infection resistant model community mediated repression of *V. cholerae* colonization in mouse model. We first demonstrated *V. cholerae* colonization difference under simplified model communities representing a resistant (SR) or susceptible (SS) state of microbiome in antibiotic treated infant mice model based on previously published data (Alavi et al., 2020). Our findings indicated mice co-infected with SR community expresses significantly higher reactive nitrogen species (RNS) and reactive oxygen species (ROS) related gene, *NOS1*, *NOS2*, and *DUOX2*, while *V. cholerae* has significant

lower expression of biofilm formation related gene. On the other hand, SS community co-infected mice showed higher expression of antioxidant enzyme, catalase (*CAT*). Direct measurement of H_2O_2 in the homogenates from each model microbiome indicated that SR community is capable of induced higher H_2O_2 production. Treating *V. cholerae*-containing homogenates with H_2O_2, wild-type *V. cholerae* survival rate was significantly higher when co-infected with SS, on the other hand, biofilm formation deficient *V. cholerae* does not possess this advantage. Additionally, SR community strain also demonstrated the ability to alter bile acid composition that affects *V. cholerae* growth. We also demonstrated the addition of quorum sensing (QS) signaling molecule, AI-2, from a member of resistant community to the complex susceptible community could restore restriction against *V. cholerae* colonization. Our finding suggests that this could be due direct regulation of AI-2 interacting with *V. cholerae* transcription factor altering its gene expression. Taken together, our results suggest microbiome composition affects pathogen infection through manipulating environmental stress and regulation of pathogen defense mechanism.

With the understanding of gut microbiome composition and QS effect on pathogen infection, we turn our attention to QS, microbiome, and host interaction in

chapter 3. We first show that the addition of exogenous QS signal, AI-2, shifts the microbiome structure away from no signal added microbiome after a week of inoculation into germ-free mice. Unfortunately, we did not see significant difference between different AI-2 signal source. Metatranscriptomics analysis demonstrated diverge between presence of exogenous AI-2 or not in expression profile started at an earlier time point. Results also demonstrated that bacterial relative abundance is different from transcript relative abundance indicating bacterial activity differences in the microbiome. In addition to model communities, we demonstrated QS pathways were enriched in multiple immune checkpoint inhibitors (ICI) treatment clinical cohorts. Between responder (R) and non-responder (NR) to ICI treatment, AI-2 synthase genes (*luxS*) shown differential abundance between clusters distinct based on sequence similarity, suggesting AI-2 production may not be uniform across gut commensals. The examination of immune-modulatory species reaction on AI-2 signal indicating LuxS enzymes are able to produce signal that differentially affects bacteria in a direct and indirect mechanisms depending on gut microbiome structure. These signal-dependent effects are capable of altering immune-modulatory species that are associated with immunotherapy outcomes. Here, we demonstrated the regulation of QS signal affects microbiome structure and behavior leads

to host response to immunotherapy.

Future studies and applications

With growing evidence of QS signals being able to regulate biofilm formation and virulence in pathogenic bacteria and with increasing of pathogen resistance to antibiotics, researchers have been think of using QS as potential clinical therapies. Duan and March used commensal *E. coli* Nissle 1917 as a carrier to express CAI-1. They found pretreating the infant mice with CAI-1 producing *E. coli* for 8 hours could increase mice survival by over 90%. When co-ingesting CAI-1 producing *E. coli* and *V. cholerae* also has about 25% increase in survival rate (Duan and March, 2010). Other than *V. cholerae*, QS signaling pathway are also used to potentially treat other pathogens. With the developing of a high-throughput screening, Christensen et al. discovered AHLs synthase inhibitors that can potentially use as antivirulence agent (Christensen et al., 2013). Quorum sensing signal DSF (diffusible signal factor) showed to be capable of inducing bacterial antibiotic susceptibility (Deng et al., 2014). By programing *cheZ* (motility gene), *Dnasel* (*P. aeruginosa* biofilm degradation gene), and *mcsS* (antimicrobial peptides) with *lasI* promoter to respond to AHL sensing protein, LasR, Hwang et al. reprogramed and engineered an *E. coli* strain capable of seeking and targeting pathogen *P. aeruginosa*

(Hwang et al., 2014). As previously described, *B. obeum* and *E. coli* has shown potential of restricting pathogen colonization and restoring microbiome homeostasis through the expression of AI-2 signaling molecule (Hsiao et al., 2014;Thompson et al., 2015). Xavier et al. also proposed that AI-2 can alter gut microbiota in mammalian intestine (Bivar Xavier, 2018).

QS signal communication also happens cross-kingdom. Studies reported That QS signal induces host cell apoptosis and regulating immune mediators secretion (Shiner et al., 2006). *E. coli* AI-2 signal has been found to activate NF-κB-mediated signaling pathways in HCT-8 cells (Zargar et al., 2015). Intestinal bacteria secreted AI-2 also been reported to regulate epithelium inflammatory responses (Li et al., 2019). These studies indications the importance of QS in regulating host immune response and with more understanding of host-pathogen or gut microbiome and pathogen cross-species communication, it is possible to prevent and potentially treat *V. cholerae* and other pathogen infection with QS regulation as well as improving immunotherapy treatment.

Reference

Alavi, S., and Hsiao, A. (2020). Protocol for microbiome transplantation in suckling mice during *Vibrio cholerae* infection to study commensal-pathogen interactions. *STAR Protocols* 1**,** 100200.

Alavi, S., Mitchell, J.D., Cho, J.Y., Liu, R., Macbeth, J.C., and Hsiao, A. (2020). Interpersonal Gut Microbiome Variation Drives Susceptibility and Resistance to Cholera Infection. *Cell* 181**,** 1533-1546.e1513.

Anders, S., and Huber, W. (2010). Differential expression analysis for sequence count data. *Genome Biol* 11**,** R106.

Anders, S., Pyl, P.T., and Huber, W. (2015). HTSeq--a Python framework to work with high-throughput sequencing data. *Bioinformatics* 31**,** 166-169.

Anderson, C.J., Clark, D.E., Adli, M., and Kendall, M.M. (2015). Ethanolamine Signaling Promotes Salmonella Niche Recognition and Adaptation during Infection. *PLoS Pathog* 11**,** e1005278.

Anderson, C.J., and Kendall, M.M. (2016). Location, location, location. Salmonella senses ethanolamine to gauge distinct host environments and coordinate gene expression. *Microb Cell* 3**,** 89-91.

Arques, J.L., Hautefort, I., Ivory, K., Bertelli, E., Regoli, M., Clare, S., Hinton, J.C., and Nicoletti, C. (2009). *Salmonella* induces flagellin- and MyD88-dependent migration of bacteria-capturing dendritic cells into the gut lumen. *Gastroenterology* 137**,** 579-587.

Bachmann, V., Kostiuk, B., Unterweger, D., Diaz-Satizabal, L., Ogg, S., and Pukatzki, S. (2015). Bile Salts Modulate the Mucin-Activated Type VI Secretion System of Pandemic *Vibrio cholerae*. *PLoS Negl Trop Dis* 9**,** e0004031.

Baryshev, V.A., Glagolev, A.N., and Skulachev, V.P. (1981). Sensing of ΔμH+ in phototaxis of Halobacterium halobium. *Nature* 292**,** 338-340.

Bassler, B.L., Wright, M., and Silverman, M.R. (1994). Multiple signalling systems controlling expression of luminescence in *Vibrio harveyi*: sequence and function of genes encoding a second sensory pathway. *Mol Microbiol* 13**,** 273-286.

Beghini, F., Mciver, L.J., Blanco-Miguez, A., Dubois, L., Asnicar, F., Maharjan, S., Mailyan, A., Manghi, P., Scholz, M., Thomas, A.M., Valles-Colomer, M., Weingart, G., Zhang, Y., Zolfo, M., Huttenhower, C., Franzosa, E.A., and Segata, N. (2021). Integrating taxonomic, functional, and strain-level profiling of diverse microbial communities with bioBakery 3. *Elife* 10.

Begley, M., Gahan, C.G., and Hill, C. (2005). The interaction between bacteria and bile. *FEMS Microbiol Rev* 29**,** 625-651.

Bhattacharyya, A., Chattopadhyay, R., Mitra, S., and Crowe, S.E. (2014). Oxidative stress: an essential factor in the pathogenesis of gastrointestinal mucosal diseases. *Physiol Rev* 94**,** 329-354.

Bina, X.R., Provenzano, D., Nguyen, N., and Bina, J.E. (2008). *Vibrio cholerae* RND family efflux systems are required for antimicrobial resistance, optimal virulence factor production, and colonization of the infant mouse small intestine. *Infect Immun* 76**,** 3595-3605.

Bischofs, I.B., Hug, J.A., Liu, A.W., Wolf, D.M., and Arkin, A.P. (2009). Complexity in bacterial cell-cell communication: quorum signal integration and subpopulation signaling in the *Bacillus subtilis* phosphorelay. *Proc Natl Acad Sci U S A* 106**,** 6459-6464.

Bivar Xavier, K. (2018). Bacterial interspecies quorum sensing in the mammalian gut microbiota. *Comptes Rendus Biologies* 341**,** 297-299.

Bligh, E.G., and Dyer, W.J. (1959). A rapid method of total lipid extraction and purification. *Can J Biochem Physiol* 37**,** 911-917.

Bolger, A.M., Lohse, M., and Usadel, B. (2014). Trimmomatic: a flexible trimmer for Illumina sequence data. *Bioinformatics* 30**,** 2114-2120.

Bolyen, E., Rideout, J.R., Dillon, M.R., Bokulich, N.A., Abnet, C.C., Al-Ghalith, G.A., Alexander, H., Alm, E.J., Arumugam, M., Asnicar, F., Bai, Y., Bisanz, J.E., Bittinger, K., Brejnrod, A., Brislawn, C.J., Brown, C.T., Callahan, B.J., Caraballo-Rodriguez, A.M., Chase, J., Cope, E.K., Da Silva, R., Diener, C., Dorrestein, P.C., Douglas, G.M., Durall, D.M., Duvallet, C., Edwardson, C.F., Ernst, M., Estaki, M., Fouquier, J., Gauglitz, J.M., Gibbons, S.M., Gibson, D.L., Gonzalez, A., Gorlick, K., Guo, J., Hillmann, B., Holmes, S., Holste, H., Huttenhower, C., Huttley, G.A., Janssen, S., Jarmusch, A.K., Jiang, L., Kaehler, B.D., Kang, K.B., Keefe, C.R., Keim, P., Kelley, S.T., Knights, D., Koester, I., Kosciolek, T., Kreps, J., Langille, M.G.I., Lee, J., Ley, R., Liu, Y.X., Loftfield, E., Lozupone, C., Maher, M., Marotz, C., Martin, B.D., Mcdonald, D., Mciver, L.J., Melnik, A.V., Metcalf, J.L., Morgan, S.C., Morton, J.T., Naimey, A.T., Navas-Molina, J.A., Nothias, L.F., Orchanian, S.B., Pearson, T., Peoples, S.L., Petras, D., Preuss, M.L., Pruesse, E., Rasmussen, L.B., Rivers, A., Robeson, M.S., 2nd, Rosenthal, P., Segata, N., Shaffer, M., Shiffer, A., Sinha, R., Song, S.J., Spear, J.R., Swafford, A.D., Thompson, L.R., Torres, P.J., Trinh, P., Tripathi, A., Turnbaugh, P.J., Ul-Hasan, S., Van Der Hooft, J.J.J., Vargas, F., Vazquez-Baeza, Y., Vogtmann, E., Von Hippel, M., Walters, W., et al. (2019). Reproducible, interactive, scalable and extensible microbiome data science using QIIME 2. *Nat Biotechnol* 37**,** 852-857.

Bouillaut, L., Perchat, S., Arold, S., Zorrilla, S., Slamti, L., Henry, C., Gohar, M., Declerck, N., and Lereclus, D. (2008). Molecular basis for group-specific activation of the virulence regulator PlcR by PapR heptapeptides. *Nucleic Acids Res* 36**,** 3791-3801.

Bourque, D.L., Bhuiyan, T.R., Genereux, D.P., Rashu, R., Ellis, C.N., Chowdhury, F., Khan, A.I., Alam, N.H., Paul, A., Hossain, L., Mayo-Smith, L.M., Charles, R.C., Weil, A.A., Larocque, R.C., Calderwood, S.B., Ryan, E.T., Karlsson, E.K., Qadri, F., and Harris, J.B. (2018). Analysis of the Human Mucosal Response to Cholera Reveals Sustained Activation of Innate Immune Signaling Pathways. *Infect Immun* 86.

Boyaci, H., Shah, T., Hurley, A., Kokona, B., Li, Z., Ventocilla, C., Jeffrey, P.D.,

Semmelhack, M.F., Fairman, R., Bassler, B.L., and Hughson, F.M. (2016). Structure, Regulation, and Inhibition of the Quorum-Sensing Signal Integrator LuxO. *PLoS Biology* 14**,** e1002464.

Burgueno, J.F., Fritsch, J., Santander, A.M., Brito, N., Fernandez, I., Pignac-Kobinger, J., Conner, G.E., and Abreu, M.T. (2019). Intestinal Epithelial Cells Respond to Chronic Inflammation and Dysbiosis by Synthesizing H2O2. *Front Physiol* 10**,** 1484.

Campagna, S.R., Gooding, J.R., and May, A.L. (2009). Direct quantitation of the quorum sensing signal, autoinducer-2, in clinically relevant samples by liquid chromatography-tandem mass spectrometry. *Anal Chem* 81**,** 6374-6381.

Cerda-Maira, F.A., Ringelberg, C.S., and Taylor, R.K. (2008). The bile response repressor BreR regulates expression of the *Vibrio cholerae* breAB efflux system operon. *J Bacteriol* 190**,** 7441-7452.

Chand, D., Avinash, V.S., Yadav, Y., Pundle, A.V., Suresh, C.G., and Ramasamy, S. (2017). Molecular features of bile salt hydrolases and relevance in human health. *Biochim Biophys Acta Gen Subj* 1861**,** 2981-2991.

Chen, X., Schauder, S., Potier, N., Van Dorsselaer, A., Pelczer, I., Bassler, B.L., and Hughson, F.M. (2002). Structural identification of a bacterial quorum-sensing signal containing boron. *Nature* 415**,** 545-549.

Childers, B.M., and Klose, K.E. (2007). Regulation of virulence in *Vibrio cholerae*: the ToxR regulon. *Future Microbiol* 2**,** 335-344.

Cho, J.Y., Liu, R., and Hsiao, A. (2022). Microbiota-Associated Biofilm Regulation Leads to *Vibrio cholerae* Resistance Against Intestinal Environmental Stress. *Front Cell Infect Microbiol* 12**,** 861677.

Cho, J.Y., Liu, R., Macbeth, J.C., and Hsiao, A. (2021). The Interface of *Vibrio cholerae* and the Gut Microbiome. *Gut Microbes* 13**,** 1937015.

Christensen, Q.H., Grove, T.L., Booker, S.J., and Greenberg, E.P. (2013). A high-throughput screen for quorum-sensing inhibitors that target acyl-homoserine lactone synthases. *Proceedings of the National Academy of Sciences of the United States of America* 110**,** 13815-13820.

Clemens, J.D., Nair, G.B., Ahmed, T., Qadri, F., and Holmgren, J. (2017). Cholera. *Lancet* 390**,** 1539-1549.

Colwell, R.R., and Huq, A. (1994). Environmental reservoir of *Vibrio cholerae.* The causative agent of cholera. *Ann N Y Acad Sci* 740**,** 44-54.

Colwell, R.R., Kaper, J., and Joseph, S.W. (1977). *Vibrio cholerae*, *Vibrio parahaemolyticus*, and other *Vibrios*: occurrence and distribution in Chesapeake Bay. *Science* 198**,** 394-396.

Dalia, A.B., Mcdonough, E., and Camilli, A. (2014). Multiplex genome editing by natural transformation. *Proceedings of the National Academy of Sciences* 111**,** 8937-8942.

Darkoh, C., Dupont, H.L., Norris, S.J., and Kaplan, H.B. (2015). Toxin synthesis by *Clostridium difficile* is regulated through quorum signaling. *mBio* 6**,** e02569.

Dasgupta, A., Sureka, K., Mitra, D., Saha, B., Sanyal, S., Das, A.K., Chakrabarti, P., Jackson, M., Gicquel, B., and Kundu, M. (2010). An oligopeptide transporter of *Mycobacterium tuberculosis* regulates cytokine release and apoptosis of infected macrophages. *PLoS One* 5**,** e12225.

Davar, D., Dzutsev, A.K., Mcculloch, J.A., Rodrigues, R.R., Chauvin, J.-M., Morrison, R.M., Deblasio, R.N., Menna, C., Ding, Q., and Pagliano, O. (2021). Fecal microbiota transplant overcomes resistance to anti–PD-1 therapy in melanoma patients. *Science* 371**,** 595-602.

David, L.A., Weil, A., Ryan, E.T., Calderwood, S.B., Harris, J.B., Chowdhury, F., Begum, Y., Qadri, F., Larocque, R.C., and Turnbaugh, P.J. (2015). Gut Microbial Succession

Follows Acute Secretory Diarrhea in Humans. *mBio* 6**,** e00381-00315.

Dawson, P.A., and Karpen, S.J. (2015). Intestinal transport and metabolism of bile acids. *J Lipid Res* 56**,** 1085-1099.

De Smet, I., Van Hoorde, L., Vande Woestyne, M., Christiaens, H., and Verstraete, W. (1995). Significance of bile salt hydrolytic activities of lactobacilli. *J Appl Bacteriol* 79**,** 292-301.

De Spiegeleer, B., Verbeke, F., D'hondt, M., Hendrix, A., Van De Wiele, C., Burvenich, C., Peremans, K., De Wever, O., Bracke, M., and Wynendaele, E. (2015). The quorum sensing peptides PhrG, CSP and EDF promote angiogenesis and invasion of breast cancer cells *in vitro*. *PLoS One* 10**,** e0119471.

Deng, Y., Lim, A., Lee, J., Chen, S., An, S., Dong, Y.H., and Zhang, L.H. (2014). Diffusible signal factor (DSF) quorum sensing signal and structurally related molecules enhance the antimicrobial efficacy of antibiotics against some bacterial pathogens. *BMC Microbiology* 14**,** 51-51.

Di Ciaula, A., Garruti, G., Lunardi Baccetto, R., Molina-Molina, E., Bonfrate, L., Wang, D.Q., and Portincasa, P. (2017). Bile Acid Physiology. *Ann Hepatol* 16 Suppl 1**,** S4-S14.

Dirita, V.J., and Mekalanos, J.J. (1991). Periplasmic interaction between two membrane regulatory proteins, ToxR and ToxS, results in signal transduction and transcriptional activation. *Cell* 64**,** 29-37.

Disis, M.L. (2014). Mechanism of action of immunotherapy. *Seminars in Oncology* 41**,** S3-S13.

Dong, T.G., Ho, B.T., Yoder-Himes, D.R., and Mekalanos, J.J. (2013). Identification of T6SS-dependent effector and immunity proteins by Tn-seq in *Vibrio cholerae*. *Proc Natl Acad Sci U S A* 110**,** 2623-2628.

Duan, F., and March, J.C. (2010). Engineered bacterial communication prevents *Vibrio cholerae* virulence in an infant mouse model. *Proc Natl Acad Sci U S A* 107**,** 11260-11264.

Duan, K., Dammel, C., Stein, J., Rabin, H., and Surette, M.G. (2003). Modulation of *Pseudomonas aeruginosa* gene expression by host microflora through interspecies communication. *Molecular Microbiology* 50**,** 1477-1491.

Ecdc (2021). Cholera Annual Report 2020. *Weekly Epidemiological Record* 96**,** 445-460.

El Hassani, R.A., Benfares, N., Caillou, B., Talbot, M., Sabourin, J.C., V, B., Morand, S., Gnidehou, D., Agnandji, D., Ohayon, R., Kaniewski, J., Noel-Hudson, M.S., Bidart, J.M., Schlumberger, M., Virion, A., and Dupuy, C. (2005). Dual oxidase2 is expressed all along the digestive tract. *American Journal of Physiology-Gastrointestinal and Liver Physiology* 288**,** G933-G942.

Ellis, C.N., Larocque, R.C., Uddin, T., Krastins, B., Mayo-Smith, L.M., Sarracino, D., Karlsson, E.K., Rahman, A., Shirin, T., Bhuiyan, T.R., Chowdhury, F., Khan, A.I., Ryan, E.T., Calderwood, S.B., Qadri, F., and Harris, J.B. (2015). Comparative proteomic analysis reveals activation of mucosal innate immune signaling pathways during cholera. *Infect Immun* 83**,** 1089-1103.

Engebrecht, J., Nealson, K., and Silverman, M. (1983). Bacterial bioluminescence: isolation and genetic analysis of functions from *Vibrio fischeri*. *Cell* 32**,** 773-781.

Fast, D., Kostiuk, B., Foley, E., and Pukatzki, S. (2018). Commensal pathogen competition impacts host viability. *Proc Natl Acad Sci U S A* 115**,** 7099-7104.

Feng, L., Rutherford, S.T., Papenfort, K., Bagert, J.D., Van Kessel, J.C., Tirrell, D.A., Wingreen, N.S., and Bassler, B.L. (2015). A qrr noncoding RNA deploys four different regulatory mechanisms to optimize quorum-sensing dynamics. *Cell* 160**,** 228-240.

Finkelstein, R.A. (1996). "Cholera, *Vibrio cholerae* O1 and O139, and Other Pathogenic

Vibrios," in *Medical Microbiology*. (Galveston (TX)).

Fong, J.C., and Yildiz, F.H. (2008). Interplay between cyclic AMP-cyclic AMP receptor protein and cyclic di-GMP signaling in *Vibrio cholerae* biofilm formation. *J Bacteriol* 190**,** 6646-6659.

Fong, J.C.N., Syed, K.A., Klose, K.E., and Yildiz, F.H. (2010). Role of *Vibrio* polysaccharide (vps) genes in VPS production, biofilm formation and *Vibrio cholerae* pathogenesis. *Microbiology (Reading)* 156**,** 2757-2769.

Forstermann, U., and Munzel, T. (2006). Endothelial nitric oxide synthase in vascular disease: from marvel to menace. *Circulation* 113**,** 1708-1714.

Frankel, A.E., Coughlin, L.A., Kim, J., Froehlich, T.W., Xie, Y., Frenkel, E.P., and Koh, A.Y. (2017). Metagenomic shotgun sequencing and unbiased metabolomic profiling identify specific human gut microbiota and metabolites associated with immune checkpoint therapy efficacy in melanoma patients. *Neoplasia* 19**,** 848.

Freeman, J.A., and Bassler, B.L. (1999a). A genetic analysis of the function of LuxO, a two-component response regulator involved in quorum sensing in *Vibrio harveyi*. *Mol Microbiol* 31**,** 665-677.

Freeman, J.A., and Bassler, B.L. (1999b). Sequence and function of LuxU: a two-component phosphorelay protein that regulates quorum sensing in *Vibrio harveyi*. *J Bacteriol* 181**,** 899-906.

Freestone, P.P., Haigh, R.D., Williams, P.H., and Lyte, M. (1999). Stimulation of bacterial growth by heat-stable, norepinephrine-induced autoinducers. *FEMS Microbiol Lett* 172**,** 53-60.

Fu, Y., Waldor, M.K., and Mekalanos, J.J. (2013). Tn-Seq analysis of *Vibrio cholerae* intestinal colonization reveals a role for T6SS-mediated antibacterial activity in the host. *Cell Host Microbe* 14**,** 652-663.

Fuqua, C., Winans, S.C., and Greenberg, E.P. (1996). Census and consensus in bacterial ecosystems: the LuxR-LuxI family of quorum-sensing transcriptional regulators. *Annu Rev Microbiol* 50**,** 727-751.

Gallegos, M.T., Schleif, R., Bairoch, A., Hofmann, K., and Ramos, J.L. (1997). Arac/XylS family of transcriptional regulators. *Microbiol Mol Biol Rev* 61**,** 393-410.

Galloway, W.R., Hodgkinson, J.T., Bowden, S.D., Welch, M., and Spring, D.R. (2011). Quorum sensing in Gram-negative bacteria: small-molecule modulation of AHL and AI-2 quorum sensing pathways. *Chem Rev* 111**,** 28-67.

Geiszt, M., Witta, J., Baffi, J., Lekstrom, K., and Leto, T.L. (2003). Dual oxidases represent novel hydrogen peroxide sources supporting mucosal surface host defense. *FASEB J* 17**,** 1502-1504.

Gharaibeh, R.Z., and Jobin, C. (2019). Microbiota and cancer immunotherapy: in search of microbial signals. *Gut* 68**,** 385-388.

Glagolev, A.N. (1980). Reception of the energy level in bacterial taxis. *J Theor Biol* 82**,** 171-185.

Gopalakrishnan, V., Spencer, C., Nezi, L., Reuben, A., Andrews, M., Karpinets, T., Prieto, P., Vicente, D., Hoffman, K., and Wei, S. (2018). Gut microbiome modulates response to anti-PD-1 immunotherapy in melanoma patients. *Science* 359**,** 97-103.

Gorbach, S.L., Banwell, J.G., Jacobs, B., Chatterjee, B.D., Mitra, R., Brigham, K.L., and Neogy, K.N. (1970). Intestinal microflora in Asiatic cholera. I. "Rice-water" stool. *J Infect Dis* 121**,** 32-37.

Gorelik, O., Levy, N., Shaulov, L., Yegodayev, K., Meijler, M.M., and Sal-Man, N. (2019). *Vibrio cholerae* autoinducer-1 enhances the virulence of enteropathogenic *Escherichia coli*. *Sci Rep* 9**,** 4122.

Greenberg, E.P., Hastings, J.W., and Ulitzur, S. (1979). Induction of luciferase synthesis in

Beneckea harveyi by other marine bacteria. *Archives of Microbiology* 120**,** 87-91.

Grill, J.P., Cayuela, C., Antoine, J.M., and Schneider, F. (2000). Isolation and characterization of a *Lactobacillus amylovorus* mutant depleted in conjugated bile salt hydrolase activity: relation between activity and bile salt resistance. *J Appl Microbiol* 89**,** 553-563.

Halpern, M., Senderovich, Y., and Izhaki, I. (2008). Waterfowl: the missing link in epidemic and pandemic cholera dissemination? *PLoS Pathog* 4**,** e1000173.

Halpert, M.M., Konduri, V., Liang, D., Chen, Y., Wing, J.B., Paust, S., Levitt, J.M., and Decker, W.K. (2016). Dendritic cell-secreted cytotoxic T-lymphocyte-associated protein-4 regulates the T-cell response by downmodulating bystander surface B7. *Stem Cells and Development* 25**,** 774-787.

Hammer, B.K., and Bassler, B.L. (2003). Quorum sensing controls biofilm formation in *Vibrio cholerae*. *Molecular Microbiology* 50**,** 101-114.

Hase, C.C., and Mekalanos, J.J. (1998). TcpP protein is a positive regulator of virulence gene expression in *Vibrio cholerae*. *Proc Natl Acad Sci U S A* 95**,** 730-734.

Havarstein, L.S., Coomaraswamy, G., and Morrison, D.A. (1995). An unmodified heptadecapeptide pheromone induces competence for genetic transformation in *Streptococcus pneumoniae*. *Proc Natl Acad Sci U S A* 92**,** 11140-11144.

Hawver, L.A., Jung, S.A., and Ng, W.-L. (2016). Specificity and complexity in bacterial quorum-sensing systems. *FEMS Microbiology Reviews* 40**,** 738-752.

Hay, A.J., Yang, M., Xia, X., Liu, Z., Hammons, J., Fenical, W., and Zhu, J. (2017). Calcium Enhances Bile Salt-Dependent Virulence Activation in *Vibrio cholerae*. *Infect Immun* 85.

Hay, A.J., and Zhu, J. (2015). Host intestinal signal-promoted biofilm dispersal induces *Vibrio cholerae* colonization. *Infect Immun* 83**,** 317-323.

Helmink, B.A., Khan, M.a.W., Hermann, A., Gopalakrishnan, V., and Wargo, J.A. (2019). The microbiome, cancer, and cancer therapy. *Nature Medicine* 25**,** 377-388.

Herrington, D.A., Hall, R.H., Losonsky, G., Mekalanos, J.J., Taylor, R.K., and Levine, M.M. (1988). Toxin, toxin-coregulated pili, and the *toxR* regulon are essential for *Vibrio cholerae* pathogenesis in humans. *J Exp Med* 168**,** 1487-1492.

Higgins, D.A., Pomianek, M.E., Kraml, C.M., Taylor, R.K., Semmelhack, M.F., and Bassler, B.L. (2007). The major *Vibrio cholerae* autoinducer and its role in virulence factor production. *Nature* 450**,** 883-886.

Higgins, D.E., and Dirita, V.J. (1994). Transcriptional control of toxT, a regulatory gene in the ToxR regulon of *Vibrio cholerae*. *Mol Microbiol* 14**,** 17-29.

Higgins, D.E., Nazareno, E., and Dirital, V.J. (1992). "The Virulence Gene Activator ToxT from *Vibio cholerae* Is a Member of the AraC Family of Transcriptional Activators".).

Hirakawa, H., Inazumi, Y., Masaki, T., Hirata, T., and Yamaguchi, A. (2005). Indole induces the expression of multidrug exporter genes in *Escherichia coli*. *Mol Microbiol* 55**,** 1113-1126.

Ho, B.T., Dong, T.G., and Mekalanos, J.J. (2014). A view to a kill: The bacterial type VI secretion system. *Cell Host and Microbe* 15**,** 9-21.

Hofmann, A.F. (1999). Bile Acids: The Good, the Bad, and the Ugly. *News Physiol Sci* 14**,** 24-29.

Horz, H.P., Vianna, M.E., Gomes, B.P., and Conrads, G. (2005). Evaluation of universal probes and primer sets for assessing total bacterial load in clinical samples: general implications and practical use in endodontic antimicrobial therapy. *J Clin Microbiol* 43**,** 5332-5337.

Hsiao, A., Ahmed, A.M., Subramanian, S., Griffin, N.W., Drewry, L.L., Petri, W.A., Jr., Haque, R., Ahmed, T., and Gordon, J.I. (2014). Members of the human gut microbiota involved in recovery from *Vibrio cholerae* infection. *Nature* 515**,** 423-426.

Huang, X., Duddy, O.P., Silpe, J.E., Paczkowski, J.E., Cong, J., Henke, B.R., and Bassler, B.L. (2020). Mechanism underlying autoinducer recognition in the Vibrio cholerae DPO-VqmA quorum-sensing pathway. *J Biol Chem* 295**,** 2916-2931.

Hui, F.M., and Morrison, D.A. (1991). Genetic transformation in *Streptococcus pneumoniae*: nucleotide sequence analysis shows *comA*, a gene required for competence induction, to be a member of the bacterial ATP-dependent transport protein family. *J Bacteriol* 173**,** 372-381.

Hui, F.M., Zhou, L., and Morrison, D.A. (1995). Competence for genetic transformation in *Streptococcus pneumoniae*: organization of a regulatory locus with homology to two lactococcin A secretion genes. *Gene* 153**,** 25-31.

Humbert, L., Maubert, M.A., Wolf, C., Duboc, H., Mahe, M., Farabos, D., Seksik, P., Mallet, J.M., Trugnan, G., Masliah, J., and Rainteau, D. (2012). Bile acid profiling in human biological samples: comparison of extraction procedures and application to normal and cholestatic patients. *J Chromatogr B Analyt Technol Biomed Life Sci* 899**,** 135-145.

Hung, D.T., Zhu, J., Sturtevant, D., and Mekalanos, J.J. (2006). Bile acids stimulate biofilm formation in *Vibrio cholerae*. *Mol Microbiol* 59**,** 193-201.

Huq, A., Small, E.B., West, P.A., Huq, M.I., Rahman, R., and Colwell, R.R. (1983). Ecological relationships between *Vibrio cholerae* and planktonic crustacean copepods. *Appl Environ Microbiol* 45**,** 275-283.

Huttenhower, C., Gevers, D., Knight, R., Abubucker, S., Badger, J.H., Chinwalla, A.T., Creasy, H.H., Earl, A.M., Fitzgerald, M.G., and Fulton, R.S. (2012). Structure, function and diversity of the healthy human microbiome. *Nature* 486**,** 207-214.

Hwang, I.Y., Tan, M.H., Koh, E., Ho, C.L., Poh, C.L., and Chang, M.W. (2014). Reprogramming microbes to be pathogen-Seeking killers. *ACS Synthetic Biology* 3**,** 228-237.

Imlay, J.A. (2019). Where in the world do bacteria experience oxidative stress? *Environ Microbiol* 21**,** 521-530.

Integrative, H. (2014). The Integrative Human Microbiome Project: dynamic analysis of microbiome-host omics profiles during periods of human health and disease. *Cell Host & Microbe* 16**,** 276-289.

Ismail, A.S., Valastyan, J.S., and Bassler, B.L. (2016). A Host-Produced Autoinducer-2 Mimic Activates Bacterial Quorum Sensing. *Cell Host and Microbe* 19**,** 470-480.

Jandhyala, S.M., Talukdar, R., Subramanyam, C., Vuyyuru, H., Sasikala, M., and Reddy, D.N. (2015). Role of the normal gut microbiota. *World Journal of Gastroenterology* 21**,** 8836-8847.

Janoff, E.N., Hayakawa, H., Taylor, D.N., Fasching, C.E., Kenner, J.R., Jaimes, E., and Raij, L. (1997). Nitric oxide production during *Vibrio cholerae* infection. *Am J Physiol* 273**,** G1160-1167.

Ji, G., Beavis, R., and Novick, R.P. (1997). Bacterial interference caused by autoinducing peptide variants. *Science* 276**,** 2027-2030.

Ji, G., Beavis, R.C., and Novick, R.P. (1995). Cell density control of staphylococcal virulence mediated by an octapeptide pheromone. *Proc Natl Acad Sci U S A* 92**,** 12055-12059.

Jimenez, A.G., and Sperandio, V. (2019). "Quorum sensing and the gut microbiome," in *Quorum Sensing*. Elsevier), 151-169.

Jones, B.V., Begley, M., Hill, C., Gahan, C.G., and Marchesi, J.R. (2008). Functional and

comparative metagenomic analysis of bile salt hydrolase activity in the human gut microbiome. *Proc Natl Acad Sci U S A* 105**,** 13580-13585.

Jung, S.A., Chapman, C.A., and Ng, W.-L.L. (2015). Quadruple Quorum-Sensing Inputs Control *Vibrio cholerae* Virulence and Maintain System Robustness. *PLoS Pathogens* 11**,** e1004837-e1004837.

Jung, S.A., Hawver, L.A., and Ng, W.-L. (2016). Parallel quorum sensing signaling pathways in *Vibrio cholerae*. *Current genetics* 62**,** 255-260.

Kanehisa, M. (2019). Toward understanding the origin and evolution of cellular organisms. *Protein Sci* 28**,** 1947-1951.

Kanehisa, M., Furumichi, M., Sato, Y., Ishiguro-Watanabe, M., and Tanabe, M. (2021). KEGG: integrating viruses and cellular organisms. *Nucleic Acids Res* 49**,** D545-D551.

Kanehisa, M., and Goto, S. (2000). KEGG: kyoto encyclopedia of genes and genomes. *Nucleic Acids Res* 28**,** 27-30.

Kang, D.J., Ridlon, J.M., Moore, D.R., 2nd, Barnes, S., and Hylemon, P.B. (2008). *Clostridium scindens* baiCD and baiH genes encode stereo-specific 7alpha/7beta-hydroxy-3-oxo-delta4-cholenoic acid oxidoreductases. *Biochim Biophys Acta* 1781**,** 16-25.

Karaolis, D.K., Johnson, J.A., Bailey, C.C., Boedeker, E.C., Kaper, J.B., and Reeves, P.R. (1998). A *Vibrio cholerae* pathogenicity island associated with epidemic and pandemic strains. *Proc Natl Acad Sci U S A* 95**,** 3134-3139.

Kaval, K.G., and Garsin, D.A. (2018). Ethanolamine Utilization in Bacteria. *mBio* 9.

Kawamoto, K., Horibe, I., and Uchida, K. (1989). Purification and characterization of a new hydrolase for conjugated bile acids, chenodeoxycholyltaurine hydrolase, from *Bacteroides vulgatus*. *J Biochem* 106**,** 1049-1053.

Kelly, R.C., Bolitho, M.E., Higgins, D.A., Lu, W., Ng, W.-L.L., Jeffrey, P.D., Rabinowitz, J.D., Semmelhack, M.F., Hughson, F.M., and Bassler, B.L. (2009). The *Vibrio cholerae* quorum-sensing autoinducer CAI-1: Analysis of the biosynthetic enzyme CqsA. *Nature Chemical Biology* 5**,** 891-895.

Kendall, M.M., Gruber, C.C., Parker, C.T., and Sperandio, V. (2012). Ethanolamine controls expression of genes encoding components involved in interkingdom signaling and virulence in enterohemorrhagic *Escherichia coli* O157:H7. *mBio* 3.

Kieser, S., Sarker, S.A., Sakwinska, O., Foata, F., Sultana, S., Khan, Z., Islam, S., Porta, N., Combremont, S., Betrisey, B., Fournier, C., Charpagne, A., Descombes, P., Mercenier, A., Berger, B., and Brüssow, H. (2018). Bangladeshi children with acute diarrhoea show faecal microbiomes with increased Streptococcus abundance, irrespective of diarrhoea aetiology. *Environmental Microbiology* 20**,** 2256-2269.

Kim, C.S., Gatsios, A., Cuesta, S., Lam, Y.C., Wei, Z., Chen, H., Russell, R.M., Shine, E.E., Wang, R., Wyche, T.P., Piizzi, G., Flavell, R.A., Palm, N.W., Sperandio, V., and Crawford, J.M. (2020). Characterization of Autoinducer-3 Structure and Biosynthesis in *E. coli*. *ACS Cent Sci* 6**,** 197-206.

Kim, D., Langmead, B., and Salzberg, S.L. (2015). HISAT: a fast spliced aligner with low memory requirements. *Nat Methods* 12**,** 357-360.

Kim, S.H., and Lee, W.J. (2014). Role of DUOX in gut inflammation: lessons from Drosophila model of gut-microbiota interactions. *Front Cell Infect Microbiol* 3**,** 116.

Kirn, T.J., Lafferty, M.J., Sandoe, C.M., and Taylor, R.K. (2000). Delineation of pilin domains required for bacterial association into microcolonies and intestinal colonization by *Vibrio cholerae*. *Mol Microbiol* 35**,** 896-910.

Knott, A.B., and Bossy-Wetzel, E. (2009). Nitric oxide in health and disease of the nervous system. *Antioxid Redox Signal* 11**,** 541-554.

Koch, R. (1884). An Address on Cholera and its Bacillus. *Br Med J* 2**,** 453-459.

Koetje, E.J., Hajdo-Milasinovic, A., Kiewiet, R., Bron, S., and Tjalsma, H. (2003). A plasmid-borne Rap-Phr system of *Bacillus subtilis* can mediate cell-density controlled production of extracellular proteases. *Microbiology* 149**,** 19-28.

Król, M., and Kepinska, M. (2021). Human Nitric Oxide Synthase—Its Functions, Polymorphisms, and Inhibitors in the Context of Inflammation, Diabetes and Cardiovascular Diseases. 22**,** 56.

Kumar, S., Stecher, G., Li, M., Knyaz, C., and Tamura, K. (2018). MEGA X: Molecular evolutionary genetics analysis across computing platforms. *Molecular Biology and Evolution* 35**,** 1547.

Lee, J.H., and Lee, J. (2010). Indole as an intercellular signal in microbial communities. *FEMS Microbiol Rev* 34**,** 426-444.

Lee, K.A., Thomas, A.M., Bolte, L.A., Björk, J.R., De Ruijter, L.K., Armanini, F., Asnicar, F., Blanco-Miguez, A., Board, R., Calbet-Llopart, N., Derosa, L., Dhomen, N., Brooks, K., Harland, M., Harries, M., Leeming, E.R., Lorigan, P., Manghi, P., Marais, R., Newton-Bishop, J., Nezi, L., Pinto, F., Potrony, M., Puig, S., Serra-Bellver, P., Shaw, H.M., Tamburini, S., Valpione, S., Vijay, A., Waldron, L., Zitvogel, L., Zolfo, M., De Vries, E.G.E., Nathan, P., Fehrmann, R.S.N., Bataille, V., Hospers, G.a.P., Spector, T.D., Weersma, R.K., and Segata, N. (2022). Cross-cohort gut microbiome associations with immune checkpoint inhibitor response in advanced melanoma. *Nature Medicine* 28**,** 535-544.

Lee, M.S., and Morrison, D.A. (1999). Identification of a new regulator in *Streptococcus pneumoniae* linking quorum sensing to competence for genetic transformation. *J Bacteriol* 181**,** 5004-5016.

Leiman, P.G., Basler, M., Ramagopal, U.A., Bonanno, J.B., Sauder, J.M., Pukatzki, S., Burley, S.K., Almo, S.C., and Mekalanos, J.J. (2009). Type VI secretion apparatus and phage tail-associated protein complexes share a common evolutionary origin.

Proceedings of the National Academy of Sciences of the United States of America 106**,** 4154-4159.

Lembke, M., Hofler, T., Walter, A.N., Tutz, S., Fengler, V., Schild, S., and Reidl, J. (2020). Host stimuli and operator binding sites controlling protein interactions between virulence master regulator ToxR and ToxS in *Vibrio cholerae*. *Mol Microbiol*.

Lembke, M., Pennetzdorfer, N., Tutz, S., Koller, M., Vorkapic, D., Zhu, J., Schild, S., and Reidl, J. (2018). Proteolysis of ToxR is controlled by cysteine-thiol redox state and bile salts in *Vibrio cholerae*. *Mol Microbiol* 110**,** 796-810.

Lenz, D.H., Mok, K.C., Lilley, B.N., Kulkarni, R.V., Wingreen, N.S., and Bassler, B.L. (2004). The small RNA chaperone Hfq and multiple small RNAs control quorum sensing in *Vibrio harveyi* and *Vibrio cholerae*. *Cell* 118**,** 69-82.

Li, Q., Peng, W., Wu, J., Wang, X., Ren, Y., Li, H., Peng, Y., Tang, X., and Fu, X. (2019). Autoinducer-2 of gut microbiota, a potential novel marker for human colorectal cancer, is associated with the activation of TNFSF9 signaling in macrophages. *Oncoimmunology* 8**,** e1626192.

Lina, G., Jarraud, S., Ji, G., Greenland, T., Pedraza, A., Etienne, J., Novick, R.P., and Vandenesch, F. (1998). Transmembrane topology and histidine protein kinase activity of AgrC, the agr signal receptor in *Staphylococcus aureus*. *Mol Microbiol* 28**,** 655-662.

Liu, Z., Hsiao, A., Joelsson, A., and Zhu, J. (2006). The transcriptional regulator VqmA increases expression of the quorum-sensing activator HapR in *Vibrio cholerae*. *J Bacteriol* 188**,** 2446-2453.

Liu, Z., Li, L., Wang, Q., Sadiq, F.A., Lee, Y., Zhao, J., Zhang, H., Chen, W., Li, H., and Lu, W. (2021). Transcriptome analysis reveals the genes involved in *Bifidobacterium Longum* FGSZY16M3 biofilm formation. *Microorganisms* 9**,** 385.

Logan, S.L., Thomas, J., Yan, J., Baker, R.P., Shields, D.S., Xavier, J.B., Hammer, B.K.,

and Parthasarathy, R. (2018). The *Vibrio cholerae* type VI secretion system can modulate host intestinal mechanics to displace gut bacterial symbionts. *Proceedings of the National Academy of Sciences* 115**,** E3779-E3787.

Louis, P., and O'byrne, C.P. (2010). Life in the gut: microbial responses to stress in the gastrointestinal tract. *Sci Prog* 93**,** 7-36.

Lowden, M.J., Skorupski, K., Pellegrini, M., Chiorazzo, M.G., Taylor, R.K., and Kull, F.J. (2010). Structure of *Vibrio cholerae* ToxT reveals a mechanism for fatty acid regulation of virulence genes. *Proc Natl Acad Sci U S A* 107**,** 2860-2865.

Lyte, M., Arulanandam, B.P., and Frank, C.D. (1996a). Production of Shiga-like toxins by *Escherichia coli* O157:H7 can be influenced by the neuroendocrine hormone norepinephrine. *J Lab Clin Med* 128**,** 392-398.

Lyte, M., Frank, C.D., and Green, B.T. (1996b). Production of an autoinducer of growth by norepinephrine cultured *Escherichia coli* O157:H7. *FEMS Microbiol Lett* 139**,** 155-159.

Ma, N., and Ma, X. (2019). Dietary Amino Acids and the Gut-Microbiome-Immune Axis: Physiological Metabolism and Therapeutic Prospects. *Compr Rev Food Sci Food Saf* 18**,** 221-242.

Macintyre, D.L., Miyata, S.T., Kitaoka, M., and Pukatzki, S. (2010). The *Vibrio cholerae* type VI secretion system displays antimicrobial properties. *Proceedings of the National Academy of Sciences* 107**,** 19520 -19524.

Mager, L.F., Burkhard, R., Pett, N., Cooke, N.C.A., Brown, K., Ramay, H., Paik, S., Stagg, J., Groves, R.A., Gallo, M., Lewis, I.A., Geuking, M.B., and Mccoy, K.D. (2020). Microbiome-derived inosine modulates response to checkpoint inhibitor immunotherapy. *Science* 369**,** 1481-1489.

Mallick, H., Rahnavard, A., Mciver, L.J., Ma, S., Zhang, Y., Nguyen, L.H., Tickle, T.L., Weingart, G., Ren, B., Schwager, E.H., Chatterjee, S., Thompson, K.N., Wilkinson,

J.E., Subramanian, A., Lu, Y., Waldron, L., Paulson, J.N., Franzosa, E.A., Bravo, H.C., and Huttenhower, C. (2021). Multivariable association discovery in population-scale meta-omics studies. *PLoS Comput Biol* 17**,** e1009442.

Marques, J.C., Oh, I.K., Ly, D.C., Lamosa, P., Ventura, M.R., Miller, S.T., and Xavier, K.B. (2014). LsrF, a coenzyme A-dependent thiolase, catalyzes the terminal step in processing the quorum sensing signal autoinducer-2. *Proc Natl Acad Sci U S A* 111**,** 14235-14240.

Martin-Verstraete, I., Peltier, J., and Dupuy, B. (2016). The Regulatory Networks That Control *Clostridium difficile* Toxin Synthesis. *Toxins (Basel)* 8.

Martin, R.G., and Rosner, J.L. (2001). "The AraC transcriptional activators". Elsevier Ltd).

Martino, P.D., Fursy, R., Bret, L., Sundararaju, B., and Phillips, R.S. (2003). Indole can act as an extracellular signal to regulate biofilm formation of *Escherichia coli* and other indole-producing bacteria. *Can J Microbiol* 49**,** 443-449.

Mashruwala, A.A., and Bassler, B.L. (2020). The *Vibrio cholerae* quorum-sensing protein VqmA integrates cell density, environmental, and host-derived cues into the control of virulence. *mBio* 11**,** 1-19.

Matson, J.S., Withey, J.H., and Dirita, V.J. (2007). Regulatory networks controlling *Vibrio cholerae* virulence gene expression. *Infect Immun* 75**,** 5542-5549.

Matson, V., Fessler, J., Bao, R., Chongsuwat, T., Zha, Y., Alegre, M.-L., Luke, J.J., and Gajewski, T.F. (2018). The commensal microbiome is associated with anti-PD-1 efficacy in metastatic melanoma patients. *Science* 359**,** 104-108.

Matz, C., Mcdougald, D., Moreno, A.M., Yung, P.Y., Yildiz, F.H., and Kjelleberg, S. (2005). Biofilm formation and phenotypic variation enhance predation-driven persistence of *Vibrio cholerae*. *Proc Natl Acad Sci U S A* 102**,** 16819-16824.

Mccarthy, D.J., Chen, Y., and Smyth, G.K. (2012). Differential expression analysis of

multifactor RNA-Seq experiments with respect to biological variation. *Nucleic Acids Res* 40**,** 4288-4297.

Mcclure, R., Balasubramanian, D., Sun, Y., Bobrovskyy, M., Sumby, P., Genco, C.A., Vanderpool, C.K., and Tjaden, B. (2013). Computational analysis of bacterial RNA-Seq data. *Nucleic Acids Res* 41**,** e140.

Mcquade, R.S., Comella, N., and Grossman, A.D. (2001). Control of a family of phosphatase regulatory genes (phr) by the alternate sigma factor sigma-H of *Bacillus subtilis*. *J Bacteriol* 183**,** 4905-4909.

Miller, M.B., and Bassler, B.L. (2002). Quorum Sensing in Bacteria. *Annual Review of Microbiology* 55**,** 165-199.

Miller, M.B., Skorupski, K., Lenz, D.H., Taylor, R.K., and Bassler, B.L. (2002). Parallel quorum sensing systems converge to regulate virulence in *Vibrio cholerae*. *Cell* 110**,** 303-314.

Miller, S.T., Xavier, K.B., Campagna, S.R., Taga, M.E., Semmelhack, M.F., Bassler, B.L., and Hughson, F.M. (2004). *Salmonella typhimurium* recognizes a chemically distinct form of the bacterial quorum-sensing signal AI-2. *Molecular Cell* 15**,** 677-687.

Miller, V.L., Taylor, R.K., and Mekalanos, J.J. (1987). Cholera toxin transcriptional activator *toxR* is a transmembrane DNA binding protein. *Cell* 48**,** 271-279.

Mogasale, V., Mogasale, V.V., and Hsiao, A. (2020). Economic burden of cholera in Asia. *Vaccine* 38 Suppl 1**,** A160-A166.

Molinaro, A., Wahlstrom, A., and Marschall, H.U. (2018). Role of Bile Acids in Metabolic Control. *Trends Endocrinol Metab* 29**,** 31-41.

Moreira, C.G., Weinshenker, D., and Sperandio, V. (2010). QseC mediates *Salmonella enterica* serovar typhimurium virulence *in vitro* and *in vivo*. *Infect Immun* 78**,** 914-

926.

Morfeldt, E., Taylor, D., Von Gabain, A., and Arvidson, S. (1995). Activation of alpha-toxin translation in *Staphylococcus aureus* by the trans-encoded antisense RNA, RNAIII. *EMBO J* 14**,** 4569-4577.

Nathan, C., and Ding, A. (2010). SnapShot: Reactive Oxygen Intermediates (ROI). *Cell* 140**,** 951-951 e952.

Nawrocki, K.L., Wetzel, D., Jones, J.B., Woods, E.C., and Mcbride, S.M. (2018). Ethanolamine is a valuable nutrient source that impacts *Clostridium difficile* pathogenesis. *Environ Microbiol* 20**,** 1419-1435.

Neiditch, M.B., Federle, M.J., Miller, S.T., Bassler, B.L., and Hughson, F.M. (2005). Regulation of LuxPQ Receptor Activity by the Quorum-Sensing Signal Autoinducer-2. *Molecular Cell* 18**,** 507-518.

Neiditch, M.B., Federle, M.J., Pompeani, A.J., Kelly, R.C., Swem, D.L., Jeffrey, P.D., Bassler, B.L., and Hughson, F.M. (2006). Ligand-Induced Asymmetry in Histidine Sensor Kinase Complex Regulates Quorum Sensing. *Cell* 126**,** 1095-1108.

Oiseth, S.J., and Aziz, M.S. (2017). Cancer immunotherapy: a brief review of the history, possibilities, and challenges ahead. *Journal of Cancer Metastasis and Treatment* 3**,** 250-261.

Okada, M., Sato, I., Cho, S.J., Iwata, H., Nishio, T., Dubnau, D., and Sakagami, Y. (2005). Structure of the *Bacillus subtilis* quorum-sensing peptide pheromone ComX. *Nat Chem Biol* 1**,** 23-24.

Paiva, C.N., and Bozza, M.T. (2014). Are reactive oxygen species always detrimental to pathogens? *Antioxid Redox Signal* 20**,** 1000-1037.

Papenfort, K., Forstner, K.U., Cong, J.P., Sharma, C.M., and Bassler, B.L. (2015). Differential RNA-seq of *Vibrio cholerae* identifies the VqmR small RNA as a

regulator of biofilm formation. *Proc Natl Acad Sci U S A* 112**,** E766-775.

Papenfort, K., Silpe, J.E., Schramma, K.R., Cong, J.P., Seyedsayamdost, M.R., and Bassler, B.L. (2017). A *Vibrio cholerae* autoinducer-receptor pair that controls biofilm formation. *Nat Chem Biol* 13**,** 551-557.

Patankar, A.V., and Gonzalez, J.E. (2009). Orphan LuxR regulators of quorum sensing. *FEMS Microbiol Rev* 33**,** 739-756.

Pell, L.G., Kanelis, V., Donaldson, L.W., Howell, P.L., and Davidson, A.R. (2009). The phage λ major tail protein structure reveals a common evolution for long-tailed phages and the type VI bacterial secretion system. *Proceedings of the National Academy of Sciences of the United States of America* 106**,** 4160-4165.

Peng, H.L., Novick, R.P., Kreiswirth, B., Kornblum, J., and Schlievert, P. (1988). Cloning, characterization, and sequencing of an accessory gene regulator (agr) in *Staphylococcus aureus*. *J Bacteriol* 170**,** 4365-4372.

Pereira, C.S., Thompson, J.A., and Xavier, K.B. (2013). "AI-2-mediated signalling in bacteria". John Wiley & Sons, Ltd (10.1111).

Polgar, O., and Bates, S. (2005). ABC transporters in the balance: is there a role in multidrug resistance? *Biochemical Society Transactions* 33**,** 241-245.

Pozzi, G., Masala, L., Iannelli, F., Manganelli, R., Havarstein, L.S., Piccoli, L., Simon, D., and Morrison, D.A. (1996). Competence for genetic transformation in encapsulated strains of *Streptococcus pneumoniae*: two allelic variants of the peptide pheromone. *J Bacteriol* 178**,** 6087-6090.

Provenzano, D., and Klose, K.E. (2000). Altered expression of the ToxR-regulated porins OmpU and OmpT diminishes *Vibrio cholerae* bile resistance, virulence factor expression, and intestinal colonization. *Proc Natl Acad Sci U S A* 97**,** 10220-10224.

Ribet, D., and Cossart, P. (2015). How bacterial pathogens colonize their hosts and invade

deeper tissues. *Microbes and Infection* 17**,** 173-183.

Ridlon, J.M., Kang, D.J., and Hylemon, P.B. (2006). Bile salt biotransformations by human intestinal bacteria. *J Lipid Res* 47**,** 241-259.

Robinson, M.D., Mccarthy, D.J., and Smyth, G.K. (2009). edgeR: a Bioconductor package for differential expression analysis of digital gene expression data. *Bioinformatics* 26**,** 139-140.

Roilides, E., Simitsopoulou, M., Katragkou, A., Walsh, T.J., Ghannoum, M., Parsek, M., Whiteley, M., and Mukherjee, P. (2015). How Biofilms Evade Host Defenses. 3**,** 3.3.22.

Routy, B., Le Chatelier, E., Derosa, L., Duong, C.P., Alou, M.T., Daillère, R., Fluckiger, A., Messaoudene, M., Rauber, C., and Roberti, M.P. (2018). Gut microbiome influences efficacy of PD-1-based immunotherapy against epithelial tumors. *Science* 359**,** 91-97.

Russell, A.B., Peterson, S.B., and Mougous, J.D. (2014). "Type VI secretion system effectors: Poisons with a purpose". NIH Public Access).

Rutherford, S.T., and Bassler, B.L. (2012). Bacterial quorum sensing: its role in virulence and possibilities for its control. *Cold Spring Harb Perspect Med* 2.

Rutherford, S.T., Van Kessel, J.C., Shao, Y., and Bassler, B.L. (2011). AphA and LuxR/HapR reciprocally control quorum sensing in vibrios. *Genes Dev* 25**,** 397-408.

Sack, D.A., Sack, R.B., Nair, G.B., and Siddique, A.K. (2004). Cholera. *The Lancet* 363**,** 223-233.

Sayin, S.I., Wahlstrom, A., Felin, J., Jantti, S., Marschall, H.U., Bamberg, K., Angelin, B., Hyotylainen, T., Oresic, M., and Backhed, F. (2013). Gut microbiota regulates bile acid metabolism by reducing the levels of tauro-beta-muricholic acid, a naturally

occurring FXR antagonist. *Cell Metab* 17**,** 225-235.

Schauder, S., Shokat, K., Surette, M.G., and Bassler, B.L. (2001). The LuxS family of bacterial autoinducers: biosynthesis of a novel quorum-sensing signal molecule. *Mol Microbiol* 41**,** 463-476.

Shao, Y., and Bassler, B.L. (2014). Quorum regulatory small RNAs repress type VI secretion in *Vibrio cholerae*. *Mol Microbiol* 92**,** 921-930.

Shaw, C.E., and Taylor, R.K. (1990). *Vibrio cholerae* O395 *tcpA* pilin gene sequence and comparison of predicted protein structural features to those of type 4 pilins. *Infect Immun* 58**,** 3042-3049.

Shi, L., Sheng, J., Chen, G., Zhu, P., Shi, C., Li, B., Park, C., Wang, J., Zhang, B., and Liu, Z. (2020). Combining IL-2-based immunotherapy with commensal probiotics produces enhanced antitumor immune response and tumor clearance. *Journal for ImmunoTherapy of Cancer* 8.

Shiner, E.K., Terentyev, D., Bryan, A., Sennoune, S., Martinez-Zaguilan, R., Li, G., Gyorke, S., Williams, S.C., and Rumbaugh, K.P. (2006). *Pseudomonas aeruginosa* autoinducer modulates host cell responses through calcium signalling. *Cell Microbiol* 8**,** 1601-1610.

Silpe, J.E., and Bassler, B.L. (2019). A Host-Produced Quorum-Sensing Autoinducer Controls a Phage Lysis-Lysogeny Decision. *Cell* 176**,** 268-280.e213.

Simonet, V.C., Basle, A., Klose, K.E., and Delcour, A.H. (2003). The *Vibrio cholerae* porins OmpU and OmpT have distinct channel properties. *J Biol Chem* 278**,** 17539-17545.

Skorupski, K., and Taylor, R.K. (1997). Control of the ToxR virulence regulon in *Vibrio cholerae* by environmental stimuli. *Mol Microbiol* 25**,** 1003-1009.

Somboonwit, C., Menezes, L.J., Holt, D.A., Sinnott, J.T., and Shapshak, P. (2017). Current

views and challenges on clinical cholera. *Bioinformation* 13**,** 405-409.

Sommer, F., and Backhed, F. (2015). The gut microbiota engages different signaling pathways to induce Duox2 expression in the ileum and colon epithelium. *Mucosal Immunol* 8**,** 372-379.

Song, X.N., Qiu, H.B., Xiao, X., Cheng, Y.Y., Li, W.W., Sheng, G.P., Li, X.Y., and Yu, H.Q. (2014). Determination of autoinducer-2 in biological samples by high-performance liquid chromatography with fluorescence detection using pre-column derivatization. *J Chromatogr A* 1361**,** 162-168.

Song, Z., Cai, Y., Lao, X., Wang, X., Lin, X., Cui, Y., Kalavagunta, P.K., Liao, J., Jin, L., Shang, J., and Li, J. (2019). Taxonomic profiling and populational patterns of bacterial bile salt hydrolase (BSH) genes based on worldwide human gut microbiome. *Microbiome* 7**,** 9-9.

Sperandio, V., Torres, A.G., Jarvis, B., Nataro, J.P., and Kaper, J.B. (2003). Bacteria-host communication: the language of hormones. *Proc Natl Acad Sci U S A* 100**,** 8951-8956.

Stojkova, P., Spidlova, P., and Stulik, J. (2019). Nucleoid-Associated Protein HU: A Lilliputian in Gene Regulation of Bacterial Virulence. *Front Cell Infect Microbiol* 9**,** 159.

Sturme, M.H., Kleerebezem, M., Nakayama, J., Akkermans, A.D., Vaugha, E.E., and De Vos, W.M. (2002). Cell to cell communication by autoinducing peptides in gram-positive bacteria. *Antonie Van Leeuwenhoek* 81**,** 233-243.

Subramanian, S., Huq, S., Yatsunenko, T., Haque, R., Mahfuz, M., Alam, M.A., Benezra, A., Destefano, J., Meier, M.F., Muegge, B.D., Barratt, M.J., Vanarendonk, L.G., Zhang, Q., Province, M.A., Petri Jr, W.A., Ahmed, T., and Gordon, J.I. (2014). Persistent gut microbiota immaturity in malnourished Bangladeshi children. *Nature* 510**,** 417.

Sun, Z., He, X., Brancaccio, V.F., Yuan, J., and Riedel, C.U. (2014). Bifidobacteria exhibit LuxS-dependent autoinducer 2 activity and biofilm formation. *PLoS One* 9**,** e88260.

Taga, M.E., Miller, S.T., and Bassler, B.L. (2003). Lsr-mediated transport and processing of AI-2 in *Salmonella typhimurium*. *Mol Microbiol* 50**,** 1411-1427.

Taga, M.E., Semmelhack, J.L., and Bassler, B.L. (2001). The LuxS-dependent autoinducer AI-2 controls the expression of an ABC transporter that functions in AI-2 uptake in *Salmonella typhimurium*. *Mol. Microbiol.* 42**,** 777-793.

Tamayo, R., Patimalla, B., and Camilli, A. (2010). Growth in a Biofilm Induces a Hyperinfectious Phenotype in *Vibrio cholerae*. *Infection and Immunity* 78**,** 3560-3569.

Tamplin, M.L., Gauzens, A.L., Huq, A., Sack, D.A., and Colwell, R.R. (1990). Attachment of *Vibrio cholerae* serogroup O1 to zooplankton and phytoplankton of Bangladesh waters. *Appl Environ Microbiol* 56**,** 1977-1980.

Taylor, B.L. (1983). Role of proton motive force in sensory transduction in bacteria. *Annu Rev Microbiol* 37**,** 551-573.

Taylor, C.T., and Colgan, S.P. (2017). Regulation of immunity and inflammation by hypoxia in immunological niches. *Nat Rev Immunol* 17**,** 774-785.

Thiel, V., Vilchez, R., Sztajer, H., Wagner-Dobler, I., and Schulz, S. (2009). Identification, quantification, and determination of the absolute configuration of the bacterial quorum-sensing signal autoinducer-2 by gas chromatography-mass spectrometry. *Chembiochem* 10**,** 479-485.

Thoendel, M., Kavanaugh, J.S., Flack, C.E., and Horswill, A.R. (2011). Peptide signaling in the staphylococci. *Chem Rev* 111**,** 117-151.

Thompson, J.A., Oliveira, R.A., Djukovic, A., Ubeda, C., and Xavier, K.B. (2015). Manipulation of the quorum sensing signal AI-2 affects the antibiotic-treated gut

microbiota. *Cell Rep* 10**,** 1861-1871.

Thompson, J.A., Oliveira, R.A., and Xavier, K.B. (2016). "Chemical conversations in the gut microbiota". Taylor & Francis).

Thursby, E., and Juge, N. (2017). Introduction to the human gut microbiota. *Biochemical Journal* 474**,** 1823-1836.

Tjaden, B. (2015). *De novo* assembly of bacterial transcriptomes from RNA-seq data. *Genome Biol* 16**,** 1.

Tjaden, B. (2020). A computational system for identifying operons based on RNA-seq data. *Methods* 176**,** 62-70.

Van Der Kooij, M., Joosse, A., Speetjens, F., Hospers, G., Bisschop, C., De Groot, J., Koornstra, R., Blank, C., and Kapiteijn, E. (2017). Anti-PD1 treatment in metastatic uveal melanoma in the Netherlands. *Acta Oncologica* 56**,** 101-103.

Von Bodman, S.B., Willey, J.M., and Diggle, S.P. (2008). Cell-cell communication in bacteria: united we stand. *J Bacteriol* 190**,** 4377-4391.

Waldor, M.K., and Mekalanos, J.J. (1996). Lysogenic conversion by a filamentous phage encoding cholera toxin. *Science* 272**,** 1910-1914.

Wang, H., Xing, X., Wang, J., Pang, B., Liu, M., Larios-Valencia, J., Liu, T., Liu, G., Xie, S., Hao, G., Liu, Z., Kan, B., and Zhu, J. (2018). Hypermutation-induced *in vivo* oxidative stress resistance enhances *Vibrio cholerae* host adaptation. *PLoS Pathogens* 14.

Waters, C.M., and Bassler, B.L. (2005). Quorum sensing: cell-to-cell communication in bacteria. *Annu Rev Cell Dev Biol* 21**,** 319-346.

Waters, C.M., Lu, W., Rabinowitz, J.D., and Bassler, B.L. (2008). Quorum Sensing Controls Biofilm Formation in *Vibrio cholerae* through Modulation of Cyclic Di-

GMP Levels and Repression of vpsT. *Journal of Bacteriology* 190**,** 2527-2536.

Watnick, P.I., and Kolter, R. (1999). Steps in the development of a *Vibrio cholerae* El Tor biofilm. *Molecular Microbiology* 34**,** 586-595.

Watve, S., Barrasso, K., Jung, S.A., Davis, K.J., Hawver, L.A., Khataokar, A., Palaganas, R.G., Neiditch, M.B., Perez, L.J., and Ng, W.-L. (2019). Ethanolamine regulates CqsR quorum-sensing signaling in *Vibrio cholerae*. 589390.

Watve, S., Barrasso, K., Jung, S.A., Davis, K.J., Hawver, L.A., Khataokar, A., Palaganas, R.G., Neiditch, M.B., Perez, L.J., and Ng, W.L. (2020). Parallel quorum-sensing system in *Vibrio cholerae* prevents signal interference inside the host. *PLoS Pathog* 16**,** e1008313.

Watve, S.S., Thomas, J., and Hammer, B.K. (2015). CytR Is a Global Positive Regulator of Competence, Type VI Secretion, and Chitinases in *Vibrio cholerae*. *PLoS One* 10**,** e0138834.

Wei, Y., Perez, L.J., Ng, W.L., Semmelhack, M.F., and Bassler, B.L. (2011). Mechanism of *Vibrio cholerae* autoinducer-1 biosynthesis. *ACS Chem Biol* 6**,** 356-365.

Wickham, H. (2016). *ggplot2: Elegant Graphics for Data Analysis.* Springer-Verlag New York.

Winzer, K., Hardie, K.R., Burgess, N., Doherty, N., Kirke, D., Holden, M.T.G., Linforth, R., Cornell, K.A., Taylor, A.J., Hill, P.J., and Williams, P. (2002). LuxS: its role in central metabolism and the *in vitro* synthesis of 4-hydroxy-5-methyl-3(2H)-furanone. *Microbiology (Reading)* 148**,** 909-922.

Wu, H., Li, M., Guo, H., Zhou, H., Li, B., Xu, Q., Xu, C., Yu, F., and He, J. (2019a). Crystal structure of the *Vibrio cholerae* VqmA-ligand-DNA complex provides insight into ligand-binding mechanisms relevant for drug design. *J Biol Chem* 294**,** 2580-2592.

Wu, H., Li, M., Peng, C., Yin, Y., Guo, H., Wang, W., Xu, Q., Zhou, H., Xu, C., Yu, F., and

He, J. (2019b). Large conformation shifts of *Vibrio cholerae* VqmA dimer in the absence of target DNA provide insight into DNA-binding mechanisms of LuxR-type receptors. *Biochemical and Biophysical Research Communications* 520**,** 399-405.

Wu, T., Hu, E., Xu, S., Chen, M., Guo, P., Dai, Z., Feng, T., Zhou, L., Tang, W., Zhan, L., Fu, X., Liu, S., Bo, X., and Yu, G. (2021). clusterProfiler 4.0: A universal enrichment tool for interpreting omics data. *Innovation (N Y)* 2**,** 100141.

Wynendaele, E., Verbeke, F., D'hondt, M., Hendrix, A., Van De Wiele, C., Burvenich, C., Peremans, K., De Wever, O., Bracke, M., and De Spiegeleer, B. (2015). Crosstalk between the microbiome and cancer cells by quorum sensing peptides. *Peptides* 64**,** 40-48.

Xavier, K.B., and Bassler, B.L. (2005a). Interference with AI-2-mediated bacterial cell-cell communication. *Nature* 437**,** 750-753.

Xavier, K.B., and Bassler, B.L. (2005b). Regulation of uptake and processing of the quorum-sensing autoinducer AI-2 in *Escherichia coli*. *Journal of Bacteriology* 187**,** 238-248.

Xavier, K.B., Miller, S.T., Lu, W., Kim, J.H., Rabinowitz, J., Pelczer, I., Semmelhack, M.F., and Bassler, B.L. (2007). Phosphorylation and processing of the quorum-sensing molecule autoinducer-2 in enteric bacteria. *ACS Chem Biol* 2**,** 128-136.

Xu, X., Stern, A.M., Liu, Z., Kan, B., and Zhu, J. (2010). Virulence regulator AphB enhances *toxR* transcription in *Vibrio cholerae*. *BMC Microbiol* 10**,** 3.

Xue, T., Zhao, L., Sun, H., Zhou, X., and Sun, B. (2009). LsrR-binding site recognition and regulatory characteristics in *Escherichia coli* AI-2 quorum sensing. *Cell Res* 19**,** 1258-1268.

Yan, J., Sharo, A.G., Stone, H.A., Wingreen, N.S., and Bassler, B.L. (2016). *Vibrio cholerae* biofilm growth program and architecture revealed by single-cell live

imaging. *Proc Natl Acad Sci U S A* 113**,** E5337-5343.

Yang, M., Liu, Z., Hughes, C., Stern, A.M., Wang, H., Zhong, Z., Kan, B., Fenical, W., and Zhu, J. (2013). Bile salt-induced intermolecular disulfide bond formation activates *Vibrio cholerae* virulence. *Proc Natl Acad Sci U S A* 110**,** 2348-2353.

Yildiz, F.H., and Schoolnik, G.K. (1999). *Vibrio cholerae* O1 El Tor: identification of a gene cluster required for the rugose colony type, exopolysaccharide production, chlorine resistance, and biofilm formation. *Proc Natl Acad Sci U S A* 96**,** 4028-4033.

Yin, W., Wang, Y., Liu, L., and He, J. (2019). Biofilms: The Microbial "Protective Clothing" in Extreme Environments. *Int J Mol Sci* 20.

Yu, G.C., Wang, L.G., Han, Y.Y., and He, Q.Y. (2012). clusterProfiler: an R Package for Comparing Biological Themes Among Gene Clusters. *Omics-a Journal of Integrative Biology* 16**,** 284-287.

Zargar, A., Quan, D.N., Carter, K.K., Guo, M., Sintim, H.O., Payne, G.F., and Bentley, W.E. (2015). Bacterial secretions of nonpathogenic *Escherichia coli* elicit inflammatory pathways: a closer investigation of interkingdom signaling. *mBio* 6**,** e00025.

Zhao, W., Caro, F., Robins, W., and Mekalanos, J.J. (2018). Antagonism toward the intestinal microbiota and its effect on *Vibrio cholerae* virulence. *Science* 359**,** 210-213.

Zheng, J., Shin, O.S., Cameron, D.E., and Mekalanos, J.J. (2010). Quorum sensing and a global regulator TsrA control expression of type VI secretion and virulence in *Vibrio cholerae*. *Proc Natl Acad Sci U S A* 107**,** 21128-21133.

Zhu, J., and Mekalanos, J.J. (2003). Quorum sensing-dependent biofilms enhance colonization in *Vibrio cholerae*. *Developmental Cell* 5**,** 647-656.

Zhu, J., Miller, M.B., Vance, R.E., Dziejman, M., Bassler, B.L., and Mekalanos, J.J. (2002). Quorum-sensing regulators control virulence gene expression in *Vibrio cholerae*.

Proceedings of the National Academy of Sciences 99**,** 3129-3134.